

PACIFIC EARTHQUAKE ENGINEERING RESEARCH CENTER

Update of the BC Hydro Subduction Ground-Motion Model using the NGA-Subduction Dataset

Norman Abrahamson

Nicolas Kuehn

University of California, Berkeley

Zeynep Gulerce

Middle East Technical University

Nicolas Gregor

Consultant

Yousef Bozognia

Grace Parker

Jonathan Stewart

University of California, Los Angeles

Brian Chiou

California Department of Transportation

I. M. Idriss

University of California, Davis

Kenneth Campbell

CoreLogic, Inc.

Robert Youngs

Wood Environmental & Infrastructure Solutions, Inc.

PEER Report No. 2018/02

Pacific Earthquake Engineering Research Center
Headquarters at the University of California, Berkeley

June 2018

Disclaimer

The opinions, findings, and conclusions or recommendations expressed in this publication are those of the author(s) and do not necessarily reflect the views of the study sponsor(s) or the Pacific Earthquake Engineering Research Center.

Update of the BCHydro Subduction Ground-Motion Model Using the NGA-Subduction Dataset

Norman Abrahamson

Nicolas Kuehn

University of California, Berkeley

Zeynep Gulerce

Middle East Technical University

Nicholas Gregor

Consultant

Yousef Bozorgnia

Grace Parker

Jonathan Stewart

University of California, Los Angeles

I.M. Idriss

University of California, Davis

Kenneth Campbell

CoreLogic, Inc.

Robert Youngs

Wood Environmental and Infrastructure Solutions, Inc.

PEER Report 2018/02

Pacific Earthquake Engineering Research Center
Headquarters at the University of California, Berkeley

June 2018

ABSTRACT

An update to the BCHydro ground-motion model for subduction earthquakes has been developed using the 2018 PEER NGA-SUB dataset. The full NGA-SUB database includes over 70,000 recordings from 1880 earthquakes. A subset of 8144 recordings from 181 earthquake is used in this study. The update modifies the BCHydro model to include regional terms for the V_{S30} scaling, large distance (linear R) scaling, and constant terms, which is consistent with the regionalization approach used in the NGA-West2 ground-motion models. A total of six regions were considered: Cascadia, Central America, Japan, New Zealand, South America, and Taiwan. Region-independent terms are used for the small-magnitude scaling, geometrical spreading, depth to top of rupture (Z_{TOR}) scaling, and intraslab/interface scaling. The break in the magnitude scaling at large magnitudes for intraslab earthquakes is based on thickness of the intraslab and is subduction-zone dependent. The magnitude scaling for large magnitudes is constrained based on finite-fault simulations as given in the 2016 BCHydro model. Nonlinear site response is also constrained to be the same as the 2016 BCHydro model. The sparse ground-motion data from Cascadia show a factor of 2–3 lower ground motions than for other regions. Without a sound physical basis for this large reduction, the Cascadia model is adjusted to be consistent with the average from all regions for the center range of the data: $M = 6.5$, $R = 100$ km, $V_{S30} = 400$ m/sec. Epistemic uncertainty is included using the scaled backbone approach, with high and low models based on the differences in the average ground motions for the different regions. The lower range of the epistemic uncertainty does not encompass the the full range of the very low short-period ground motions in Cascadia. For the Cascadia region, the ground-motion model is considered applicable to distance up to 800 km, magnitudes of 5.0 to 9.5, and periods from 0 to 10 sec. The intended use of this update is to provide an improved ground-motion model for consideration for use in the development of 2020 U.S. national uniform-hazard maps. It is not intended to be used for other regions around the world. This updated ground-motion model will be superseded by the suite of NGA-SUB ground-motion models when they are completed.

ACKNOWLEDGMENTS

This updated ground-motion model is the result of collaboration by the NGA-SUB developer group. The work was partially supported by both funding and in-kind support from FM Global, Pacific Gas & Electric Company, and Caltrans. The U.S. Geological Survey partially supported Stewart and Bozorgnia for the NGA-SUB database development and the ground-motion model development. Many other members of the NGA-SUB developer group have participated without financial support from PEER, providing in-kind contributions of their expertise. Silvia M, ...

A key input to this study is the NGA-SUB ground-motion data base which is a result of several years effort by the database team. In particular, we want to acknowledge the efforts of Tadahiro Kishida, Silvia Mazzoni, Victor Contreras, Sean Ahdi and Robert Darragh to develop the NGA-SUB flat file that was used in this study.

Any opinions, findings, and conclusions or recommendations expressed in this material are those of the authors and do not necessarily reflect those of the sponsoring agencies or the Pacific Earthquake Engineering Research Center and the Regents of the University of California.

CONTENTS

ABSTRACT.....	III
ACKNOWLEDGMENTS	V
CONTENTS.....	VII
LIST OF TABLES	X
LIST OF FIGURES	XII
1 INTRODUCTION.....	1
2 DATASET SELECTION	3
2.1 Selection criteria for Regions.....	3
2.2 Selection Criteria for Earthquakes	5
2.3 Selection Criteria for Recordings	6
3 REGRESSION ANALYSIS	10
3.1 Functional Form.....	10
3.2 Regression Analysis	13
3.3 Residuals	13
3.4 Regional Differences	35
4 MODEL RESULTS	38
4.1 Adjusting the Cascadia Model.....	38
4.2 Model Coefficients	45
4.3 Epistemic Uncertainty	50
4.4 Median Model Comparisons.....	54
4.5 Standard Deviation	79
5 CONCLUSIONS AND FUTURE WORK	83
REFERENCES.....	86
PEER REPORTS: ONE HUNDRED SERIES.....	99

LIST OF TABLES

Table 2.1	Event classes.	6
Table 2.2	Distribution of the selected earthquakes and recordings.	8
Table 3.1	Region-specific parameters.....	12
Table 4.1	Period-independent coefficients.....	45
Table 4.2	Period-dependent coefficients for the Cascadia model.....	46
Table 4.3	Period-dependent coefficients for the Cascadia model.....	47
Table 4.4	Epistemic uncertainty in the adjustment term (in LN units).....	51
Table 4.5	Aleatory variability terms (in LN units)	81

LIST OF FIGURES

Figure 2.1	Scaling of PGA with rupture distance for the $M_w > 6$ events in the Alaska database.	4
Figure 2.2	Distribution of the residuals from preliminary analysis for events in the Taiwan dataset that includes data from the TW and CWB seismic networks.	5
Figure 2.3	Distribution of the residuals from preliminary analysis with rupture distance (left: data from Japan, right: data from South America).	7
Figure 2.4	Number of earthquakes and number of recordings in the selected subset by period.	8
Figure 2.5	Magnitude-distance distributions for the final subset (for PGA).	9
Figure 3.1	Smoothing of coefficient a_2 (global geometrical spreading for interface).	15
Figure 3.2	Smoothing of coefficient a_{12} (global V_{S30} scaling).	16
Figure 3.3	Smoothing of coefficient a_{14} (global additional geometrical spreading for intraslab).	17
Figure 3.4	Smoothing of coefficient a_4 (global small magnitude scaling).	18
Figure 3.5	Smoothing of coefficient a_{18} (Cascadia $VS30$ scaling).	19
Figure 3.6	Smoothing of coefficient a_{25} (Cascadia linear R scaling).	20
Figure 3.7	Smoothing of coefficient a_{11} (global Z_{TOR} scaling for intraslab).	21
Figure 3.8	Smoothing of coefficient a_{10} (global intraslab constant term).	22
Figure 3.9	Between-event residuals: (a) PGA , (b) $T = 0.1$ sec, and (c) $T = 0.2$ sec.	23
Figure 3.10	Between-event residuals: (a) $T = 0.5$ sec, (b) $T = 1$ sec, and (c) $T = 3$ sec.	24
Figure 3.12(a)	Within-event residuals for Cascadia: PGA and $T = 0.1$ sec.	26
Figure 3.12(b)	Within-event residuals for Cascadia: $T = 0.2$ sec and $T = 0.5$ sec.	27
Figure 3.12(c)	Within-event residuals for Cascadia: $T = 1$ sec and $T = 3$ sec.	28
Figure 3.13(a)	Within-event residuals for Japan: PGA and $T = 0.1$ sec.	29
Figure 3.13(b)	Within-event residuals for Japan: $T = 0.2$ sec and $T = 0.5$ sec.	30
Figure 3.13(c)	Within-event residuals for Japan: $T = 1$ sec and $T = 3$ sec.	31
Figure 3.14(a)	Within-event residuals for other regions: PGA and $T = 0.1$ sec.	32
Figure 3.14(b)	Within-event residuals for other regions: $T = 0.2$ sec and $T = 0.5$ sec.	33
Figure 3.14(c)	Within-event residuals for other regions: $T = 1$ sec and $T = 3$ sec.	34
Figure 3.15	Regional differences in the linear $VS30$ term (a_{12}).	36

Figure 3.16	Regional differences in the linear R term (a_6).	37
Figure 4.1	Median spectra for different regions for intraslab, M7, $Z_{TOR} = 50$ km, $R_{rup} = 100$ km, and $V_{S30}=400$ m/sec.	39
Figure 4.2	Median spectra for different regions for interface, M7, $Z_{TOR} = 20$ km, $R_{rup} = 100$ km, and $V_{S30}=400$ m/sec.	40
Figure 4.3	Adjustment to the constant term for Cascadia for intraslab earthquakes.....	41
Figure 4.4	Adjustment to the constant term for Cascadia for interface earthquakes.	42
Figure 4.5	Smoothed adjustment for the constant term for Cascadia.	43
Figure 4.6	Comparison of adjusted Cascadia median for M6.8, $V_{S30} = 400$ m/sec, $R_{rup}=83$ km.	44
Figure 4.7	Magnitude scaling of spectra for $R_{rup}=80$ km and $V_{S30}=760$ m/s.	48
Figure 4.8	Distance scaling of spectra for M=9 interface earthquakes and $V_{S30}=760$ m/s.....	49
Figure 4.9	ZTOR scaling of spectra for M=7 intraslab events and $V_{S30}=760$ m/s.....	50
Figure 4.10	Recommended epistemic uncertainty in the Cascadia adjustment term for intraslab earthquakes.....	52
Figure 4.11	Recommended epistemic uncertainty in the Cascadia adjustment term for interface earthquakes.	53
Figure 4.12(a)	Median attenuation comparison for PGA for M9, $V_{S30} = 760$ m/sec. The symbols are shown on the updated BCHydro model to make these models stand out on the plot.....	56
Figure 4.12(b)	Median attenuation comparison for $T = 0.2$ sec for M9, $V_{S30} = 760$ m/sec.....	57
Figure 4.12(c)	Median attenuation comparison for $T = 1$ sec, for M9, $V_{S30} = 760$ m/sec.....	58
Figure 4.12(d)	Median attenuation comparison for $T = 3$ sec, for M9, $V_{S30} = 760$ m/sec.....	59
Figure 4.13(a)	Median attenuation comparison for intraslab events, PGA, for M7, $V_{S30} = 760$ m/sec.	60
Figure 4.13(b)	Median attenuation comparison for intraslab events, $T = 0.2$, for M7, $V_{S30} = 760$ m/sec.	61
Figure 4.13(c)	Median attenuation comparison for intraslab events, $T = 1$, for M7, $V_{S30} = 760$ m/sec.	62
Figure 4.13(d)	Median attenuation comparison for intraslab events, $T = 3$, for M7, $V_{S30} = 760$ m/sec.	63
Figure 4.14(a)	Magnitude scaling for PGA for interface earthquakes. ($R_{rup}=75$ km, $V_{S30}=760$ m/s)	64

Figure 4.14(b) Magnitude scaling for $T=0.2$ sec for interface earthquakes. ($R_{rup}=75$ km, $V_{S30}=760$ m/s)	65
Figure 4.14(c) Magnitude scaling for $T=1$ sec for interface earthquakes. ($R_{rup}=75$ km, $V_{S30}=760$ m/s)	66
Figure 4.14(d) Magnitude scaling for $T=3$ sec for interface earthquakes. ($R_{rup}=75$ km, $V_{S30}=760$ m/s)	67
Figure 4.15(a) Magnitude scaling for PGA for intraslab earthquakes. ($R_{rup}=75$ km, $V_{S30}=760$ m/s, $Z_{TOR}=50$ km)	68
Figure 4.15(b) Magnitude scaling for $T=0.2$ sec for intraslab earthquakes. ($R_{rup}=75$ km, $V_{S30}=760$ m/s, $Z_{TOR}=50$ km)	69
Figure 4.15(c) Magnitude scaling for $T=1$ sec for intraslab earthquakes. ($R_{rup}=75$ km, $V_{S30}=760$ m/s, $Z_{TOR}=50$ km)	70
Figure 4.15(d) Magnitude scaling for $T=3$ sec for intraslab earthquakes. ($R_{rup}=75$ km, $V_{S30}=760$ m/s, $Z_{TOR}=50$ km)	71
Figure 4.16 Median spectrum comparison for interface events, $R_{rup} = 75$ km, for M8, $V_{S30} = 760$ m/sec.	72
Figure 4.17 Median spectrum comparison for interface events, $R_{rup} = 75$ km, for M9, $V_{S30} = 760$ m/sec.	73
Figure 4.18 Median spectrum comparison for interface events, $R_{rup} = 300$ km, for M8, $V_{S30} = 760$ m/sec.	74
Figure 4.19 Median spectrum comparison for interface events, $R_{rup} = 300$ km, for M9, $V_{S30} = 760$ m/sec.	75
Figure 4.20 Median spectrum comparison for intraslab events, $R_{rup}=75$ km, for M6.5, $V_{S30} = 760$ m/sec.	76
Figure 4.21 Median spectrum comparison for intraslab events, $R_{rup} = 75$ km, for M7.5, $V_{S30} = 760$ m/sec.	77
Figure 4.22 Median spectrum comparison for intraslab events, $R_{rup} = 300$ km, for M6.5, $V_{S30} = 760$ m/sec.	78
Figure 4.23 Median spectrum comparison for intraslab events, $R_{rup} = 300$ km, for M7.5, $V_{S30} = 760$ m/sec.	79
Figure 4.24 Smoothed phi and tau models.	82

1 Introduction

The U.S. Geological Survey (USGS) is in the process of reviewing and updating the seismic source characterization and ground-motion characterization models used in the national seismic hazard mapping project for the 2020 update of the national uniform-hazard maps. To give the USGS adequate time to review the new models, any new models for consideration need to be provided to the USGS in the June 2018 time frame. Currently, the NGA-SUB project is developing a suite of alternative ground-motion models (GMMs) for subduction zones based on a greatly expanded dataset and additional finite-fault numerical simulations. The full set of NGA-SUB GMMs with improved model parametrization will not be completed in time for consideration by the USGS in the 2020 update. To meet the USGS review time requirements, the NGA-SUB developers developed a single GMM that is an update of the 2016 BCHydro GMM [Abrahamson et al. 2016]. This updated BCHydro GMM uses the expanded dataset to regionalize V_{S30} , linear R , and constant terms in the GMM, similar to the approach to regionalization used by the NGA-West2 GMMs (Gregor et al, [2014]). This approach provides an improved subduction ground-motion model that includes region-specific terms for Cascadia and meets the schedule for consideration by the USGS as part of the 2020 update of the national uniform-hazard maps.

In this report, the updated GMM is called the updated BCHydro model to reflect the original model used as the starting point, but it does not imply that BCHydro reviewed or approved this update.

2 Dataset Selection

The NGA subduction (NGA-SUB) database includes recordings from seven different regions: Alaska, Cascadia, Central America, Japan, New Zealand, South America, and Taiwan as described by Kishida et al. [2018]. The full dataset includes over 70,000 3-component recordings. The June 12, 2018, version of the NGA-SUB dataset was used for this study. Given the large size of the NGA-SUB dataset, QA checks of the meta data and response spectral values are still ongoing at the time of this study. Therefore, for the current study, the parts of the dataset that show questionable scaling and which are still under review are excluded. The main criteria used for selecting the subset of data for use in this study can be grouped into three main headings: selection criteria for regions, selection criteria for earthquakes, and selection criteria for recordings.

Data selection is an iterative process. After the initial selection is made, preliminary regression analyses are performed and, using residuals, outlier data are identified and evaluated. Based on the evaluation of the outlier data, the data selection is modified and the process repeated. The selection criteria listed below the is final result of this interactive process. As examples of the process, some residual plots from the preliminary regression analyses are shown before the model is discussed.

2.1 SELECTION CRITERIA FOR REGIONS

A preliminary analysis of the June 12, 2018, version of the dataset showed that the distance scaling of the recordings from earthquakes in the Alaska region are unusual. For example, the distance scaling of PGA for $M > 6$ earthquakes in Alaska is shown in Figure 2.1. The large scatter (factor of 100) and lack of attenuation with distance indicate that this version of the dataset may include some errors in the distances or response spectral values from the Alaska region. Therefore, all of the recordings in the Alaska dataset are excluded from this analysis.

An analysis of distance scaling from Taiwan earthquakes also showed unusually large scatter for the smaller magnitude earthquakes. The metadata for some of the smaller magnitude Taiwanese events in the June 12, 2018, version of the dataset contain some errors that are currently being corrected. For this study, rather than determine which of the earthquakes have meta data errors, all of the Taiwanese earthquakes with $M < 5.5$ have excluded. A second issue for the Taiwan data is the data from the “TW” network. The ground motions from the TW network appear to be biased to much lower values than the other networks. As an example, Figure 2.2 compares the residuals for the CWB and TW networks from a preliminary regression analysis. Given the

apparent bias from the TW network, all of the recordings from this network are excluded. The TW network represents about 10% of the recordings in Taiwan dataset.

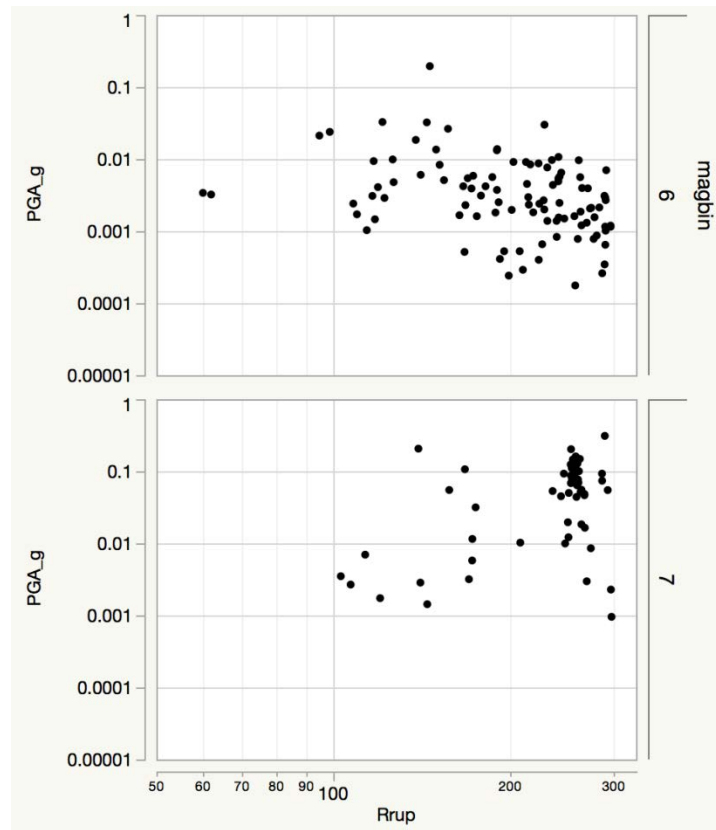


Figure 2.1 Scaling of PGA with rupture distance for the Mw > 6 events in the Alaska database.

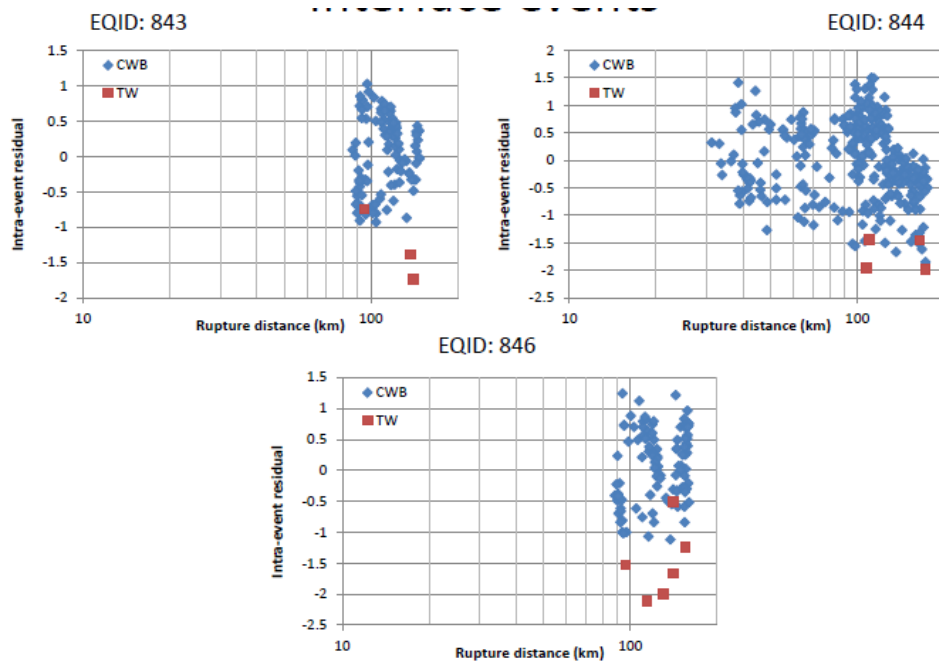


Figure 2.2 Distribution of the residuals from preliminary analysis for events in the Taiwan dataset that includes data from the TW and CWB seismic networks.

2.2 SELECTION CRITERIA FOR EARTHQUAKES

The ground-motion model is developed for two event types: interface and intraslab earthquakes. The NGA-SUB dataset includes six event classifications shown in Table 2.1. For interface events, only class 0 events were used. For intraslab events, both class 1 and class 5 (event from lower part of a double seismic zone) are used. To avoid potential event classification issues, the unusually shallow intra-slab events ($Z_{TOR} < 20$ km) and unusually deep interface events ($Z_{TOR} > 50$ km) are excluded.

For all earthquakes, the minimum magnitude of 5 was used, which is consistent with the 2016 BChydro model. The minimum of 3 recordings per event (after all of the selection criteria have been met) is applied.

Table 2.1 Event classes.

Event class index	Event class description
0	Subduction interface event
1	Subduction intraslab event
2	Shallow crustal/overriding plate event
3	Mantle event
4	Outer rise event
5	Intraslab, lower double seismic zone event
-999	Unknown
-888	Interface event with small confidence
-777	Intraslab event with small confidence
-666	Shallow crustal/overriding plate events with small confidence
-444	Outer rise event with small confidence

2.3 SELECTION CRITERIA FOR RECORDINGS

To avoid potential bias in the ground motions, the following selection criteria are applied:

- Remove recordings with multiple event flag equal to 1 (time history that includes more than one earthquake)
- Remove recordings with late *P*-trigger
- Remove recordings that have missing data in magnitude, distance and V_{S30} fields
- Remove stations with GMX first letter N, Z, and F (non-free-field stations)
- Remove downhole recordings with instrument depth >2 m

The distance scaling can be strongly influenced by wave propagation from earthquakes in the forearc to stations in the backarc. Ground-motion data from the Japan region show much faster attenuation for backarc stations; however, a preliminary analysis of the data in the Cascadia region showed no difference between the attenuation for stations located in the forearc from those located in the backarc. To avoid the lower ground motions from the backarc stations in other regions affecting the Cascadia ground-motion model, recordings in the backarc for regions other than Cascadia are removed. For the Cascadia region, stations location in both forearc and backarc regions are included.

For regions other than Cascadia, the distance is limited to 300 km as the main use of the global data is to constrain the magnitude scaling, short-distance scaling, and depth scaling. To capture the large-distance scaling in Cascadia, data out to a distance of 800 km from the Cascadia region are included. Two of the four earthquakes in the Cascadia region are from Washington and two are from northern California. The attenuation beyond 300 km is different for the Washington

and Northern California recordings. To capture the large distance scaling in Washington, the two northern California earthquakes are also limited to 300 km. Data out to 800 km is only included for the two Washington earthquakes.

The large-distance slope of the recordings from the Tohoku earthquake is quite different than the others; see Figure 2.3. This difference can affect the event terms estimated in the regression analysis. In this case, including the Tohoku data beyond 300 km would lead to smaller (more negative) event terms. To have the event terms representative of the Tohoku ground motions in the 100-km range, the recordings from the Tohoku earthquake with $R_{\text{rup}} > 200$ km are removed.

The data includes an estimate of the maximum distance, R_{max} , for which the dataset is not affected by censoring of the ground motions. Censoring can occur when there are missing recordings (not triggered or no stations installed) that would have shown lower ground motions than the recorded ground motions. The procedure for estimating R_{max} will be described in the NGA-SUB database report which is under preparation. The recordings with $R_{\text{rup}} > R_{\text{max}}$ are removed to avoid a bias to larger ground motions at large distances. This criterion has the largest effects on the Taiwan dataset. Finally, a small number of outlier recordings and events, identified by visual inspection, are removed.

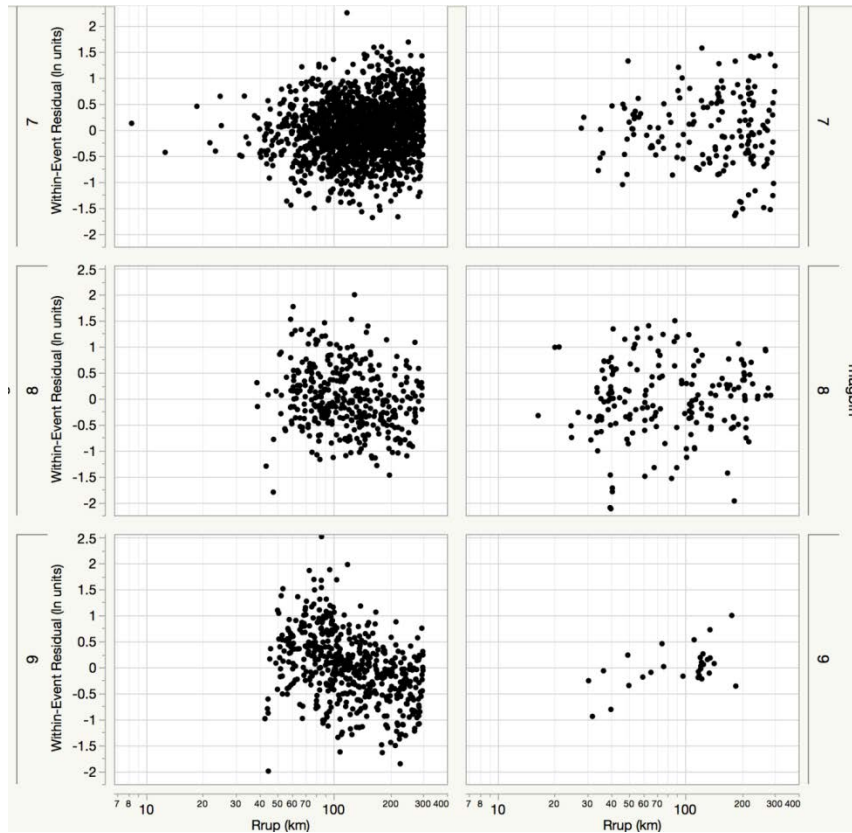


Figure 2.3 Distribution of the residuals from preliminary analysis with rupture distance (left: data from Japan, right: data from South America).

Regional distribution of the recordings used in the regression is given in Table 2.2. As defined in the NGA-West2 database (Ancheta, [2014]), the response spectral values for the selected recordings are only used in the regression analysis for spectral frequencies greater than 1.25 times the high-pass corner frequency used in the record processing. This requirement produces a dataset that varies as a function of period. The period dependence of the number of earthquakes and number of recordings used in the regression analysis is shown in Figure 2.4, which shows a slight drop in the number of recordings and earthquakes between 5–6 sec. The magnitude-distance distribution of the selected data set for short periods is shown in Figure 2.5.

Table 2.2 **Distribution of the selected earthquakes and recordings.**

Number	Region	Number of earthquakes	Number of recordings
1	Alaska	0	0
2	Cascadia	4	144
3	Central America	12	78
4	Japan	73	4953
5	New Zealand	34	541
6	South America	47	636
7	Taiwan	11	1792
Total Used		181	8144
Total in NGA-SUB		1,880	71,343

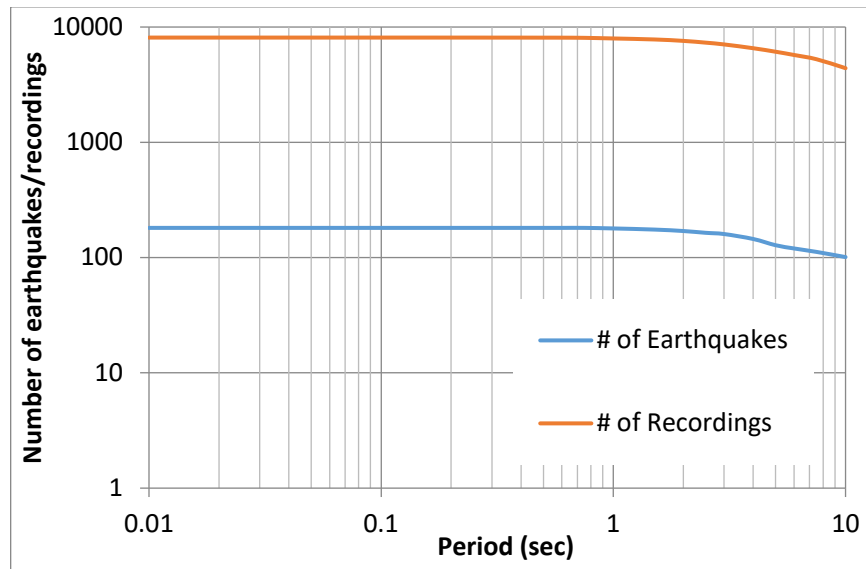


Figure 2.4 **Number of earthquakes and number of recordings in the selected subset by period.**

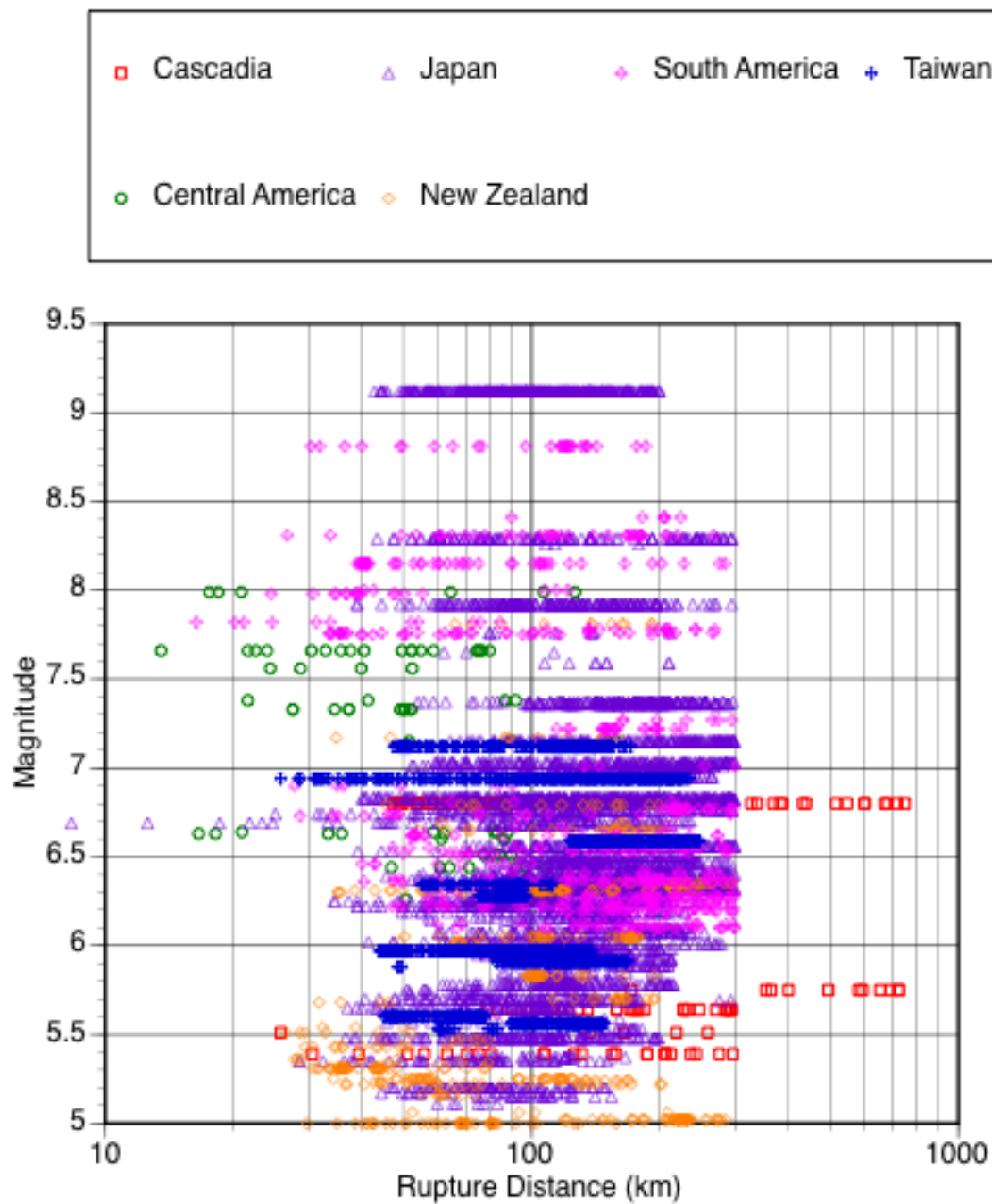


Figure 2.5 Magnitude-distance distributions for the final subset (for *PGA*).

3 Regression Analysis

3.1 FUNCTIONAL FORM

The functional form for the updated BCHydro ground-motion model is based on the functional form used in the 2016 BCHydro model with the backarc scaling removed. The base model is given by:

$$\begin{aligned} \ln(PSA(g)) = & a_1 + a_4(C_{1_slab} - C_{1_inter})F \\ & + (a_2 + a_{14}F + a_3(M - 7.8)) \ln(R_{rup} + C_4 \exp((M - 6)a_9)) + a_6 R_{rup} \\ & + a_{10}F + f_{mag}(M) + f_{ZTOR}(Z_{TOR}, F) + f_{site}(PGA_{1000}, V_{S30}) \end{aligned}$$

where

M = moment magnitude

R_{rup} = rupture distance in km

F = event type (0 for interface and 1 for intraslab)

Z_{TOR} = depth of the top of rupture (km)

PGA_{1000} = median peak horizontal acceleration for $V_{S30} = 1000$ m/sec

The magnitude scaling is given by:

$$f_{mag}(M) = \begin{cases} a_4(M - C_1) + a_{13}(10 - M)^2 & \text{for } M \leq C_1 \\ a_5(M - C_1) + a_{13}(10 - M)^2 & \text{for } M > C_1 \end{cases}$$

where

$$C_1 = F C_{1_slab} + (1 - F) C_{1_inter}$$

The nonlinear site response scaling is given by:

$$f_{\text{site}}(\text{PGA}_{1000}, V_{S30}) = \begin{cases} a_{12} \ln\left(\frac{V_S^*}{V_{\text{lin}}}\right) - b \ln(\text{PGA}_{1000} + c) b \ln\left[\text{PGA}_{1000} + c \left(\frac{V_S^*}{V_{\text{lin}}}\right)^n\right] & \text{for } V_{S30} < V_{\text{lin}} \\ (a_{12} + b n) \ln\left(\frac{V_S^*}{V_{\text{lin}}}\right) & \text{for } V_{S30} \geq V_{\text{lin}} \end{cases}$$

where

$$V_S^* = \begin{cases} 1000 & \text{for } V_{S30} > 1000 \text{ m/sec} \\ V_{S30} & \text{for } V_{S30} \leq 1000 \text{ m/sec} \end{cases}$$

The BChydro model used a quadratic magnitude scaling with a break in the scaling for large magnitudes (**M**7.6 to **M**8.0 for interface and **M** 7.5 for intraslab). The slope of the large-magnitude scaling was constrained based on finite-fault simulations by Gregor et al. [2006] and Atkinson and Macias [2008] for interface earthquakes. For the updated BChydro model, this constraint on the large magnitude scaling is maintained, but the break points for the interface earthquakes are re-evaluated based on the event terms from the large magnitude earthquakes ($M > 8$). The break in the magnitude scaling for intraslab events is based on the intraslab thickness as described by Archuleta and Ji [2018]: for Cascadia, $C_{1_slab} = 7.2$.

For intraslab earthquakes, the 2016 BChydro model used linear scaling with Z_{TOR} with a limit of 120 km on the depth range for the scaling. A preliminary analysis showed that the Z_{TOR} scaling does not apply for depth greater than about 100 km. Therefore, the limit on the Z_{TOR} scaling is modified to be 100 km rather than 120 km. The Z_{TOR} scaling is given by:

$$f_{Z_{\text{TOR}}}(Z_{\text{TOR}}, F) = \begin{cases} \theta_{11}(Z_{\text{TOR}} - 60)F & \text{for } Z_{\text{TOR}} \leq 100 \text{ km} \\ \theta_{11}(100 - 60)F & \text{for } Z_{\text{TOR}} > 100 \text{ km} \end{cases}$$

There are regional model coefficients for the three regional terms. The indexes for these coefficients are listed in Table 3.1.

Inclusion of basin effects is beyond the scope of this update. Basin effects will be addressed in the full NGA-SUB ground-motion models currently under development.

Table 3.1 Region-specific parameters.

Term	Region	Regression coefficient
Change in V_{S30} scaling	Cascadia	a_{18}
	Central America	$a_{19} = 0$ (fixed at global value)
	Japan	a_{20}
	New Zealand	a_{21}
	South America	a_{22}
	Taiwan	a_{23}
Change in Linear R term	Cascadia	a_{25}
	Central America	a_{26}
	Japan	a_{27}
	New Zealand	a_{28}
	South America	a_{29}
	Taiwan	a_{30}
Constant	Cascadia	a_{32}
	Central America	a_{33}
	Japan	a_{34}
	New Zealand	a_{35}
	South America	a_{36}
	Taiwan	a_{37}

3.2 REGRESSION ANALYSIS

The random-effects model was used for the regression analysis following the procedure described by Abrahamson and Youngs [1992]. The regression is performed in a number of steps to arrive at a smooth model. The coefficients are smoothed to either lead to smooth spectra or to constrain the model to be consistent with basic seismological constraints. Table 3.2 lists the parameters that were regressed in each step and those which were smoothed and fixed following each step.

The large-magnitude scaling was constrained to be equal to the BCHydro scaling. The large-magnitude scaling is controlled by four terms: the magnitude dependent geometrical spreading term (a_3), the linear magnitude scaling terms for large magnitude events (a_5), the magnitude-dependent finite-fault effect term (a_9), and the quadratic magnitude term (a_8). These four coefficients are set to the values given in 2016 BCHydro model. In the first run, the global geometrical spreading term (a_2) and the global linear V_{S30} scaling term (a_{12}) are smoothed; see Figures 3.1 and 3.2.

In the second run, the additional global geometrical spreading term for intraslab events (a_{14}) is smoothed based on the smoothed geometrical spreading term in the previous step. Similarly, the linear magnitude term for small-to-moderate magnitude events (a_4) is smoothed in Step 3; see Figure 3.3. In step 4, the global large distance scaling parameter (a_6) is smoothed; see Figure 3.4. In the same step, the Z_{TOR} scaling (a_{11}) is smoothed.

The next set of runs included estimation of the regional terms for the linear V_{S30} scaling for Cascadia (a_{18}) and other regions (a_{19} - a_{23}), large-distance scaling parameters for Cascadia (a_{25}) and other regions (a_{26} - a_{30}), and the constant terms for Cascadia (a_{31}) and other regions (a_{33} - a_{37}). The regional terms for Cascadia, a_{18} and a_{25} , are smoothed, but the other regional parameters are not smoothed because they are not intended to be used.

The values of the smoothed coefficients for the median ground motion are given in the following chapter; see Table 4.1.

3.3 RESIDUALS

The between-event residuals are shown as a function of magnitude in Figures 3.9 and 3.10 for six spectral periods: PGA, $T = 0.1$ sec, $T = 0.2$ sec, $T = 0.5$ sec, $T = 1$ sec, and $T = 3$ sec. Note that there is no clear trend in magnitude, indicating that the magnitude scaling is consistent with the available recorded data. A key issue is the extrapolation to the **M**9 range. The event terms for the two largest earthquakes (Maule and Tohoku) are shown in Figure 3.11. The event terms are balanced between these two events, indicating that the selected break points in the interface magnitude scaling are not unreasonable.

The within-event residuals for the same six spectral periods are shown by region in Figures 3.12, 3.13, and 3.14. In each case, the residuals are shown as functions of the magnitude, distance, V_{S30} , and PGA_{1000} . Figure 3.12 shows the residuals for the Cascadia region; Figure 3.13 shows the residuals for the Japan region; and Figure 3.14 shows the residuals for the other regions. Overall, there is not a strong trend in the residuals as functions of the four parameters.

Table 3.2 Estimated and constrained parameters at each step of regression

Step	Estimated parameters	Parameters held fixed	Parameters smoothed after run
1	a_1 (global constant), a_2 (geometrical spreading, GS), a_4 (linear magnitude for $M < c_1$), a_6 (global linear R), a_{10} (additional global constant for intraslab events), a_{11} (Z_{TOR}), a_{12} (global linear V_{S30}), a_{14} (additional global GS for intraslab events)	a_3 (mag dep GS), a_5 (linear magnitude for $M > c_1$), a_9 (finite-fault term), a_{13} (quadratic magnitude)	a_2, a_{12}
2	$a_1, a_4, a_6, a_{10}, a_{11}, a_{14}$	$a_2, a_3, a_5, a_9, a_{12}$	a_{14}
3	$a_1, a_4, a_6, a_{10}, a_{11}$	$a_2, a_3, a_5, a_9, a_{12}, a_{14}$	a_4
4	a_1, a_6, a_{10}, a_{11}	$a_2, a_3, a_4, a_5, a_9, a_{12}, a_{14}$	a_6
5	<i>global:</i> a_{10}, a_{11} regional V_{S30} : $a_{18}, a_{20}, a_{21}, a_{22}, a_{23}$, regional R : $a_{25}, a_{26}, a_{27}, a_{28}, a_{29}, a_{30}$, regional const: $a_{32}, a_{33}, a_{34}, a_{35}, a_{36}, a_{37}$	$a_2, a_3, a_4, a_5, a_6, a_9, a_{12}, a_{14}$ $a_1 = 0$ $a_{19} = 0$ (<i>VS30 scaling for Central America fixed to the global value</i>)	a_{18}, a_{25}
7	<i>global:</i> a_{10}, a_{11} regional V_{S30} : $a_{20}, a_{21}, a_{22}, a_{23}$, regional R : $a_{26}, a_{27}, a_{28}, a_{29}, a_{30}$, regional const: $a_{32}, a_{33}, a_{34}, a_{35}, a_{36}, a_{37}$	$a_2, a_3, a_4, a_5, a_6, a_9, a_{12}, a_{14}, a_{18}, a_{25}$, $a_1 = 0$ $a_{19} = 0$	a_{11}
8	<i>global:</i> a_{10} regional V_{S30} : $a_{20}, a_{21}, a_{22}, a_{23}$, regional R : $a_{26}, a_{27}, a_{28}, a_{29}, a_{30}$, regional const: $a_{32}, a_{33}, a_{34}, a_{35}, a_{36}, a_{37}$	$a_2, a_3, a_4, a_5, a_6, a_9, a_{10}, a_{12}, a_{14}, a_{18}, a_{25}$, $a_1 = 0$ $a_{19} = 0$	a_{10}
9	regional V_{S30} : $a_{20}, a_{21}, a_{22}, a_{23}$, regional R : $a_{26}, a_{27}, a_{28}, a_{29}, a_{30}$, regional const: $a_{32}, a_{33}, a_{34}, a_{35}, a_{36}, a_{37}$	$a_2, a_3, a_4, a_5, a_6, a_9, a_{10}, a_{11}, a_{12}, a_{14}, a_{18}, a_{25}$, $a_1 = 0$ $a_{19} = 0$	a_{32}

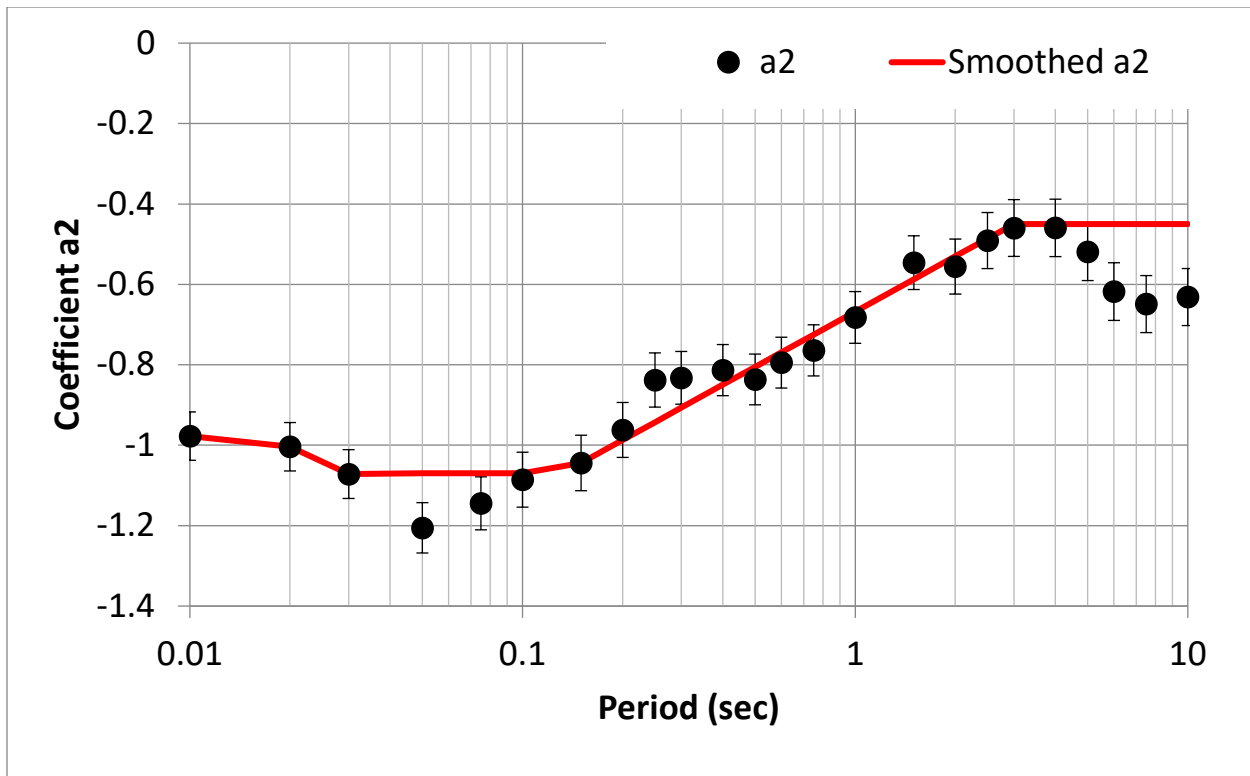


Figure 3.1 Smoothing of coefficient a_2 (global geometrical spreading for interface).

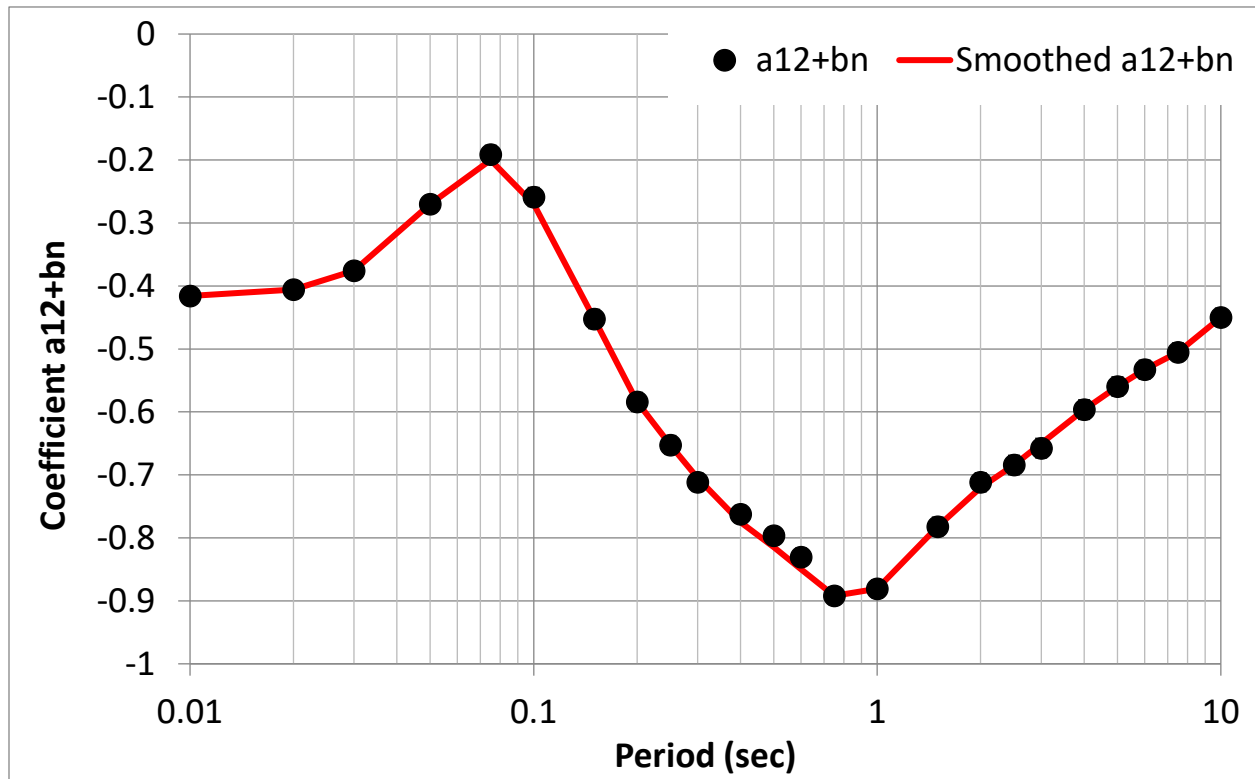


Figure 3.2 Smoothing of coefficient a_{12} (global V_{S30} scaling).

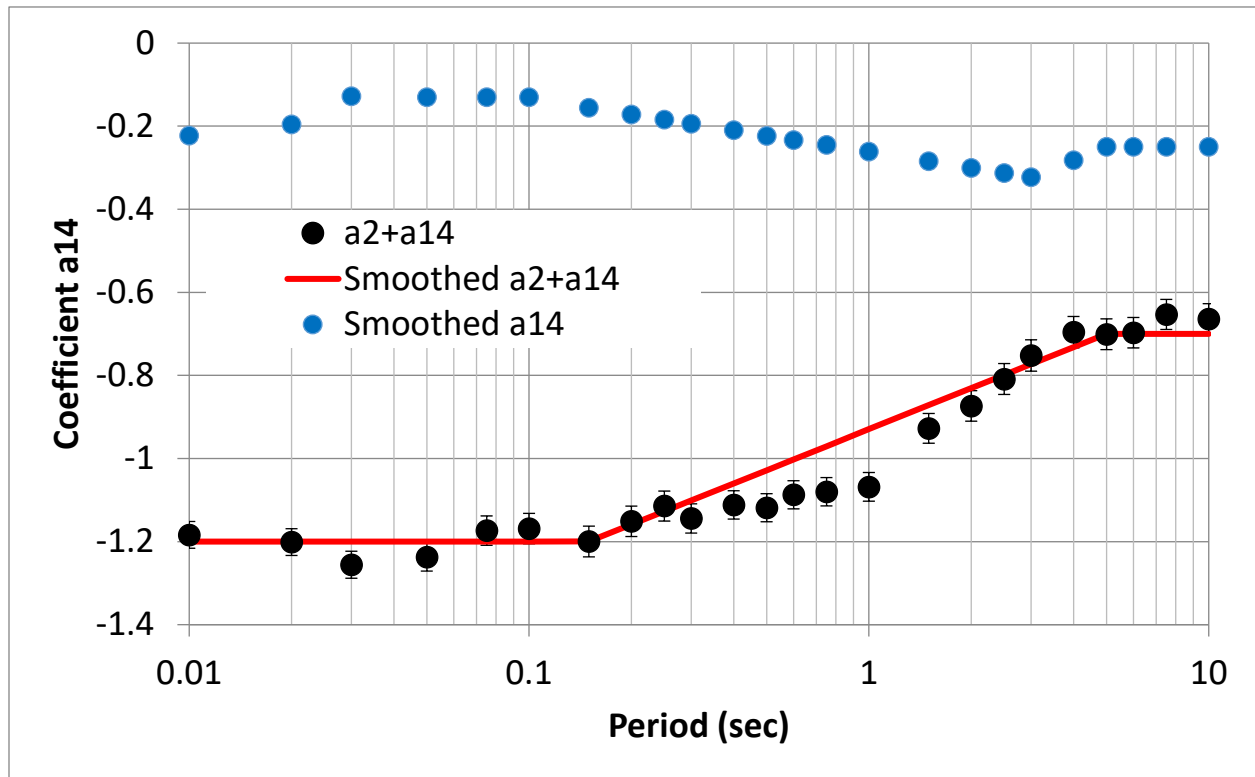


Figure 3.3 Smoothing of coefficient a_{14} (global additional geometrical spreading for intraslab).

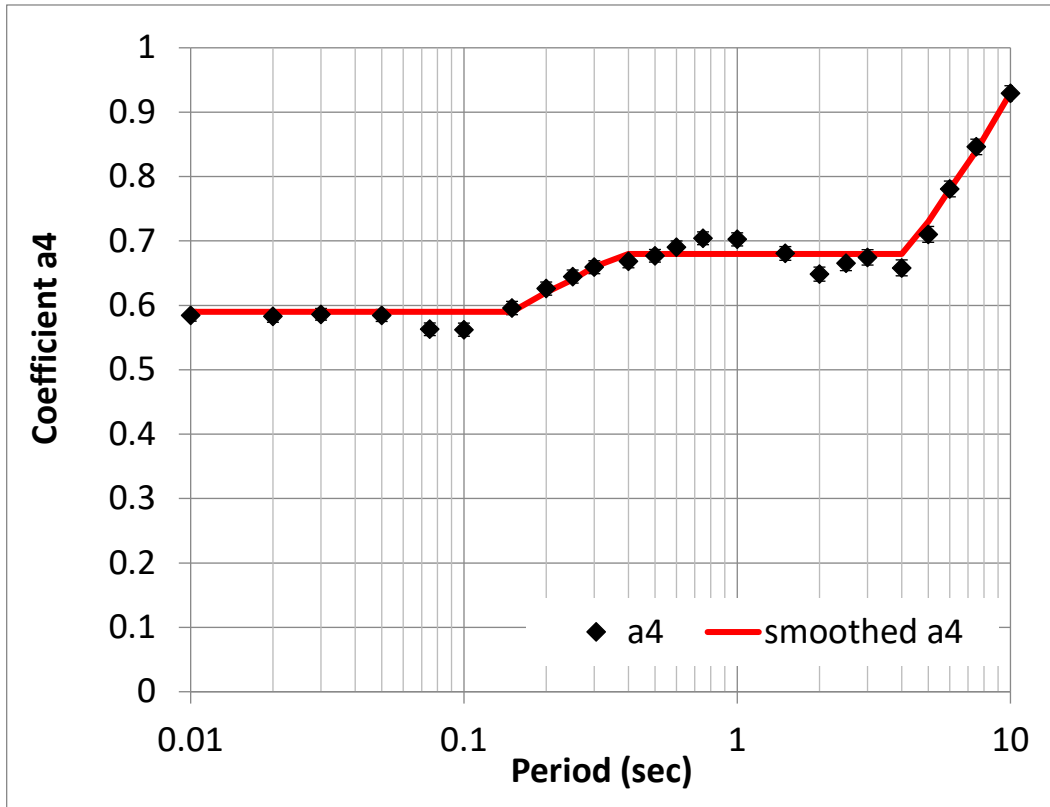


Figure 3.4 Smoothing of coefficient a_4 (global small magnitude scaling).

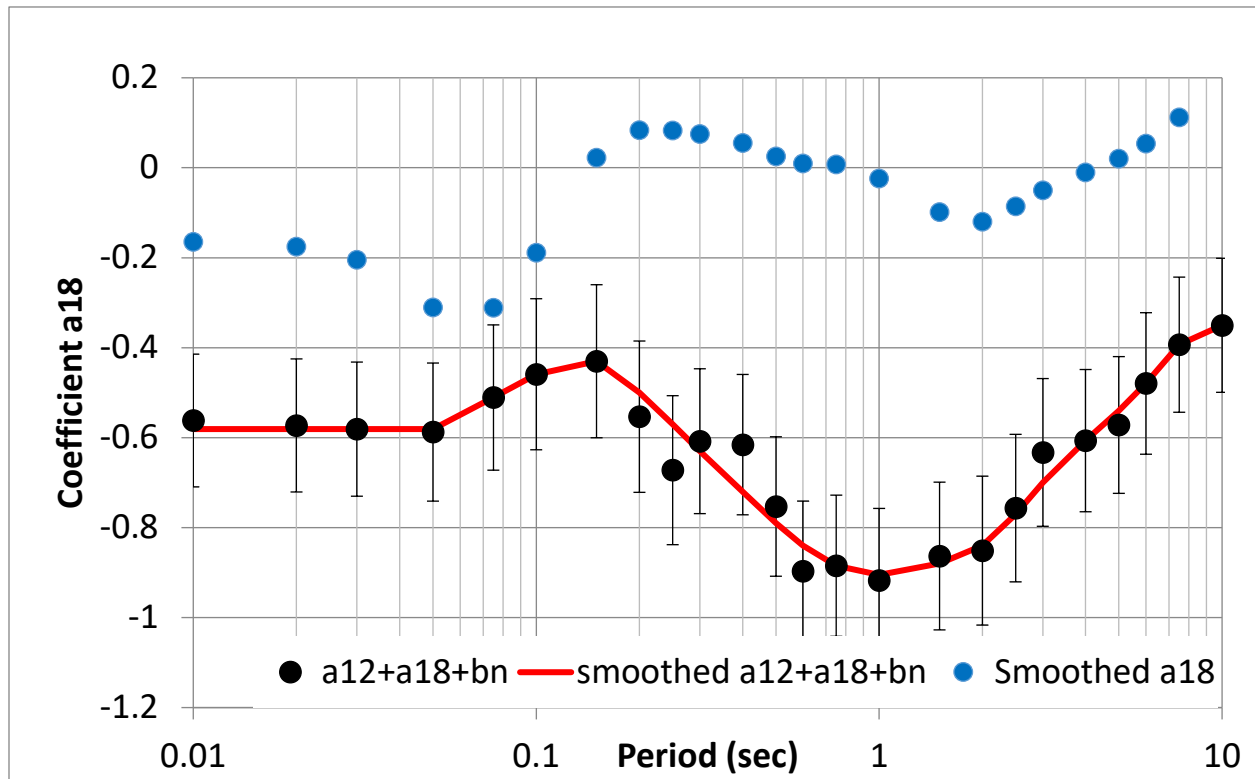


Figure 3.5 Smoothing of coefficient a_{18} (Cascadia VS30 scaling).

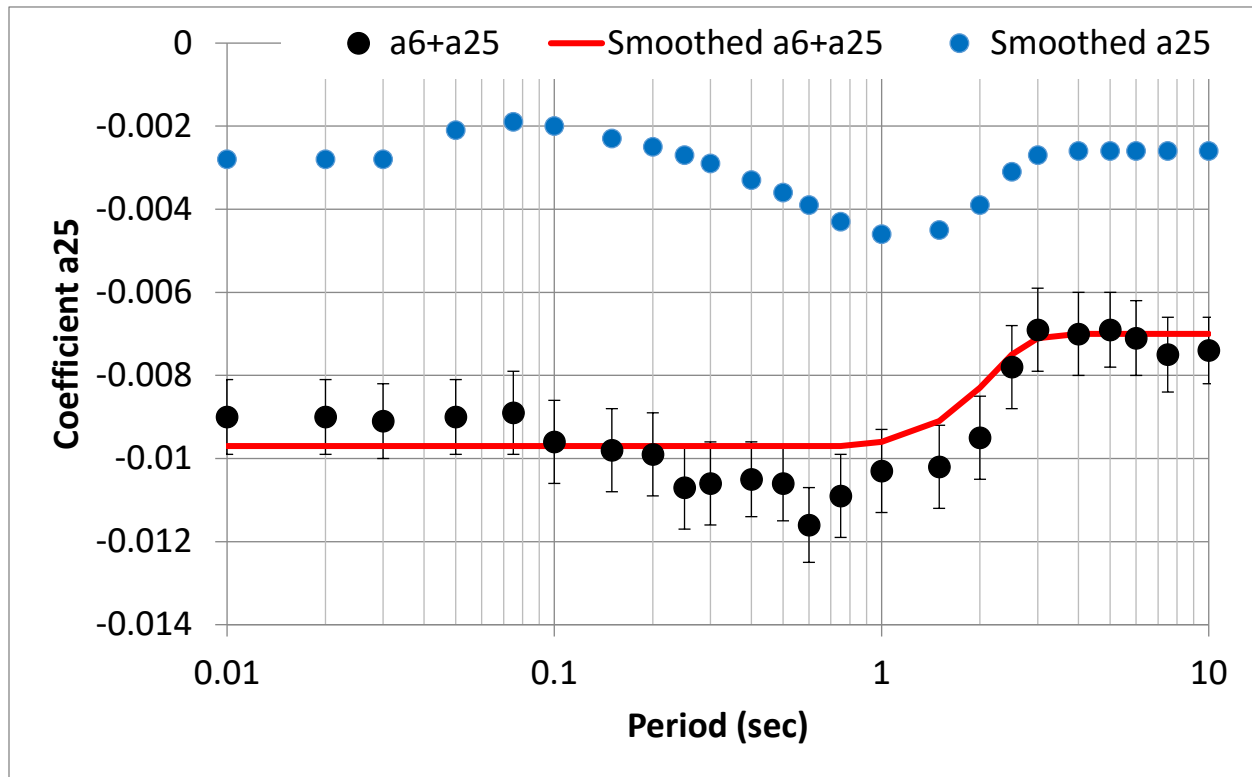


Figure 3.6 Smoothing of coefficient a_{25} (Cascadia linear R scaling).

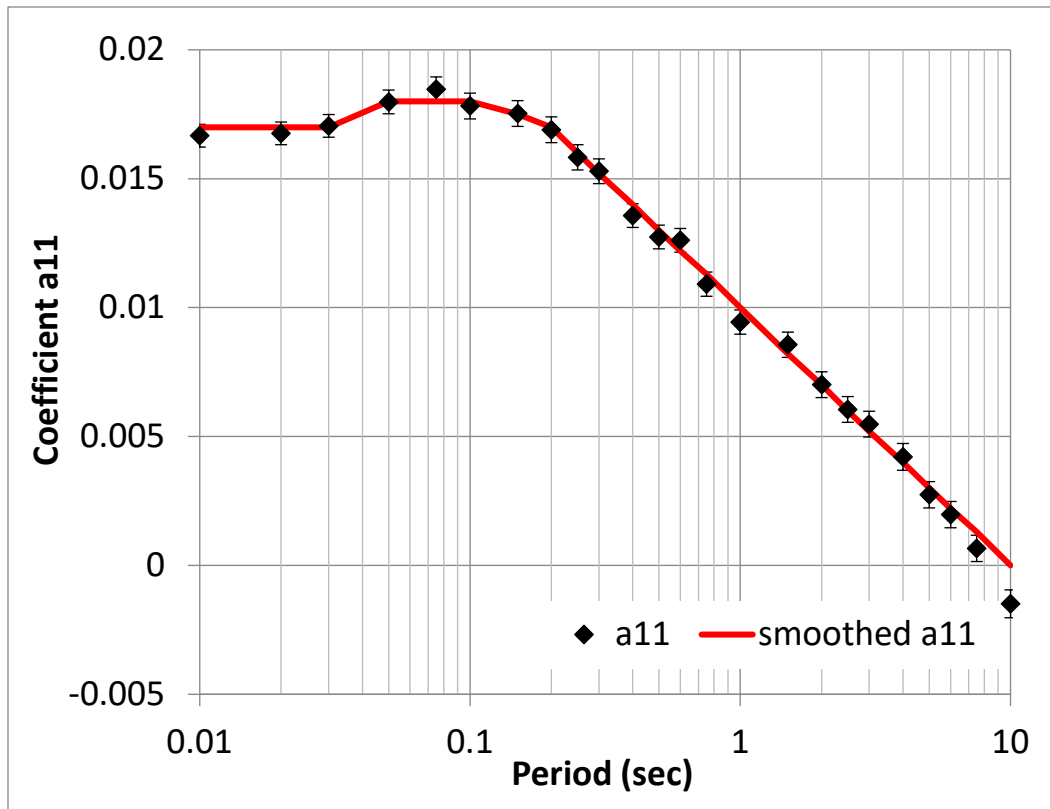


Figure 3.7 Smoothing of coefficient a_{11} (global Z_{TOR} scaling for intraslab).

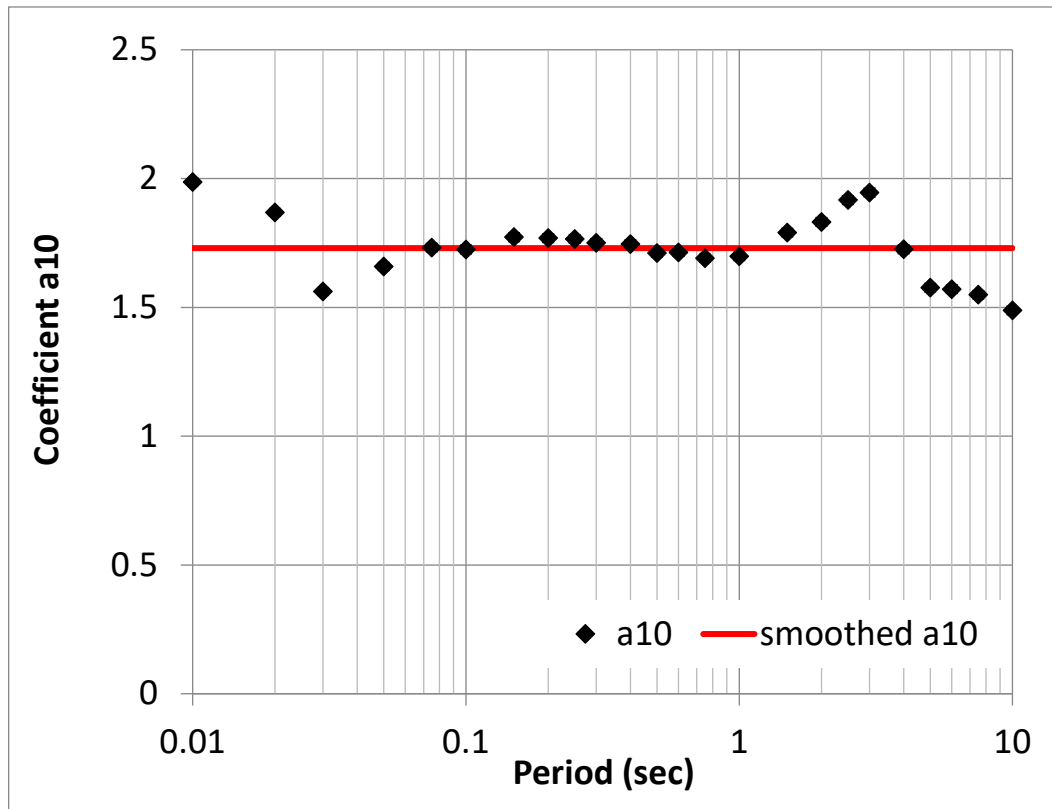


Figure 3.8 Smoothing of coefficient a_{10} (global intraslab constant term).

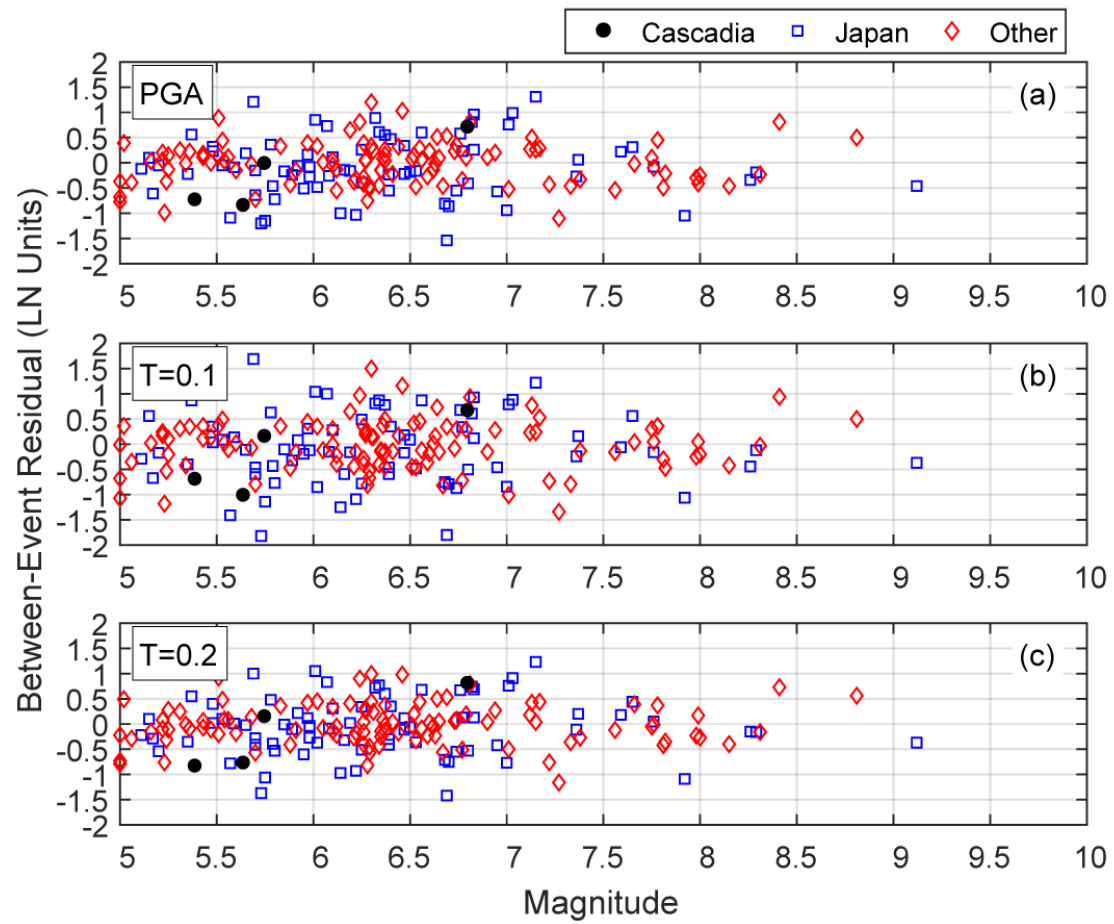


Figure 3.9 Between-event residuals: (a) PGA, (b) $T = 0.1$ sec, and (c) $T = 0.2$ sec.

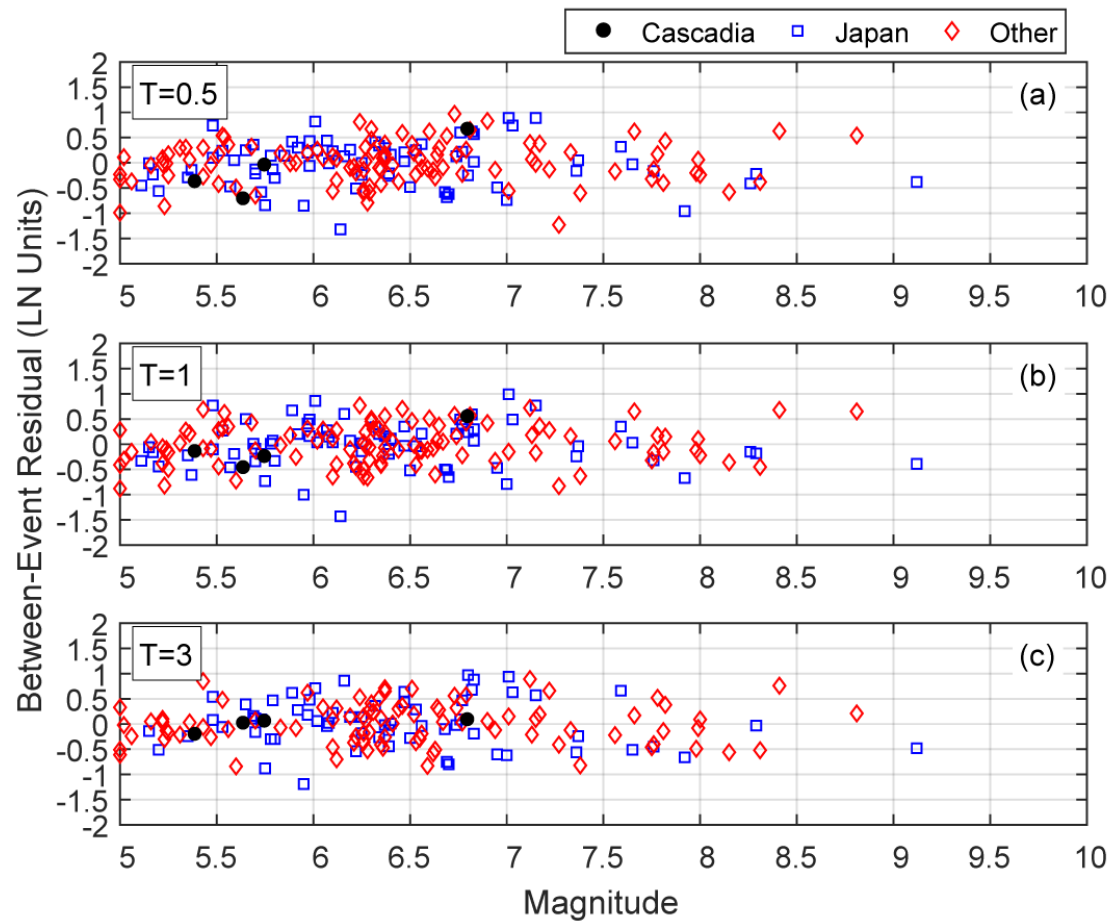


Figure 3.10 Between-event residuals: (a) $T = 0.5$ sec, (b) $T = 1$ sec, and (c) $T = 3$ sec.

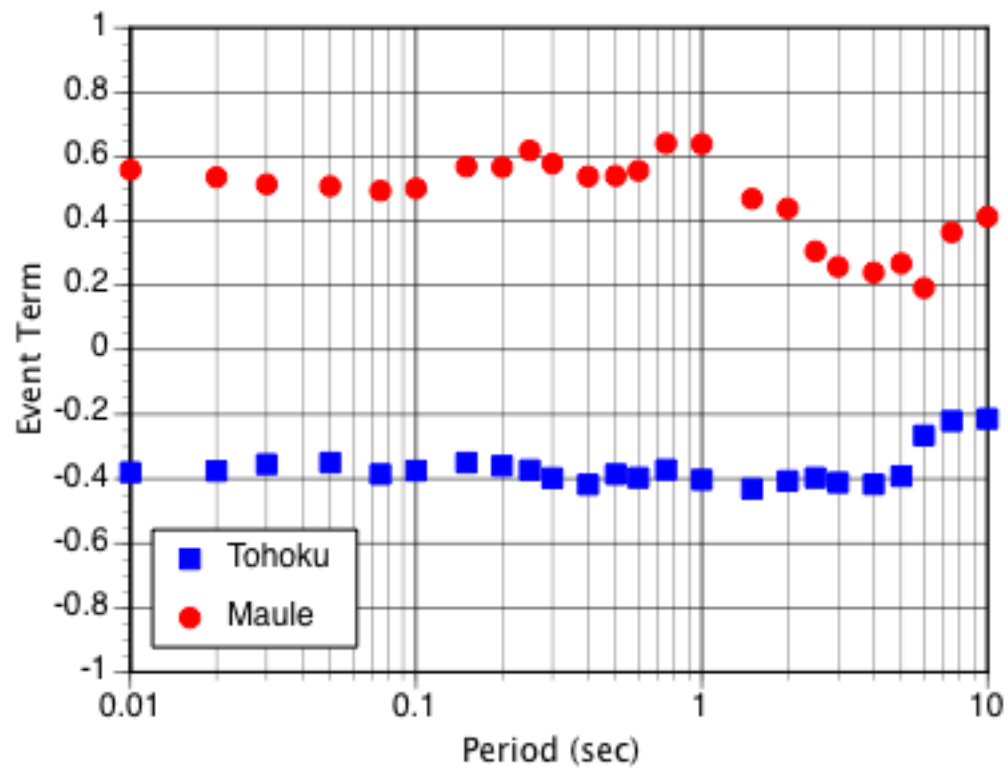


Figure 3.11 Between-event residuals for the largest events: Tohoku and Maule, Chile.

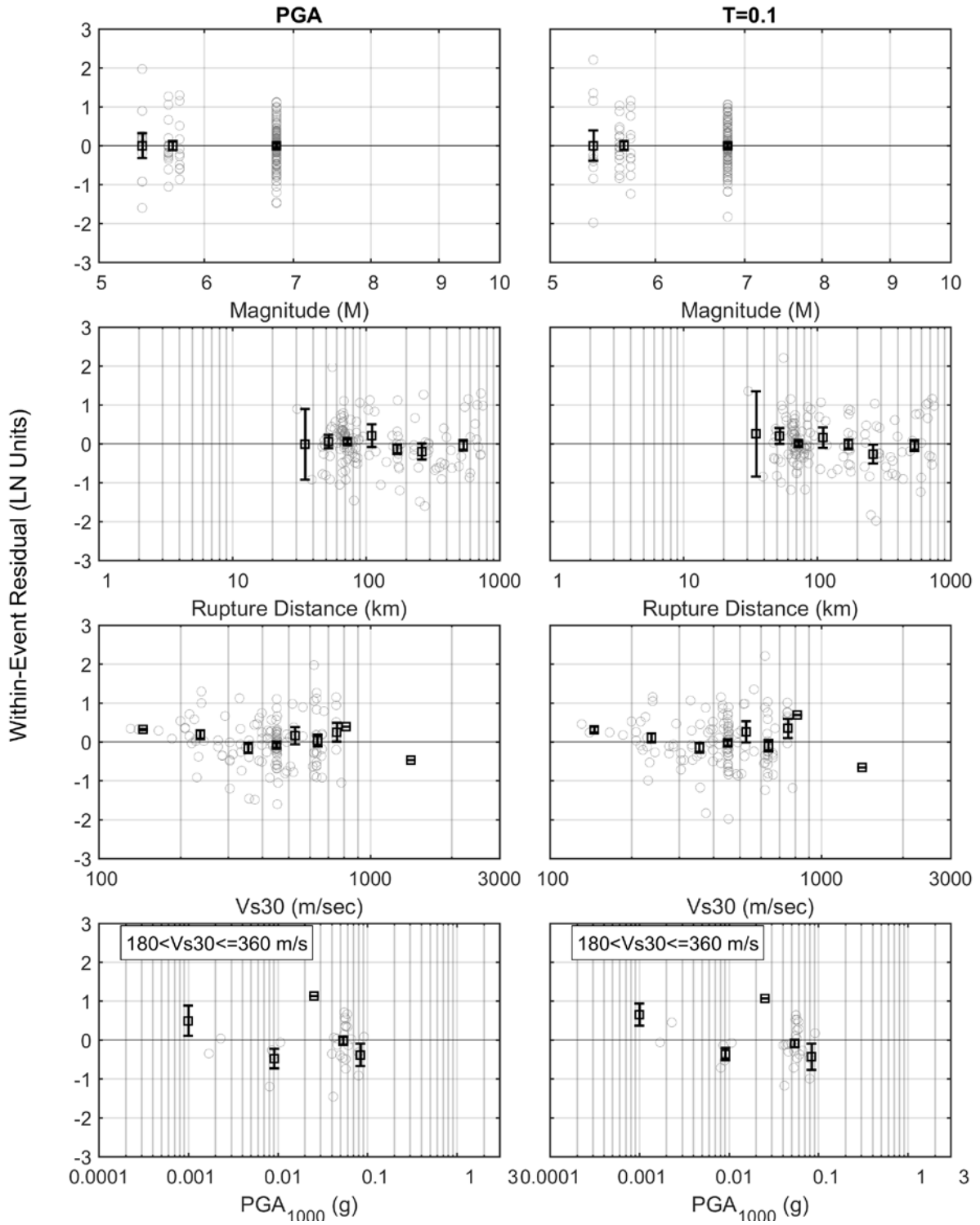


Figure 3.12(a) Within-event residuals for Cascadia: PGA and $T = 0.1$ sec.

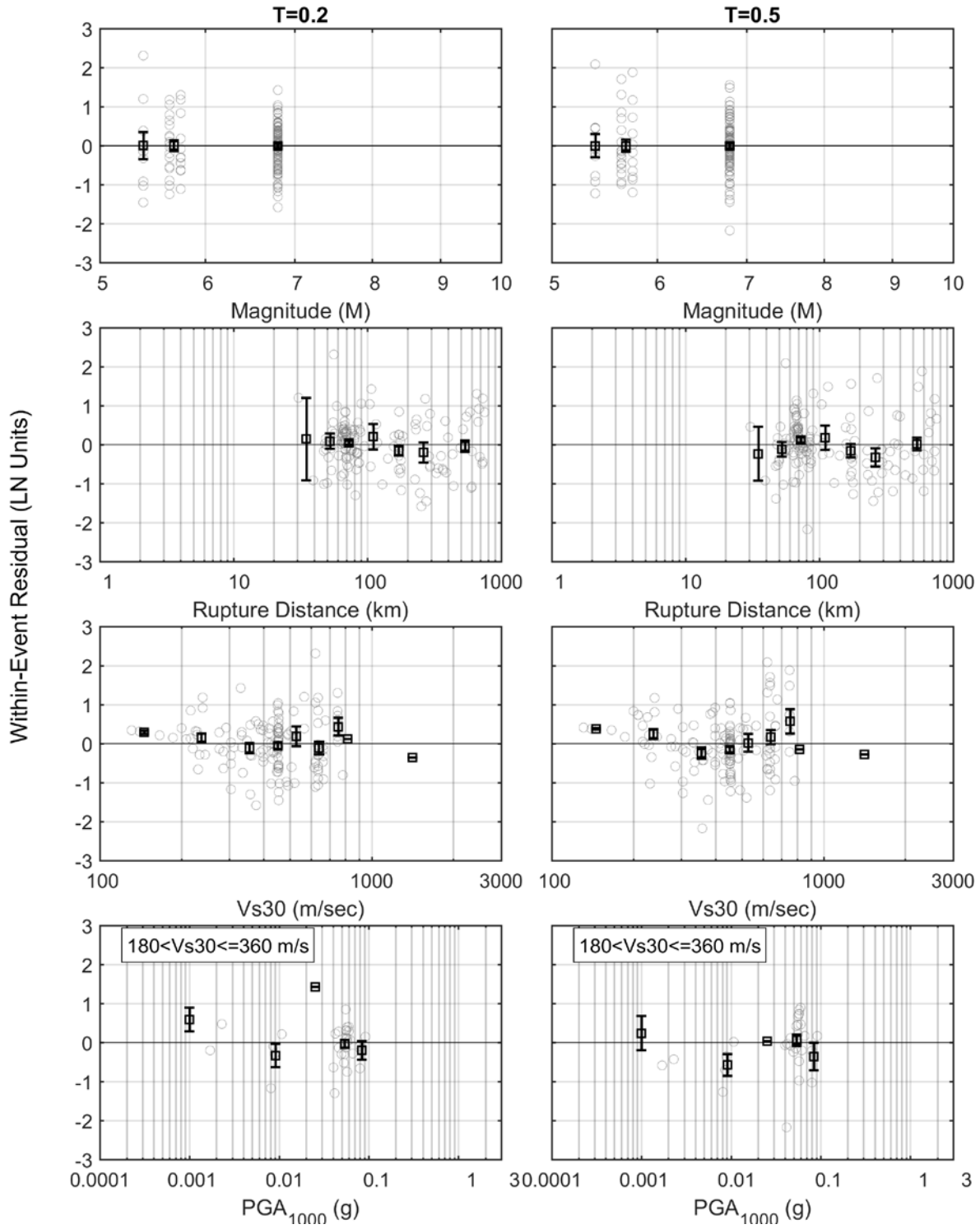


Figure 3.12(b) Within-event residuals for Cascadia: $T = 0.2$ sec and $T = 0.5$ sec.

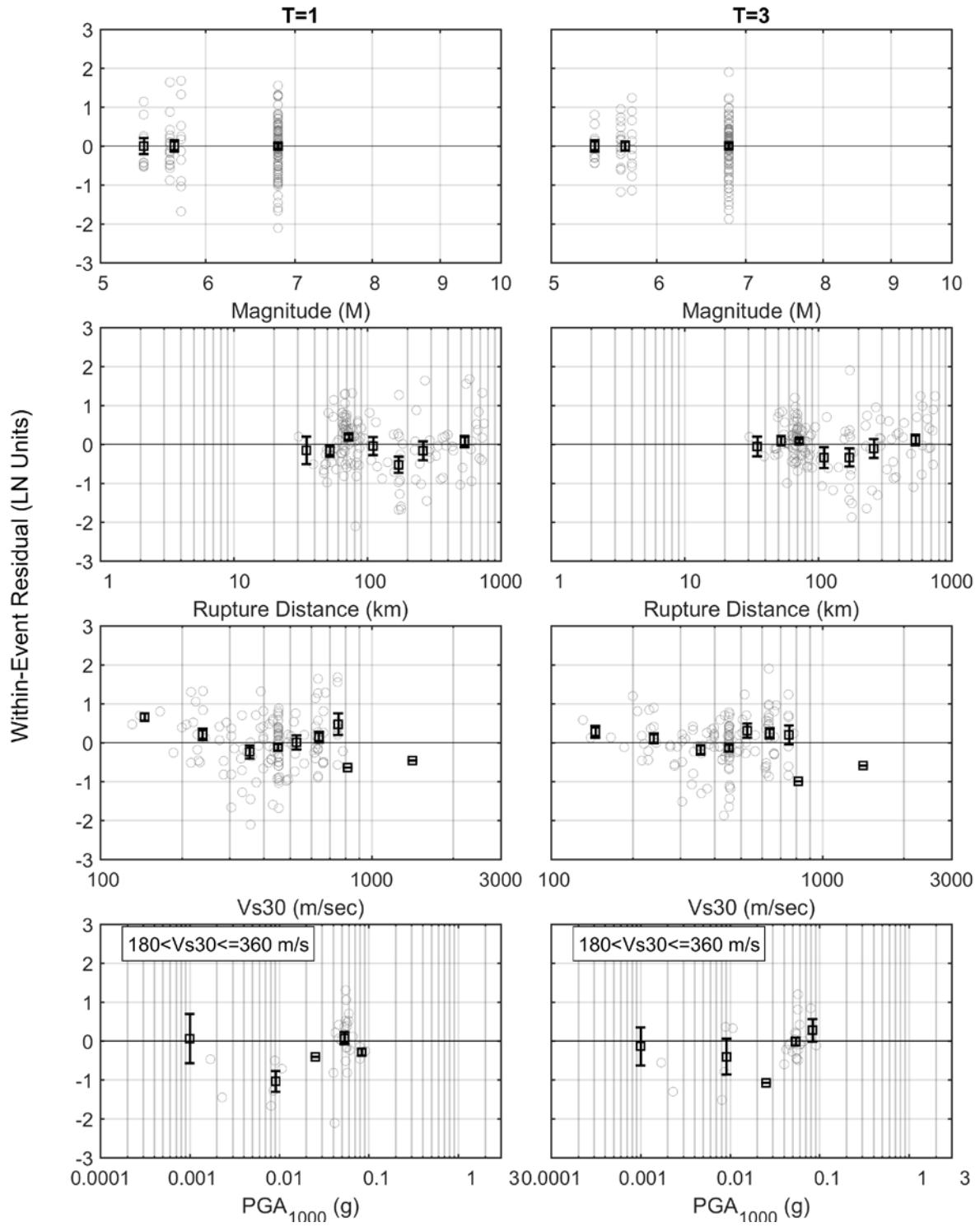


Figure 3.12(c) Within-event residuals for Cascadia: $T = 1$ sec and $T = 3$ sec.

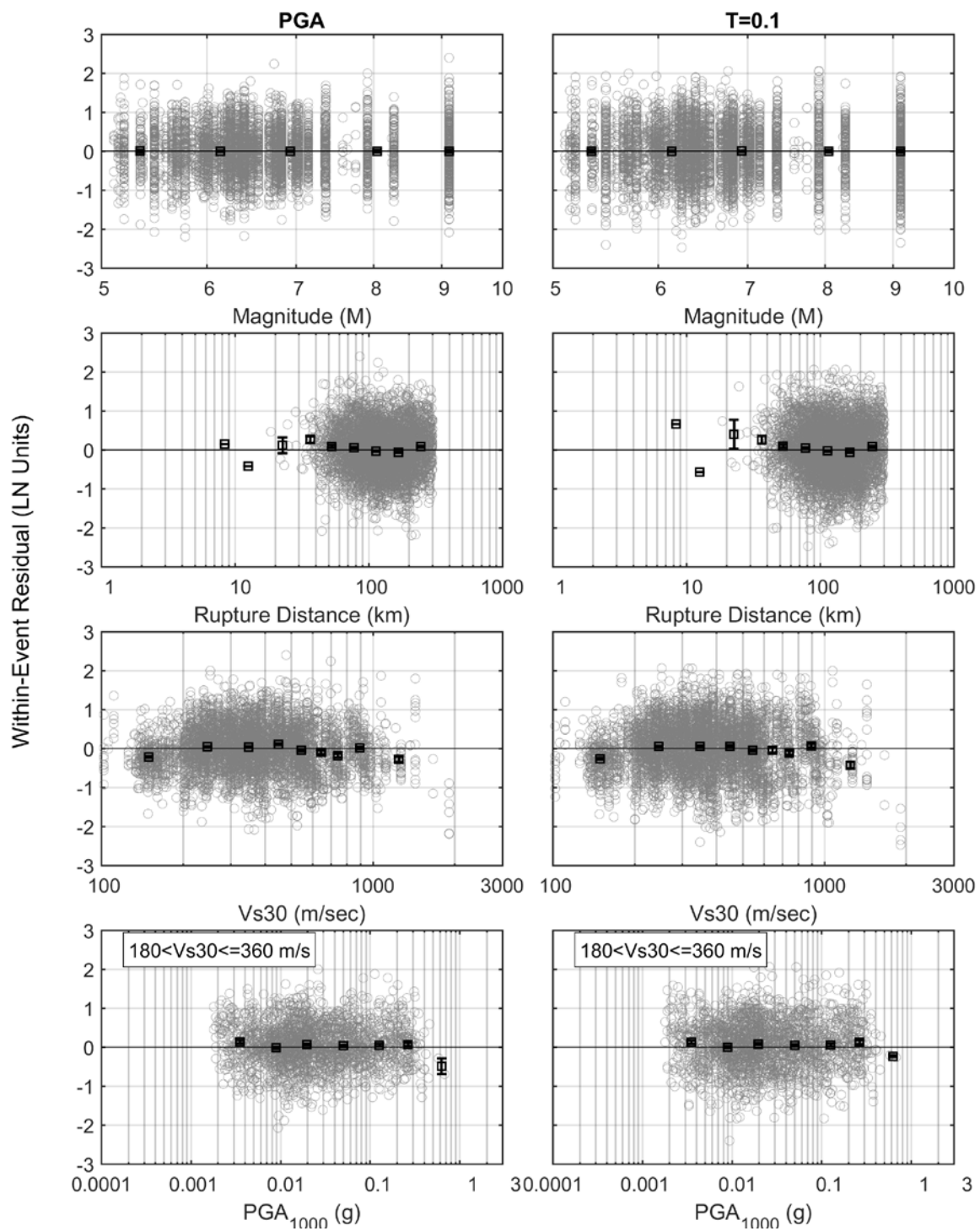


Figure 3.13(a) Within-event residuals for Japan: PGA and $T = 0.1$ sec.

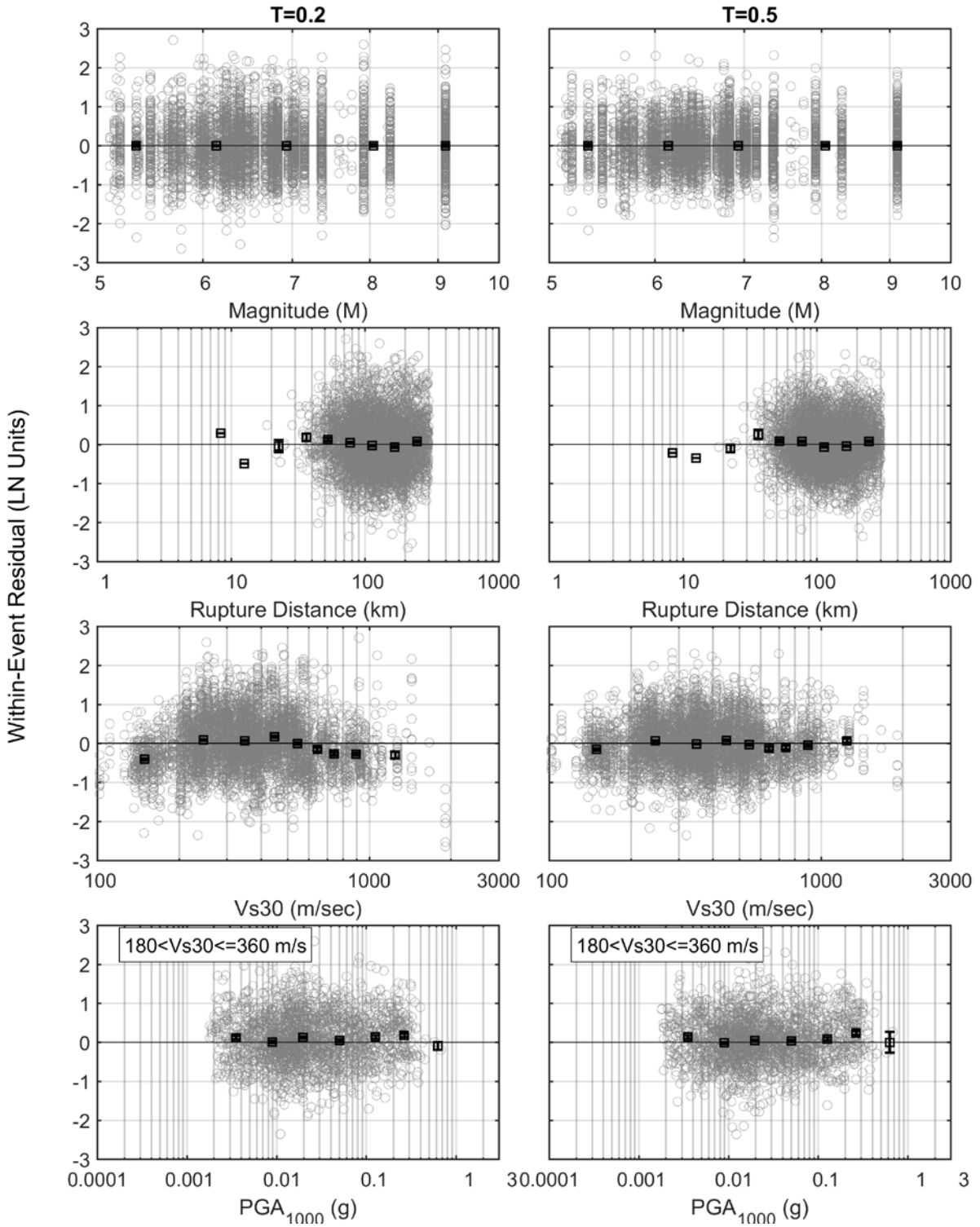


Figure 3.13(b) Within-event residuals for Japan: $T = 0.2$ sec and $T = 0.5$ sec.

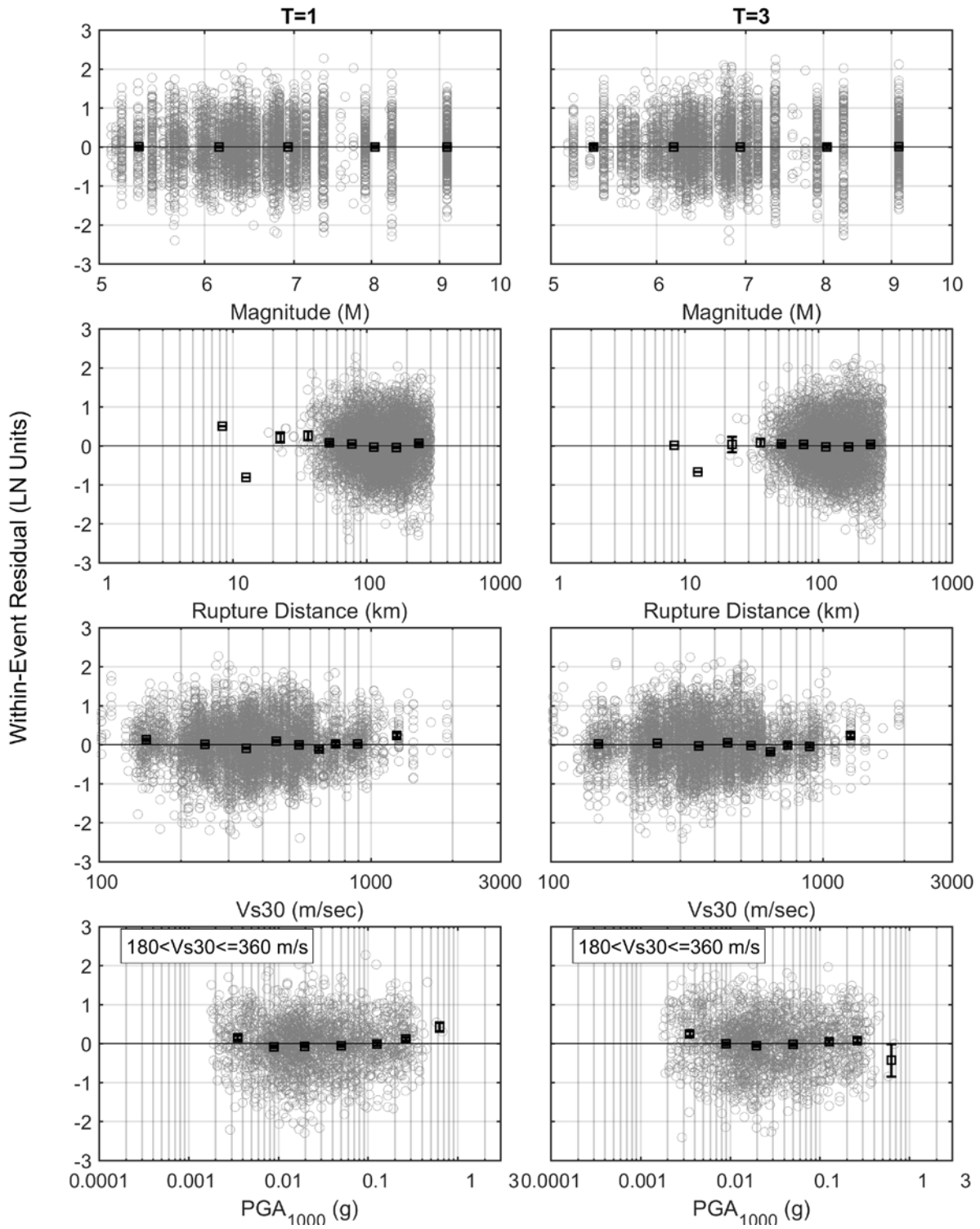


Figure 3.13(c) Within-event residuals for Japan: $T = 1$ sec and $T = 3$ sec.

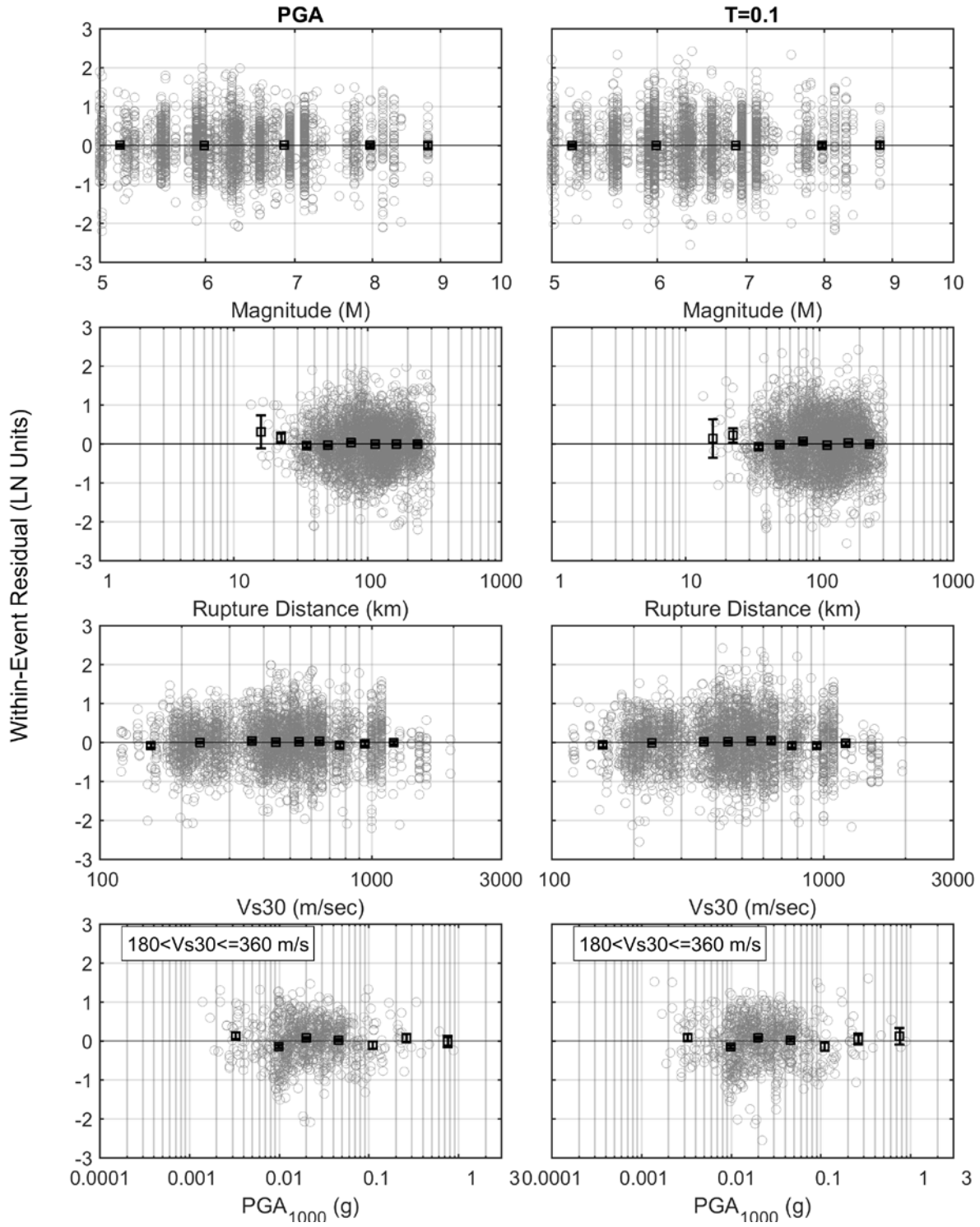


Figure 3.14(a) Within-event residuals for other regions: PGA and $T = 0.1$ sec.

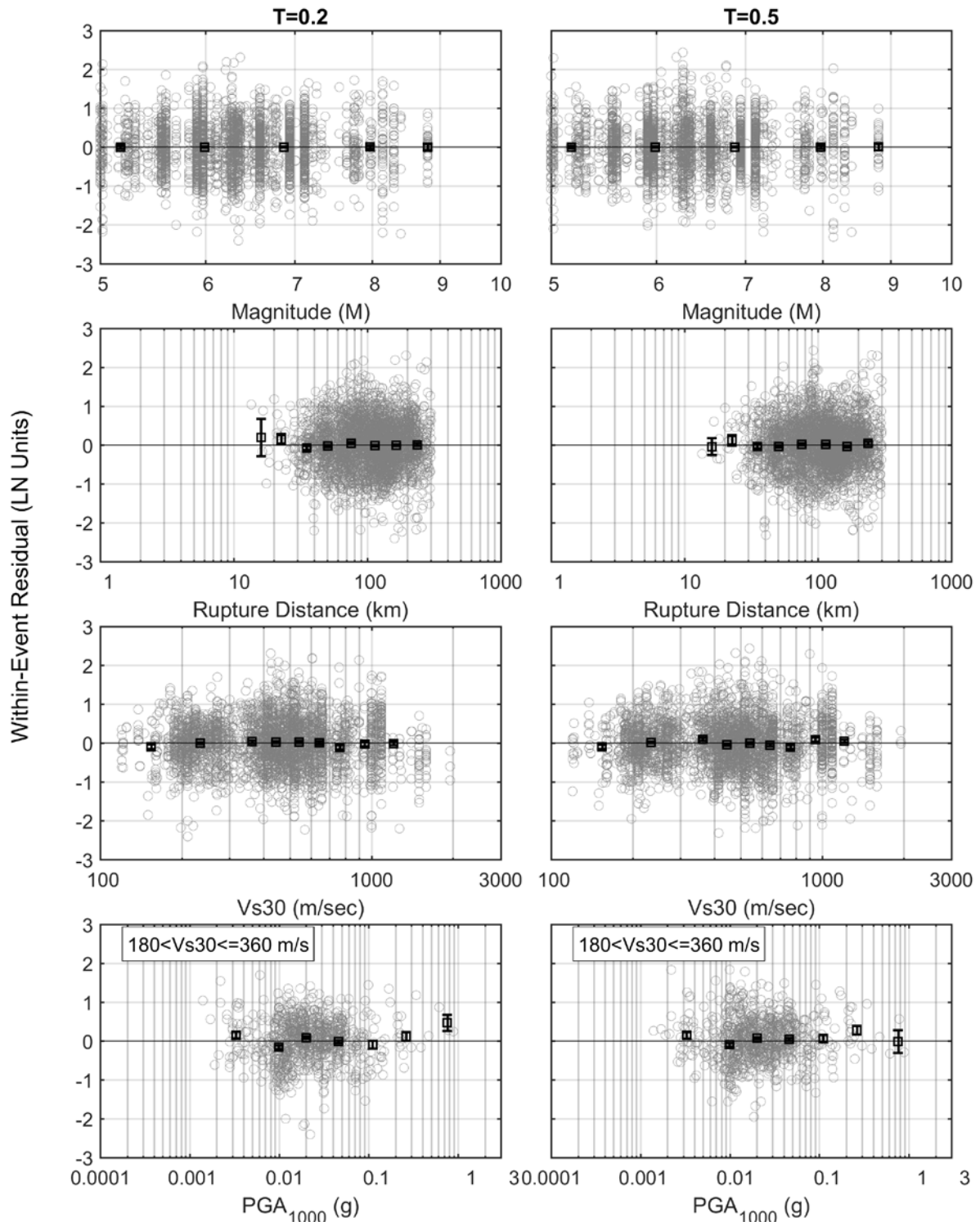


Figure 3.14(b) Within-event residuals for other regions: $T = 0.2$ sec and $T = 0.5$ sec.

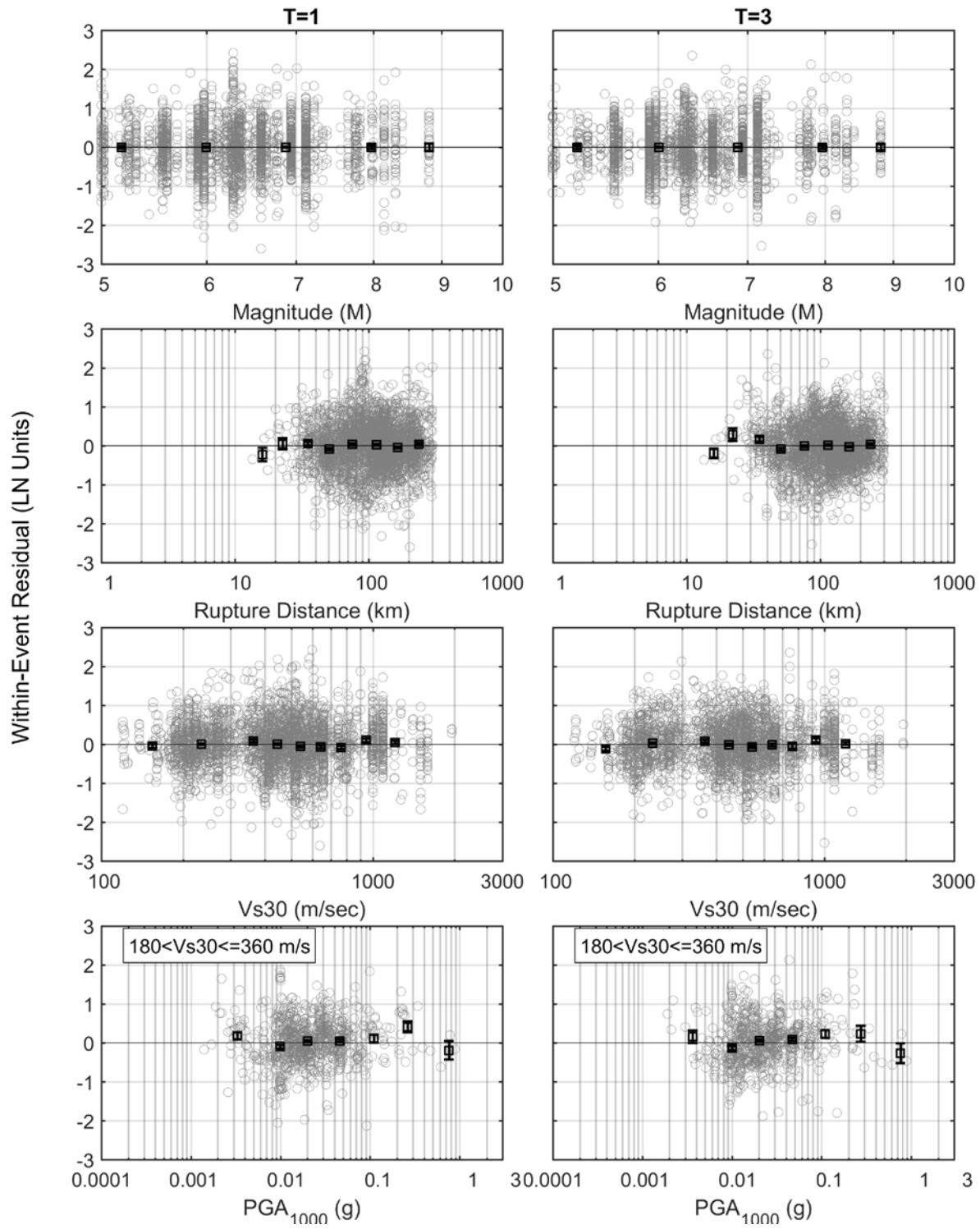


Figure 3.14(c) Within-event residuals for other regions: $T = 1$ sec and $T = 3$ sec.

3.4 REGIONAL DIFFERENCES

There are three terms that are allowed to vary regionally: the linear $\ln(V_{S30})$ scaling ($a_{12}+bn$), the linear R term (a_6), and the constant term.

The regional V_{S30} scaling coefficients are compared in Figure 3.15. For the linear V_{S30} scaling, the Central America region does not have an adequate range of V_{S30} to constrain the linear V_{S30} scaling, so it is fixed at the global model value. Overall, four of the five regions have similar trends in the V_{S30} scaling. The exception is the South America region which shows much weaker scaling for the long spectral periods. The V_{S30} scaling for the Cascadia region is similar to the global model for periods greater than 0.1 sec and has stronger scaling for periods less than 0.1 sec.

The regional linear R scaling coefficients are compared in Figure 3.16. Four of the six regions have similar trends in the linear R scaling. The Taiwan region shows almost no need for a linear R term. This is related to the limited distance range in the Taiwan data, due in part to the dimension of the Taiwan. The Central America region shows highly variability in the linear R scaling, indicating that this term is not well constrained. The linear R scaling for Cascadia shows stronger attenuation than the global average at periods between 0.1 and 3 seconds. This results in a rapid decay in the Cascadia ground motions at large distances.

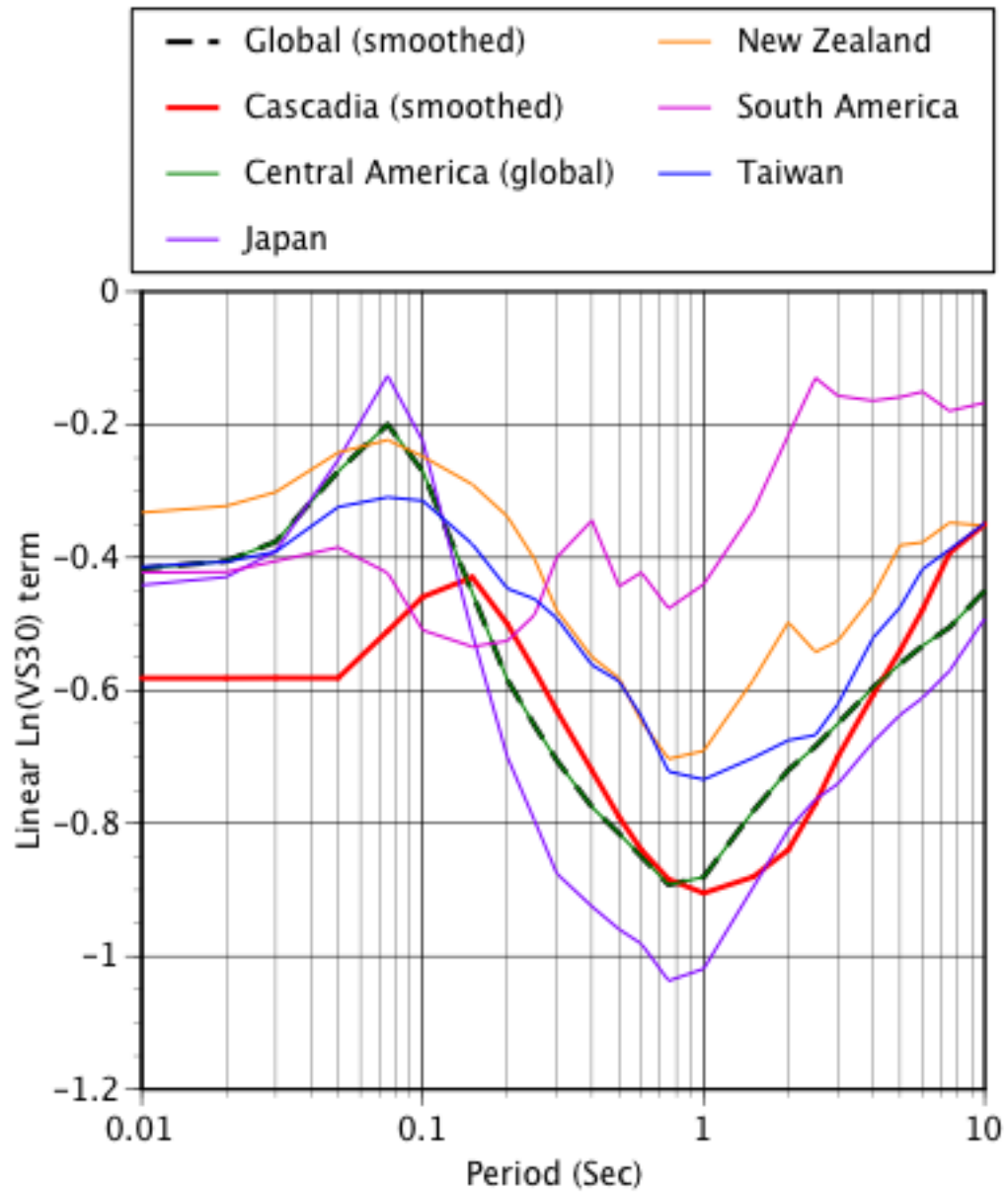


Figure 3.15 Regional differences in the linear VS30 term (a_{12}).

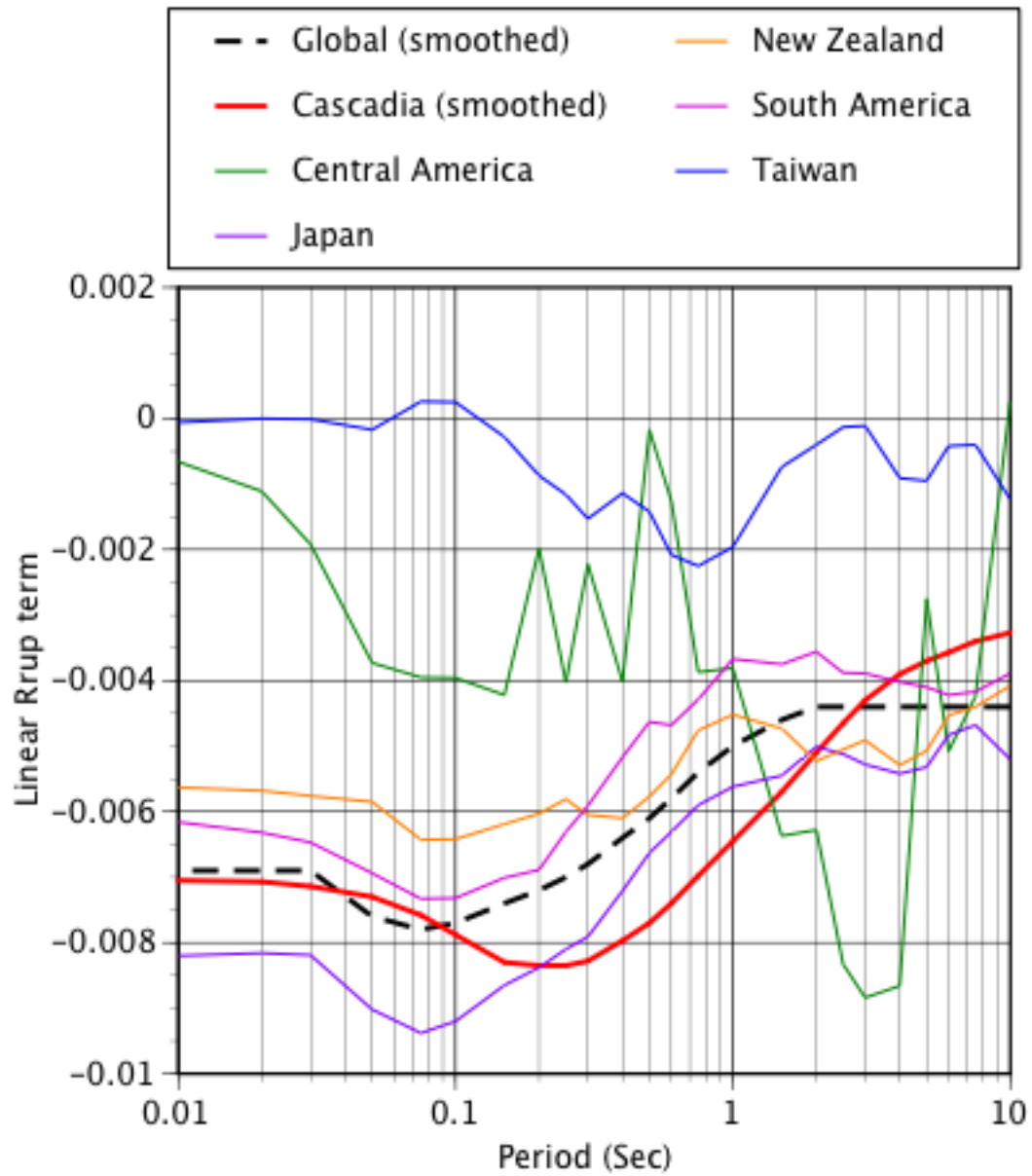


Figure 3.16 Regional differences in the linear R term (a_6).

4 Model Results

4.1 ADJUSTING THE CASCADIA MODEL

There are only four earthquakes in the Cascadia region in the selected subset. Of these four events, three have very low ground motions at short periods, leading to a median that is 2–3 times smaller than for other regions. The Cascadia median spectrum for a **M**6.5 intraslab and interface earthquakes at a distance of 100 km is compared to the median spectra for other regions in Figures 4.1 and 4.2, respectively. Other Cascadia earthquakes with **M** < 5, which are not in the selected subset, also show very low short-period ground motions. Of the four earthquakes classified as the Cascadia region, two are from Washington and two are from northern California. The largest earthquake of the four is the **M**6.8 Nisqually event. The event terms from this earthquake are much higher than the other three Cascadia events; see Figure 3.9 and 3.10.

Without a sound physical basis for the large reduction in the short-period ground motions in Cascadia as compared to other regions, and the observation that the short-period Nisqually ground-motion amplitudes are similar to other regions, the NGA-SUB developers judged that the reduction in the short-period ground motions for the small earthquakes in Cascadia should not be incorporated into the updated BCHydro ground-motion model. Therefore, the Cascadia model is adjusted so that the ground-motions for an earthquake scenario near the center of the data (**M**6.5, $R = 100$ km, $V_{S30} = 400$ m/sec) are consistent with the average over all regions.

The median ground motion for the average scenario is computed for each region using the region-specific terms. The log ratio of the median for each region to the median for Cascadia is shown in Figure 4.3 for intraslab events and in Figure 4.4 for interface events. For the intraslab events, the median is computed for all six regions, and the adjustment is based on the average term over the six regions. That is: the low Cascadia ground motions are included in the average region term for the intraslab. For the interface events, the adjustment is based on the average term over only four regions: Central America, Japan, New Zealand, and Japan. There is not enough data from Cascadia or Taiwan to constrain an interface model; therefore, they are not included in the regional average. The adjustments to the Cascadia constant term are shown in Figure 4.5. The adjustment terms are smoothed based spectral shape using all of the terms. In particular, the sum of the regional Cascadia constant term and the adjustment terms. The resulting smoothed adjustment term (keeping the Cascadia constant terms unsmoothed) are shown in Figure 4.5.

The adjusted Cascadia intraslab model is compared to the median from Nisqually data in Figure 4.6. The Nisqually data are adjusted to a V_{S30} of 400 m/sec using the V_{S30} scaling for Cascadia, and the median of the data in distance range of 70 to 120 km is shown. The adjusted Cascadia intraslab model is shown along with the 16th and 84th percentile range from the standard

deviation of the event terms. This figure shows that the average from the Nisqually data are not inconsistent with the adjusted Cascadia model. In addition, the final regression step was repeated including the data from the M6.7 1949 Olympia and M6.6 1965 Seattle earthquakes which had only two recordings for each event. Although the event terms are not well constrained, they are similar to the event terms for the Nisqually earthquake and do not show the very low short-period ground motions observed for other Cascadia earthquakes.

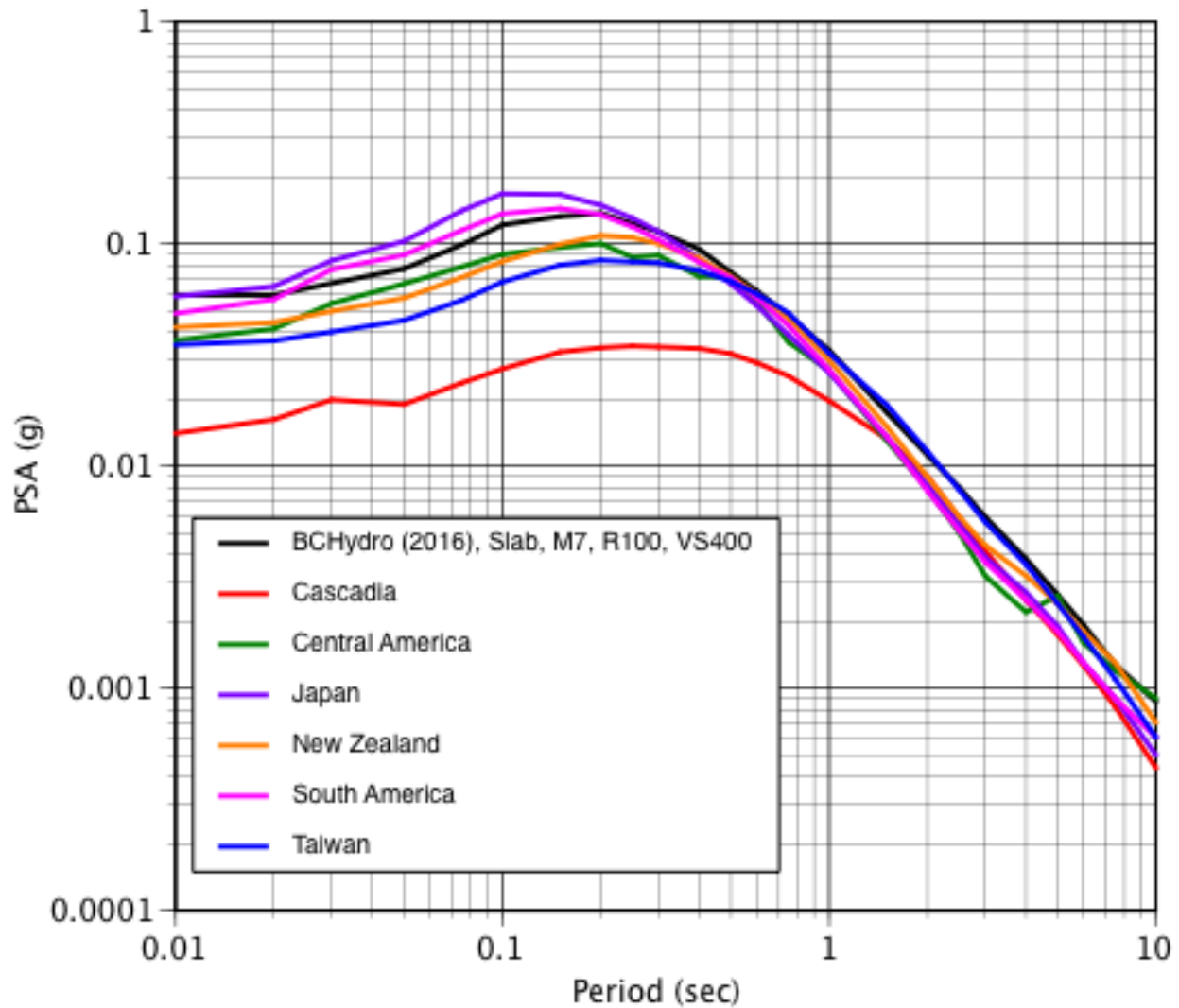


Figure 4.1 Median spectra for different regions for intraslab, M7, $Z_{TOR} = 50$ km, $R_{rup} = 100$ km, and $V_{S30} = 400$ m/sec.

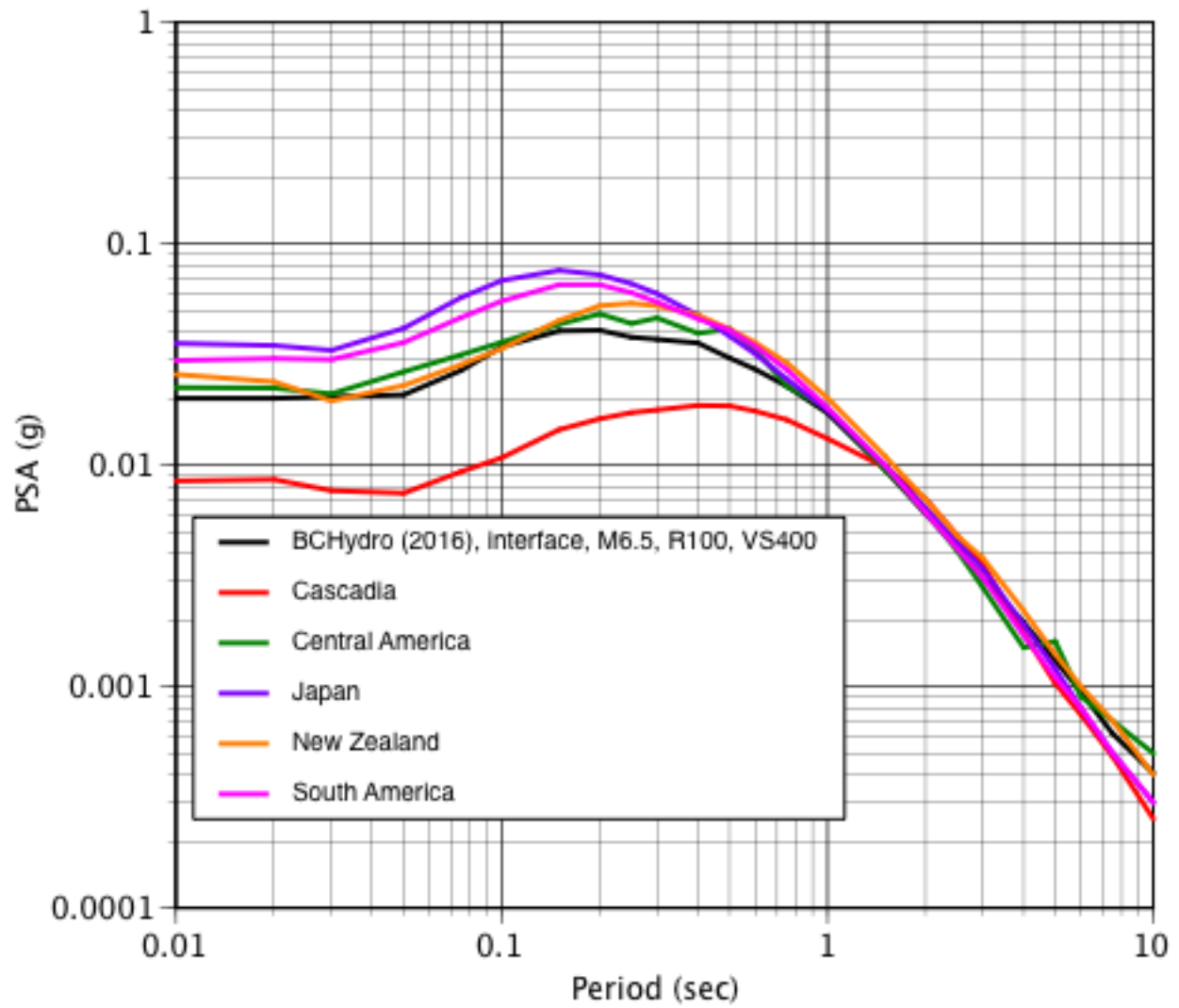


Figure 4.2 Median spectra for different regions for interface, M7, $Z_{TOR} = 20$ km, $R_{rup} = 100$ km, and $V_{S30} = 400$ m/sec.

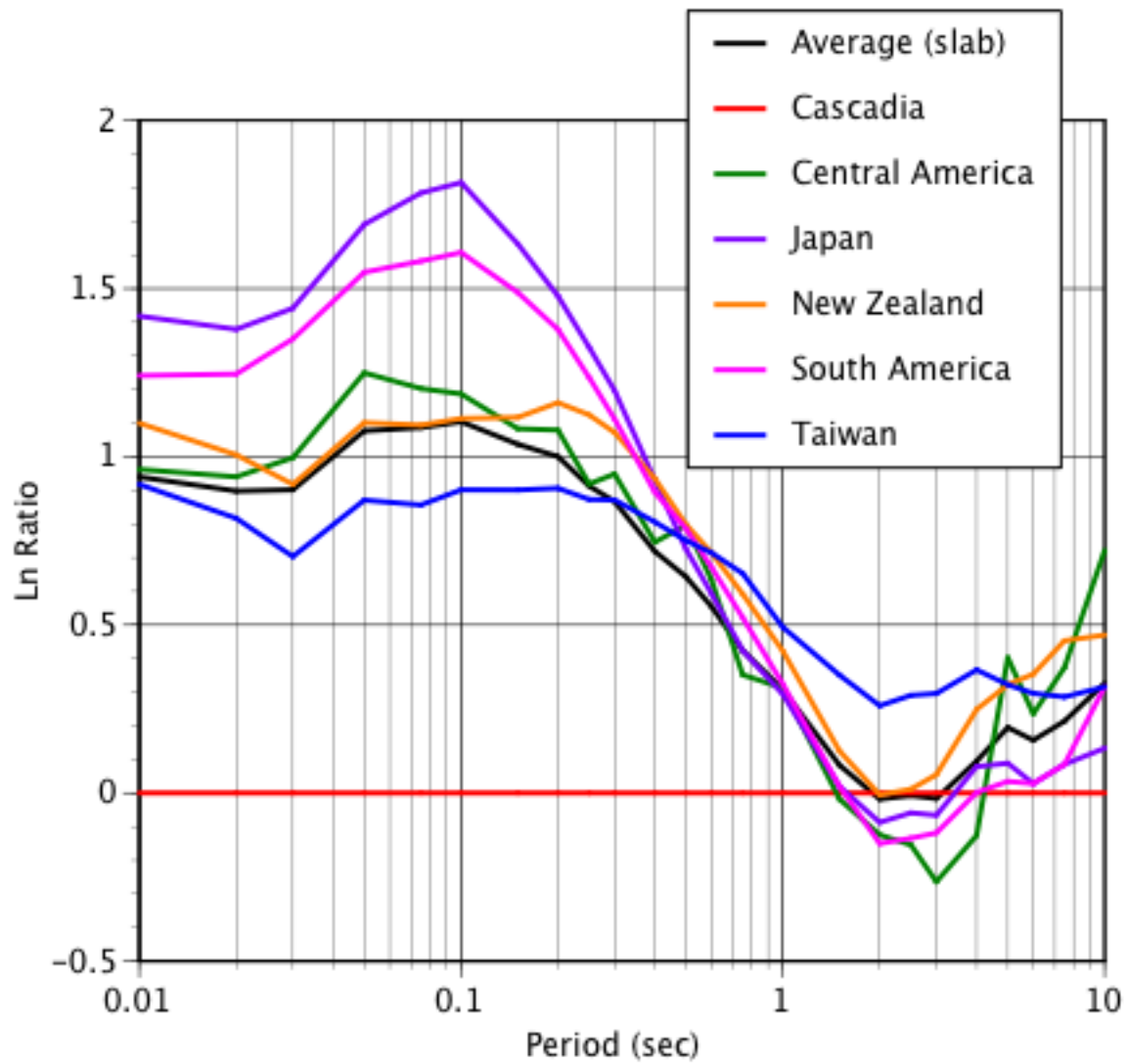


Figure 4.3 Adjustment to the constant term for Cascadia for intraslab earthquakes.

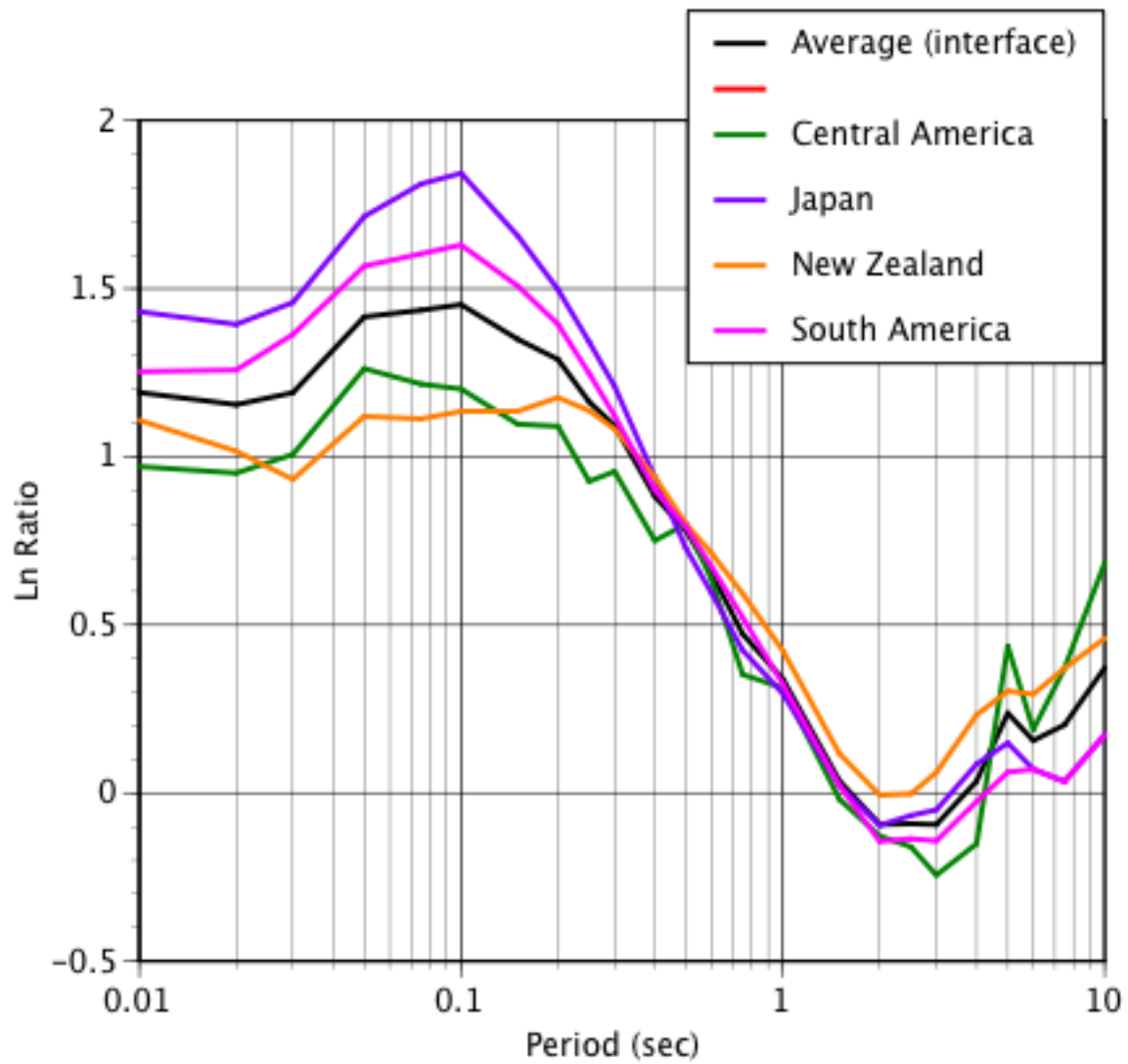


Figure 4.4 Adjustment to the constant term for Cascadia for interface earthquakes.

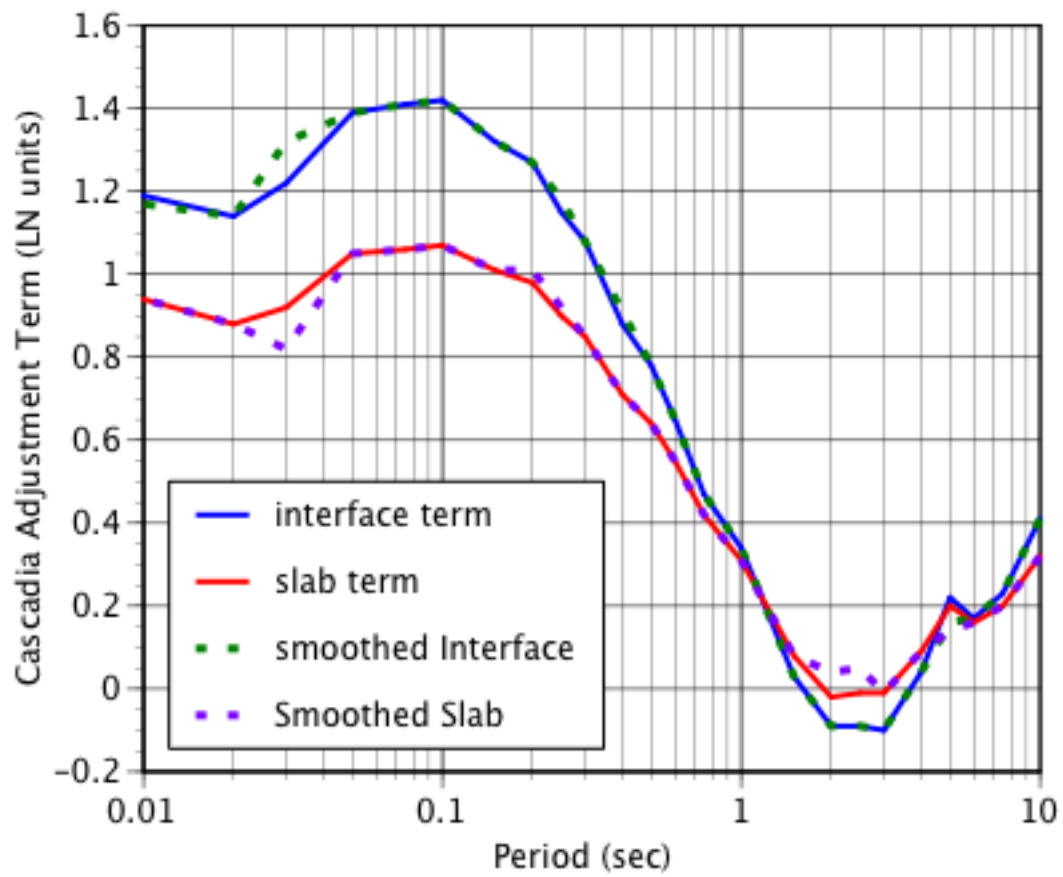


Figure 4.5 Smoothed adjustment for the constant term for Cascadia.

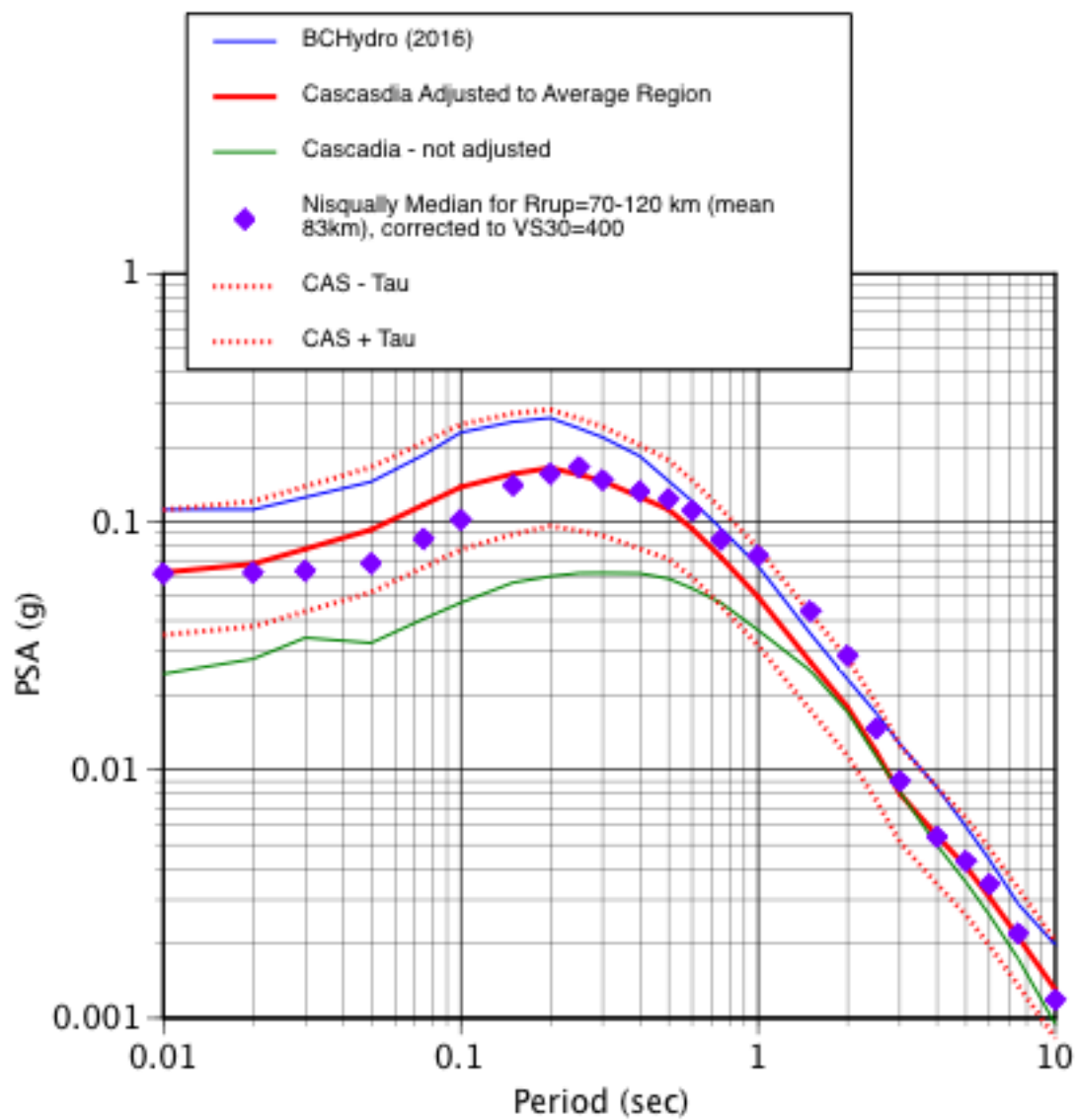


Figure 4.6 Comparison of adjusted Cascadia median for M6.8, $V_{S30} = 400$ m/sec, $R_{rup} = 83$ km.

4.2 MODEL COEFFICIENTS

The model coefficients for the adjusted Cascadia ground-motion model are listed in Tables 4.1, 4.2, and 4.3. Examples of the magnitude, distance, and ZTOR scaling of the median spectral values are shown in Figures 4.7 to 4.9. Figure 4.7 shows the spectra for M5 to M9 or a rupture distance of 80 km and a V_{S30} of 760 m/s. Figure 4.8 shows the spectra for distances of 50 to 1000 km an M9 interface earthquake and for a V_{S30} of 760 m/s. The dips in the short-period spectra ($T < 0.4$ sec) at a distance of 1000 km reflects the difficulties of applying a simple parametric form to a wide range of magnitudes and distances. Figure 4.9 shows the spectra for Z_{TOR} values of 30 to 100 km. For $Z_{TOR} > 100$ km, there is a cap on the scaling.

Table 4.1 Period-independent coefficients.

Coefficient	Period-independent values
n	1.18
c	1.88
C_4	10 km
a_3	-0.10
a_5	0.0
a_9	0.40
a_{10}	1.73

Table 4.2 Period-dependent coefficients for the Cascadia model.

Period (sec)	a_1	a_2	a_4	a_6	a_{11}	a_{12}	a_{13}	a_{14}
0.01	2.340	-1.044	0.59	-0.00705	0.0170	0.818	-0.0135	-0.223
0.02	2.360	-1.044	0.59	-0.00707	0.0170	0.857	-0.0135	-0.196
0.03	2.384	-1.080	0.59	-0.00710	0.0170	0.921	-0.0135	-0.128
0.05	2.446	-1.110	0.59	-0.00725	0.0180	1.007	-0.0138	-0.130
0.075	2.751	-1.110	0.59	-0.00758	0.0180	1.225	-0.0142	-0.130
0.10	3.019	-1.110	0.59	-0.00788	0.0180	1.457	-0.0145	-0.130
0.15	3.349	-1.084	0.59	-0.00820	0.0175	1.849	-0.0153	-0.156
0.20	3.284	-1.027	0.62	-0.00835	0.0170	2.082	-0.0162	-0.172
0.25	3.211	-0.983	0.64	-0.00835	0.0160	2.240	-0.0172	-0.184
0.30	3.145	-0.947	0.66	-0.00828	0.0152	2.341	-0.0183	-0.194
0.40	2.997	-0.890	0.68	-0.00797	0.0140	2.415	-0.0206	-0.210
0.50	2.839	-0.845	0.68	-0.00770	0.0130	2.359	-0.0231	-0.223
0.60	2.658	-0.809	0.68	-0.00740	0.0122	2.227	-0.0256	-0.233
0.75	2.346	-0.760	0.68	-0.00698	0.0113	1.949	-0.0296	-0.245
1.0	1.851	-0.698	0.68	-0.00645	0.0100	1.402	-0.0363	-0.261
1.5	1.216	-0.612	0.68	-0.00570	0.0082	0.329	-0.0493	-0.285
2.0	0.649	-0.550	0.68	-0.00510	0.0070	-0.487	-0.061	-0.301
2.5	0.082	-0.501	0.68	-0.00465	0.0060	-0.770	-0.0711	-0.313
3.0	-0.369	-0.460	0.68	-0.00430	0.0052	-0.700	-0.0798	-0.323
4.0	-1.034	-0.455	0.68	-0.00390	0.0040	-0.607	-0.0935	-0.282
5.0	-1.520	-0.450	0.73	-0.00370	0.0030	-0.540	-0.098	-0.250
6.0	-1.810	-0.450	0.78	-0.00357	0.0022	-0.479	-0.098	-0.250
7.5	-2.173	-0.450	0.84	-0.00340	0.0013	-0.393	-0.098	-0.250
10.0	-2.712	-0.450	0.93	-0.00327	0.0000	-0.350	-0.098	-0.250

Table 4.3 **Period-dependent coefficients for the Cascadia model (cont).**

Period (sec)	V_{lin}	b	C_{1_inter}	C_{1_slab}	Adjustment term for interface	Adjustment term for intraslab
0.01	865.1	-1.186	8.2	7.2	1.04	0.83
0.02	865.1	-1.219	8.2	7.2	1.05	0.79
0.03	907.8	-1.273	8.2	7.2	1.23	0.71
0.05	1053.5	-1.346	8.2	7.2	1.34	0.98
0.075	1085.7	-1.471	8.2	7.2	1.32	0.99
0.1	1032.5	-1.624	8.2	7.2	1.32	1.00
0.15	877.6	-1.931	8.2	7.2	1.21	0.92
0.2	748.2	-2.188	8.2	7.2	1.14	0.88
0.25	654.3	-2.381	8.2	7.2	1.05	0.81
0.3	587.1	-2.518	8.2	7.2	0.95	0.75
0.4	503	-2.657	8.2	7.2	0.79	0.62
0.5	456.6	-2.669	8.2	7.2	0.66	0.54
0.6	430.3	-2.599	8.2	7.2	0.54	0.46
0.75	410.5	-2.401	8.15	7.2	0.36	0.33
1.0	400	-1.955	8.1	7.2	0.24	0.23
1.5	400	-1.025	8.05	7.2	-0.08	-0.01
2.0	400	-0.299	8.0	7.2	-0.21	-0.09
2.5	400	0	7.95	7.2	-0.21	-0.05
3.0	400	0	7.9	7.2	-0.22	-0.02
4.0	400	0	7.85	7.2	-0.06	0.06
5.0	400	0	7.8	7.2	0.06	0.06
6.0	400	0	7.8	7.2	0.09	0.10
7.5	400	0	7.8	7.2	0.14	0.13
10.0	400	0	7.8	7.2	0.31	0.24

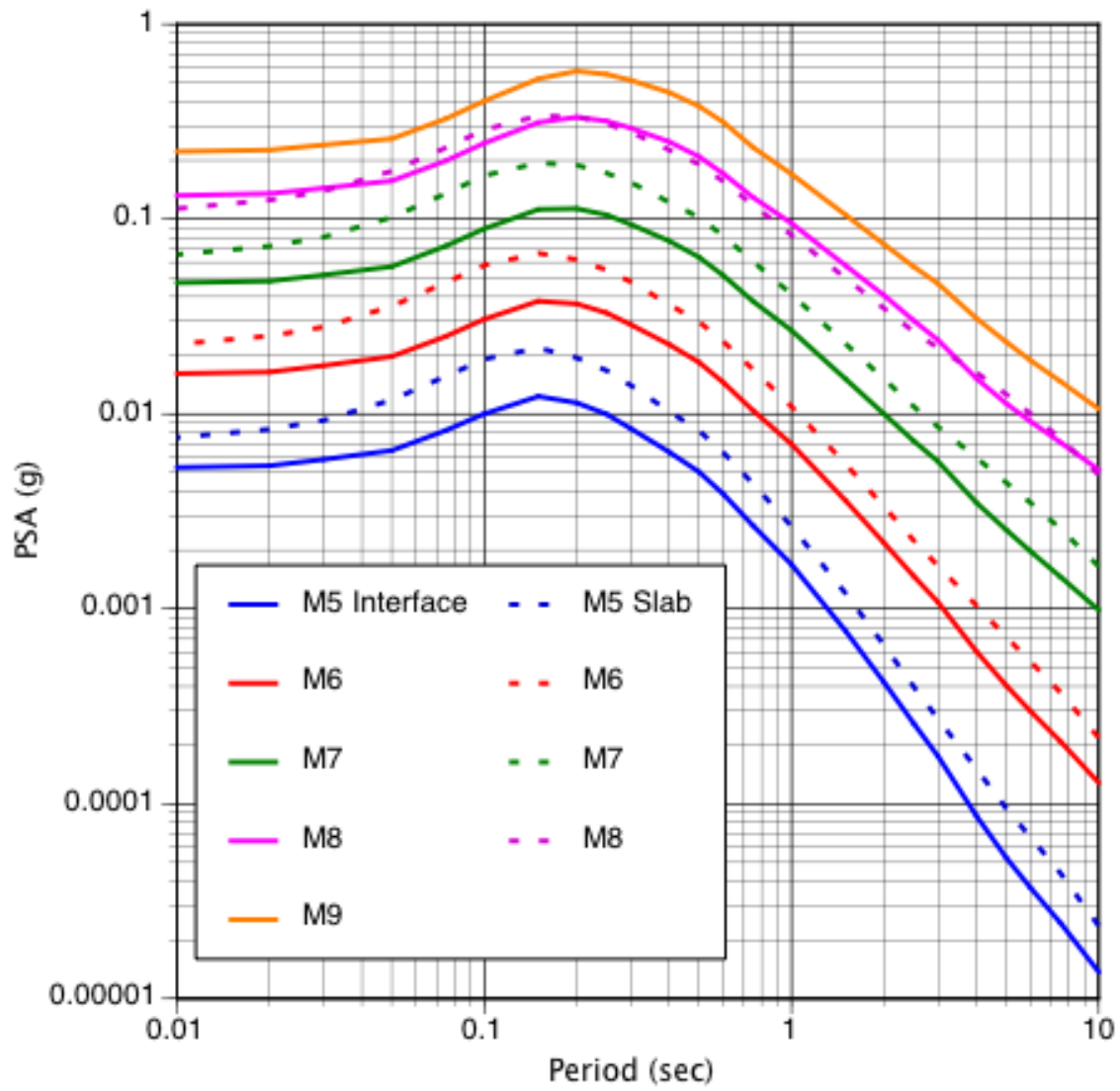


Figure 4.7 Magnitude scaling of spectra for Rrup=80 km and VS30=760 m/s.

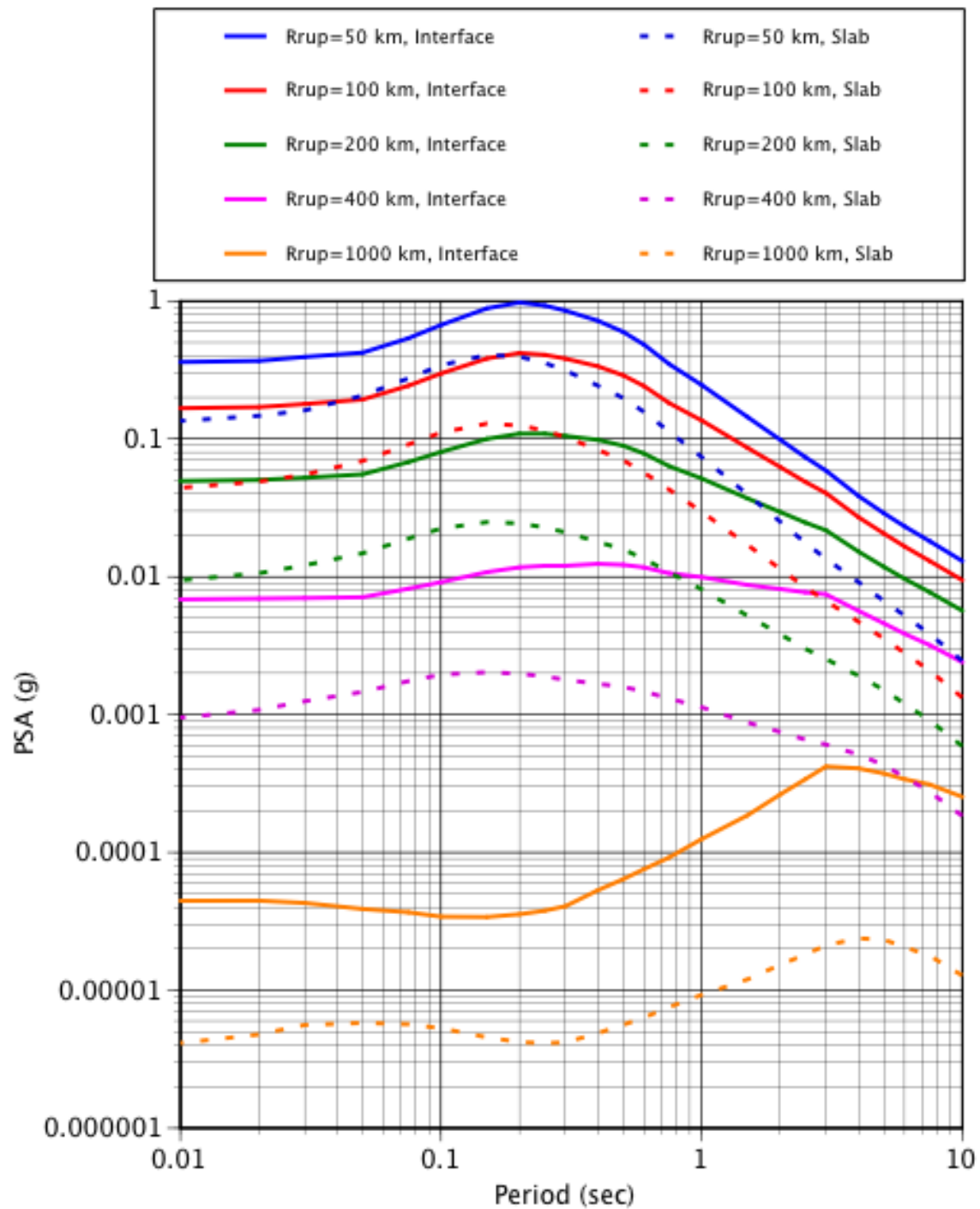


Figure 4.8 Distance scaling of spectra for M=9 interface earthquakes and VS30=760 m/s.

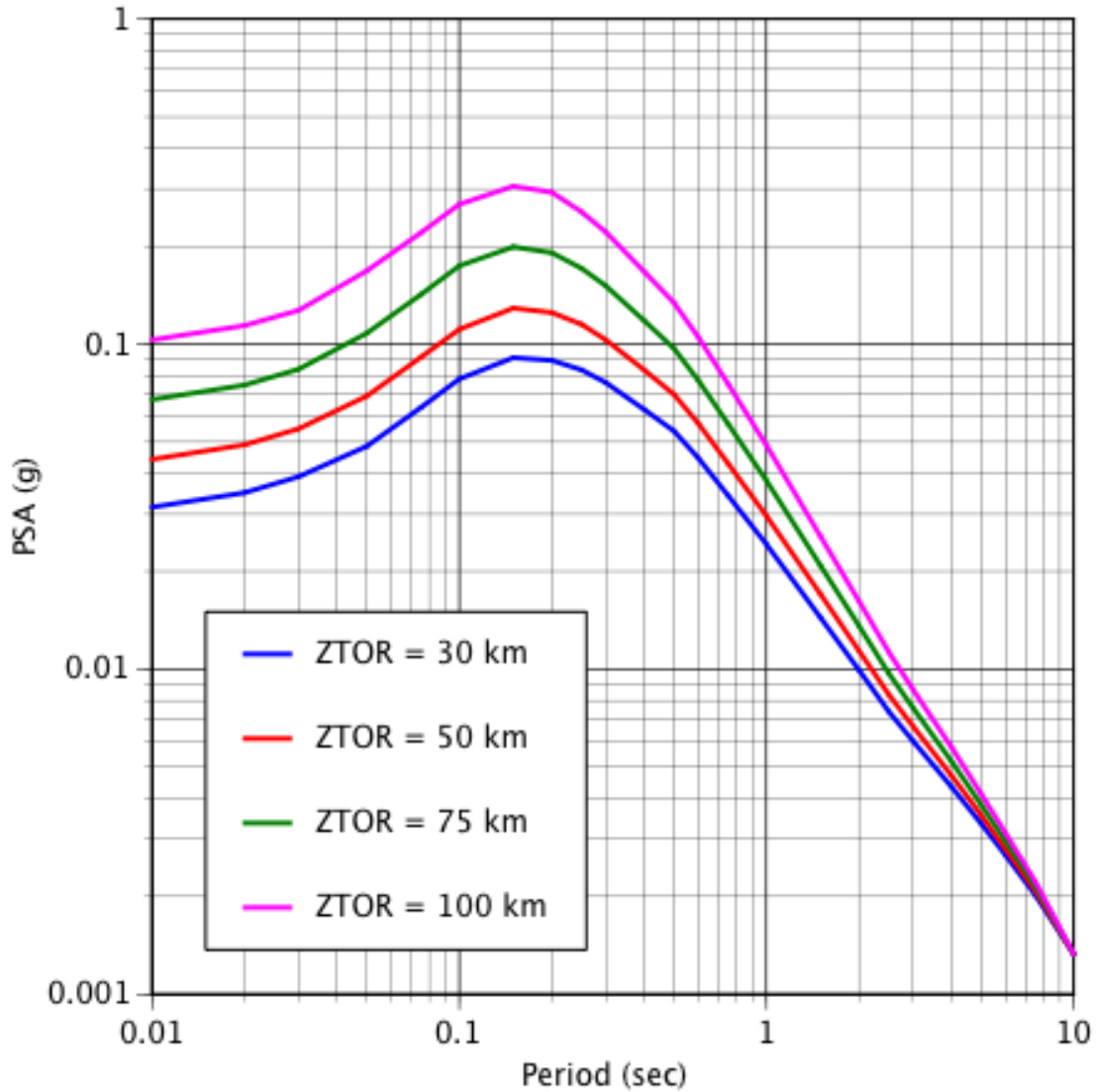


Figure 4.9 ZTOR scaling of spectra for M=7 intraslab events and VS30=760 m/s.

4.3 EPISTEMIC UNCERTAINTY

The epistemic uncertainty is modelled using the scaled backbone approach. The scale factor for the scaled backbone model is based on the range of average ground motions between the different regions. The range is shown in Figures 4.10 and 4.11 for intraslab events and interface events, respectively. The recommended high and low epistemic uncertainty range is shown by the heavy black lines in these figures. At short periods, the recommended epistemic uncertainty does not capture the lower range of the Cascadia events.

While a reduction in the epistemic uncertainty range for the interface at long periods could be justified by the range of the models shown in Figure 4.11, preliminary results using random effects for the constant scale factor between regions leads to a standard deviation at long periods

that is similar for interface and intraslab events and is also larger than indicated by the range of the interface models shown in Figure 4.11. The epistemic range shown in Figure 4.10 and 4.11 are generally consistent with the preliminary random-effects results if a three-point distribution (± 1.65 sigma) is used. The epistemic uncertainty is listed in Table 4.4. For this range, epistemic weights of 0.2, 0.6, and 0.2 are appropriate for the low, central, and high models.

This epistemic uncertainty is a minimum uncertainty that only reflects the epistemic uncertainty in the adjustment factor applied to the Cascadia model. It does not capture the epistemic uncertainty in the magnitude and distance scaling. Other published ground-motion models can be used to capture the alternative magnitude and distance scaling.

Table 4.4 Epistemic uncertainty in the adjustment term (in LN units).

Period (sec)	Interface Low	Interface High	Slab Low	Slab High
0.01	-0.3	0.3	-0.5	0.5
0.02	-0.3	0.3	-0.5	0.5
0.03	-0.3	0.3	-0.5	0.5
0.05	-0.3	0.3	-0.5	0.5
0.075	-0.3	0.3	-0.5	0.5
0.1	-0.3	0.3	-0.5	0.5
0.15	-0.3	0.3	-0.5	0.5
0.2	-0.3	0.3	-0.5	0.5
0.25	-0.3	0.3	-0.46	0.46
0.3	-0.3	0.3	-0.42	0.42
0.4	-0.3	0.3	-0.38	0.38
0.5	-0.3	0.3	-0.34	0.34
0.6	-0.3	0.3	-0.3	0.3
0.75	-0.3	0.3	-0.3	0.3
1.0	-0.3	0.3	-0.3	0.3
1.5	-0.3	0.3	-0.3	0.3
2.0	-0.3	0.3	-0.3	0.3
2.5	-0.3	0.3	-0.3	0.3
3.0	-0.3	0.3	-0.3	0.3
4.0	-0.3	0.3	-0.3	0.3
5.0	-0.3	0.3	-0.3	0.3
6.0	-0.3	0.3	-0.3	0.3
7.5	-0.3	0.3	-0.5	0.5
10.0	-0.3	0.3	-0.5	0.5

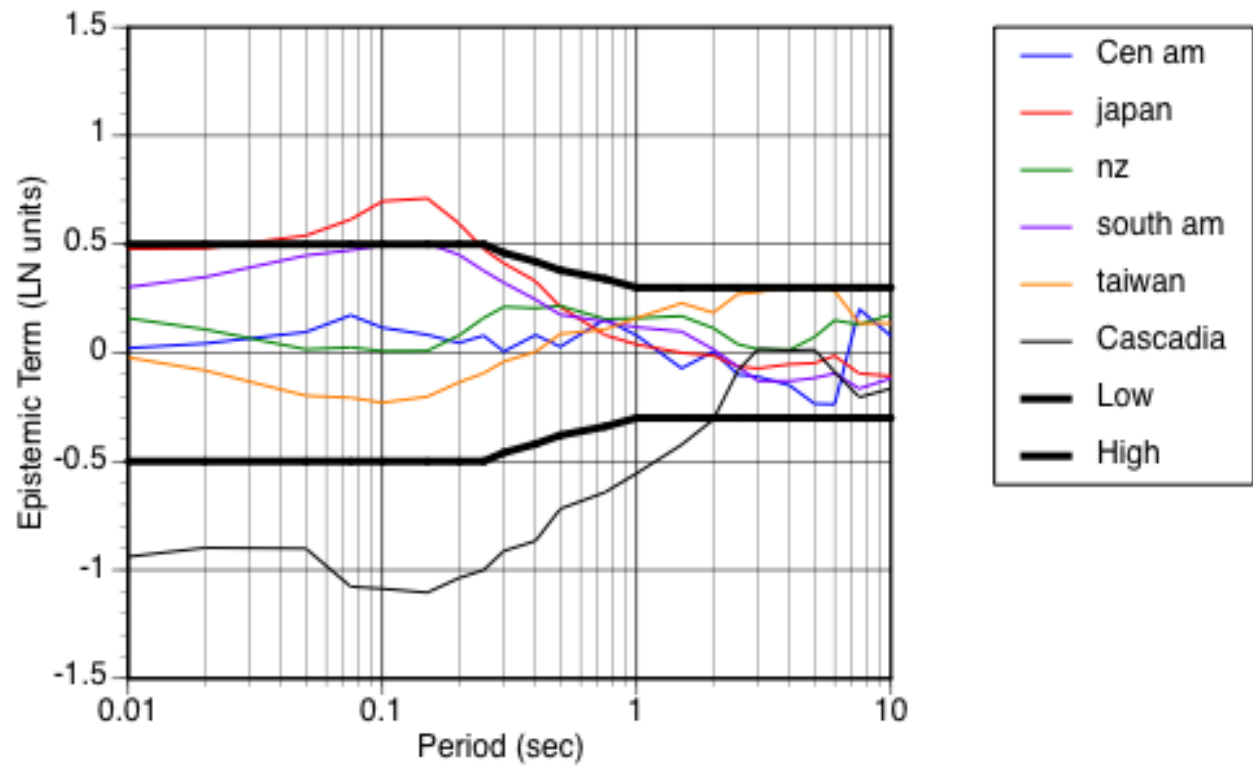


Figure 4.10 Recommended epistemic uncertainty in the Cascadia adjustment term for intraslab earthquakes.

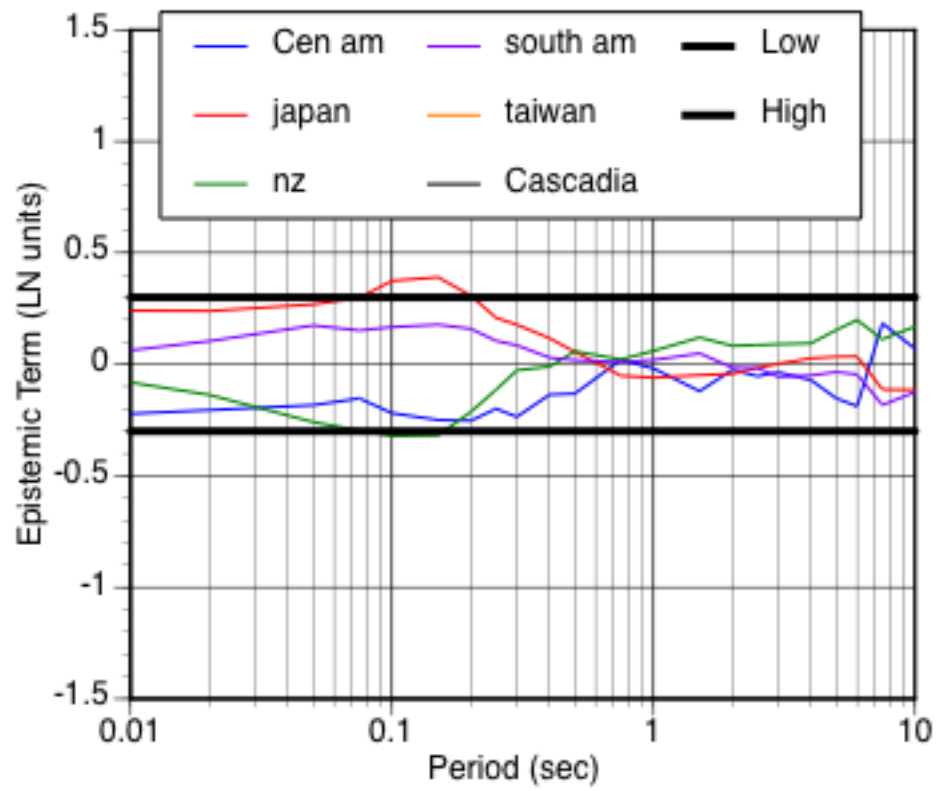


Figure 4.11 Recommended epistemic uncertainty in the Cascadia adjustment term for interface earthquakes.

4.4 MEDIAN MODEL COMPARISONS

The updated BCHydro model is compared with several current GMMs for subduction earthquakes in this section:

<u>GMM</u>	<u>Abbreviation in plots</u>
Zhao et al [2006]	Z06
Zhao et al [2016]	Z16
Atkinson and Boore [2003,2008] class B	AB, B
Atkinson and Boore [2003,2008] class C	AB, C
Atkinson and Boore [2003,2008] Cascadia, class B	AB-Cas, B
Atkinson and Boore [2003,2008] Cascadia, class C	AB-Cas, C
Atkinson and Macias [2009]	AM
Gregor et al [2006]	G06
Abrahamson et al [2016] central mag break	BCH-Cen
Abrahamson et al [2016] lower mag break	BCH-Low
Abrahamson et al [2016] higher mag break	BCH-Low
Updated BCHydro central model	BCH-381
Updated BCHydro high model	BCH-382
Updated BCHydro low model	BCH-383

The two Zhao models are based on Japanese ground motion data. The Atkinson and Boore models and the Abrahamson et al [2016] models are global models. The Atkinson and Macias [2009] and Gregor [2006] models are based on numerical simulations for interface earthquakes in Cascadia.

Figures 4.12a to 4.12d compare the distance scaling for **M**9 interface earthquakes for four spectral periods (PGA, $T=0.2$ sec, $T=1$ sec, and $T=3$ sec). Figures 4.13a to 4.13d compare the distance scaling for **M**7 intraslab earthquakes for these same four spectral periods. The Gregor et al (2006) and Atkinson and Macias (2009) models are only for interface and are not plotted in the intraslab scaling comparison. For both interface and intraslab events, the distance scaling of the updated BCHydro model is similar to the scaling of the Zhao et al. model [2006] (for Japan). Compared to the 2016 BCHydro model, the updated BCHydro model has steeper distance scaling at short periods (PGA), similar distance scaling at intermediate periods ($T = 1$ sec), and flatter distance scaling at long periods ($T = 3$).

Figures 4.14a to 4.14d compare the magnitude scaling for interface earthquakes and Figures 4.15a to 4.15d compare the magnitude scaling for intraslab earthquakes. The magnitude scaling for the updated BCHydro model is similar to the scaling in the Zhao et al (2006) model.

Figures 4.16 to 4.19 compare the response spectra for **M8** and **M9** interface earthquakes at distances of 75 and 300 km. At 75 km distance, the spectral shapes of the updated BCHydro model are similar to the spectral shapes of the 2016 BCHydro model; however, at 300 km distance, the spectral content is very different, with the updated model showing a shift to longer spectral periods due to the greater attenuation in the Cascadia model.

Figures 4.20 to 4.23 compare the response spectra for **M6.5** and **M7.5** intraslab earthquakes at distances of 75 and 300 km. At both 75 km and 300 km distance, the spectral shape of the updated BCHydro model is similar to the 2016 BCHydro model at long periods, but show lower short-period ground motions.

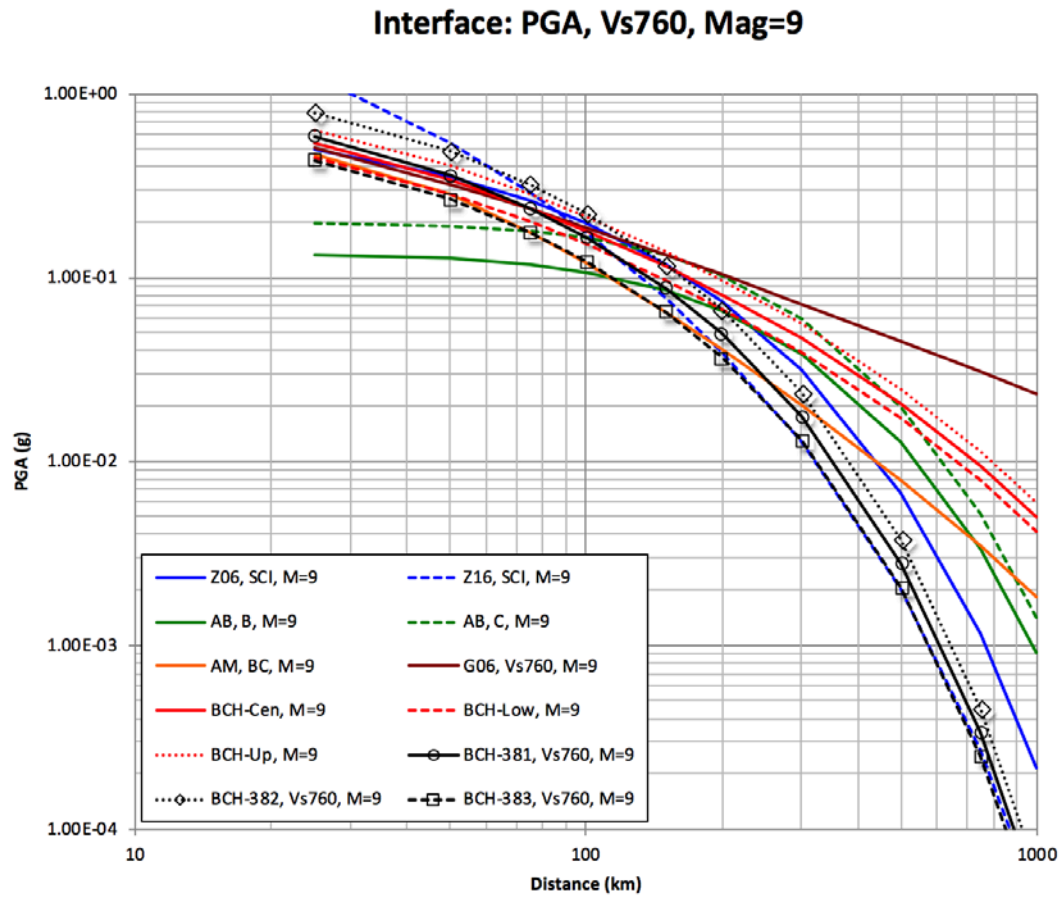


Figure 4.12(a) Median attenuation comparison for PGA for M9, $V_{S30} = 760$ m/sec. The symbols are shown on the updated BChydro model to make these models stand out on the plot.

Interface: T=0.2s, Vs760, Mag=9

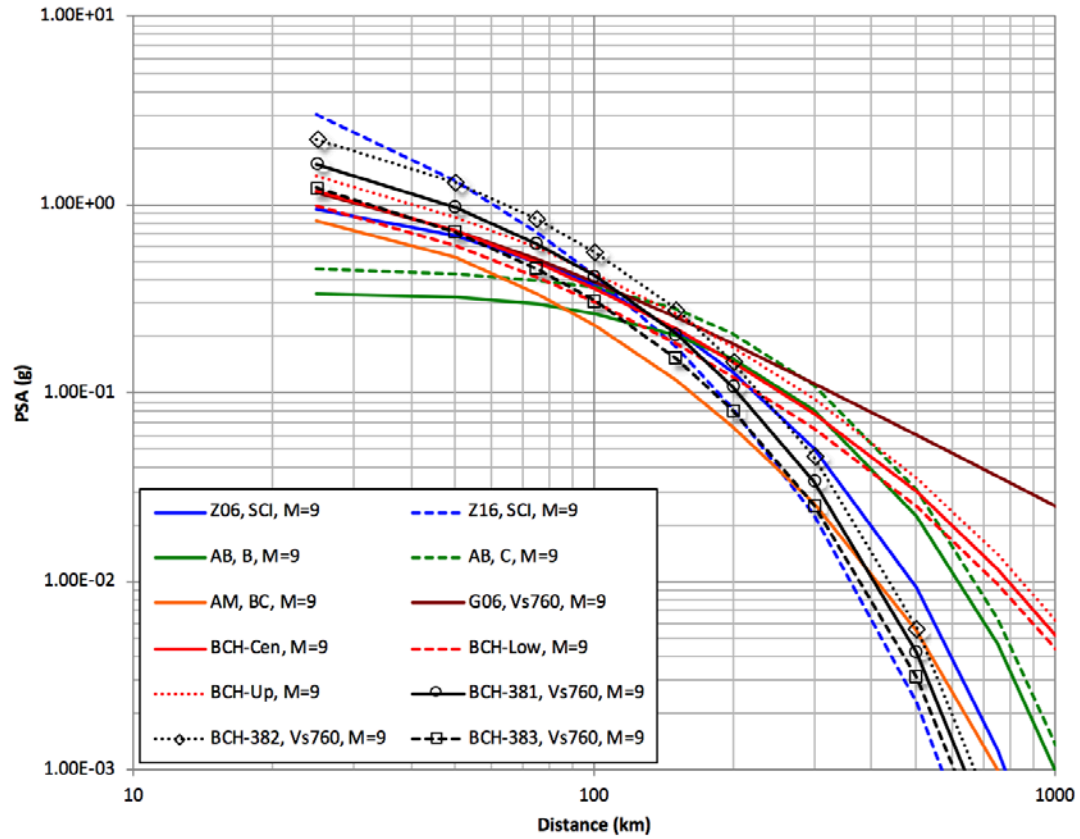


Figure 4.12(b) Median attenuation comparison for $T = 0.2$ sec for $M9$, $V_{S30} = 760$ m/sec.

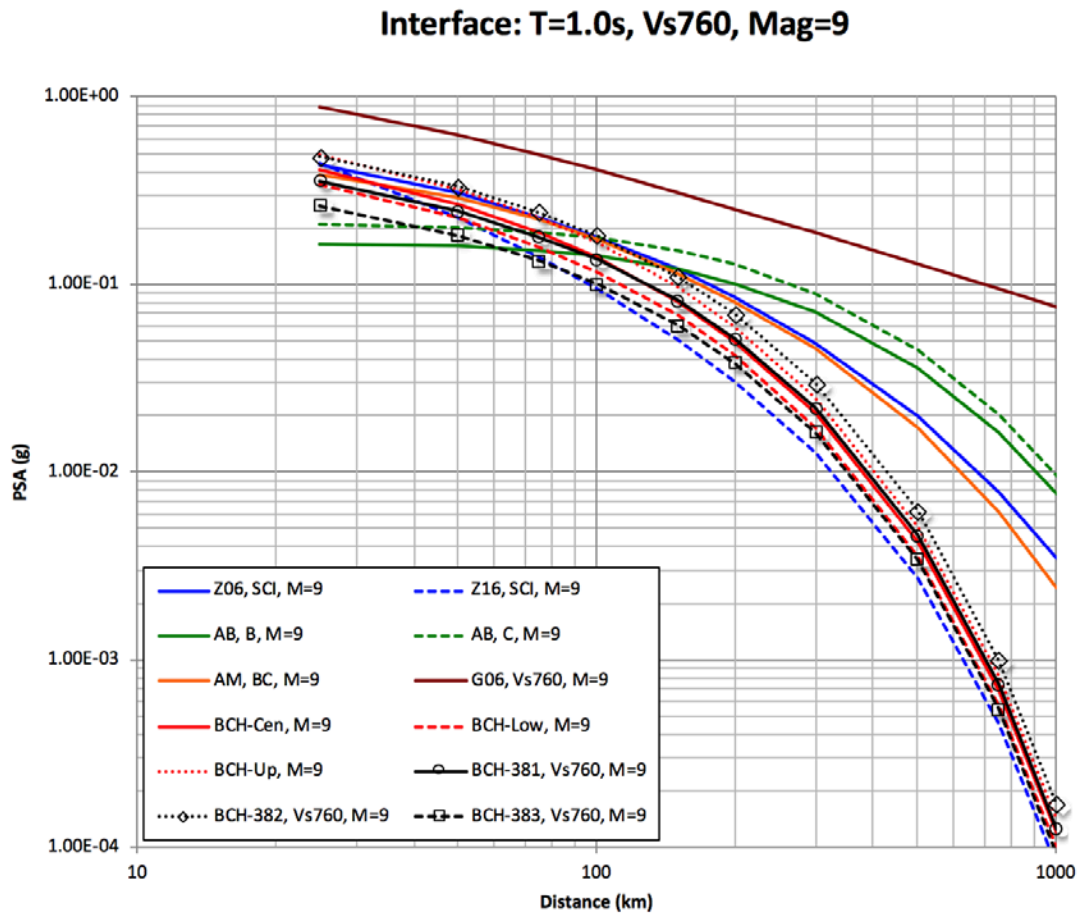


Figure 4.12(c) Median attenuation comparison for $T = 1$ sec, for M9, $V_{S30} = 760$ m/sec.

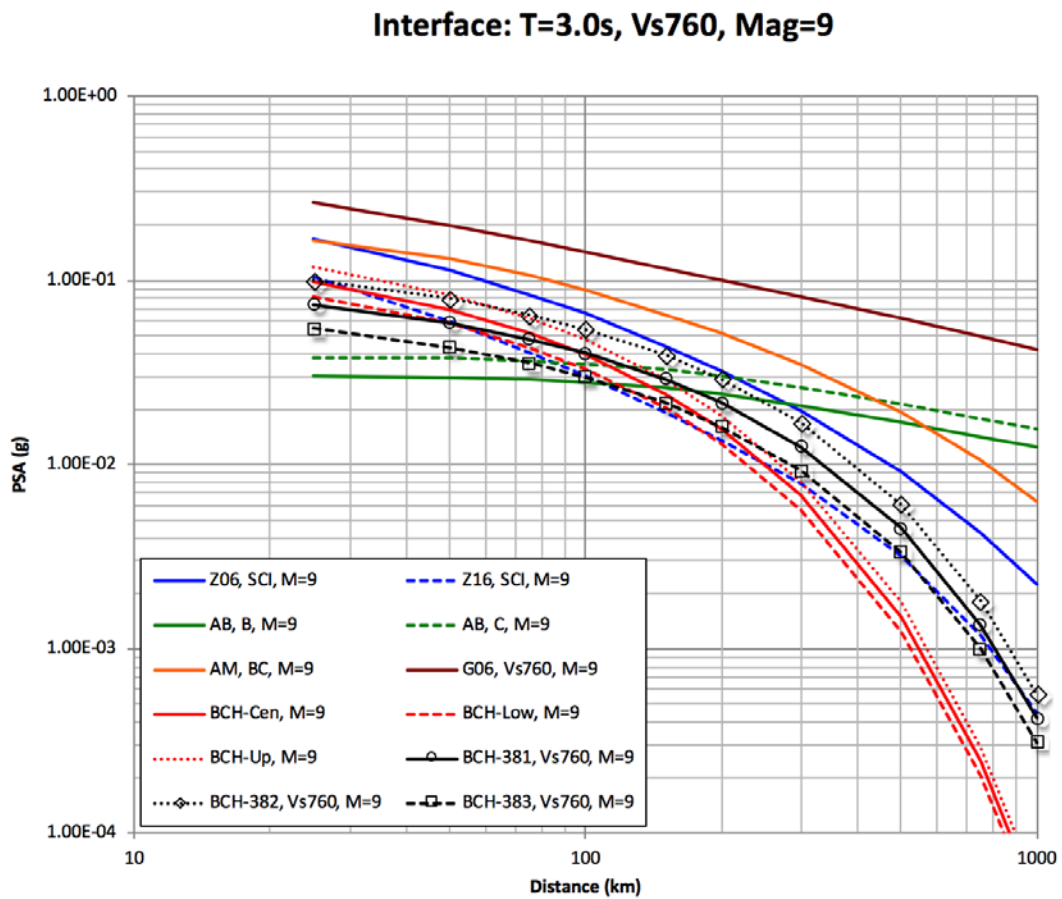


Figure 4.12(d) Median attenuation comparison for $T = 3$ sec, for M9, $V_{s30} = 760$ m/sec.

Slab: PGA, Vs760, Mag=7

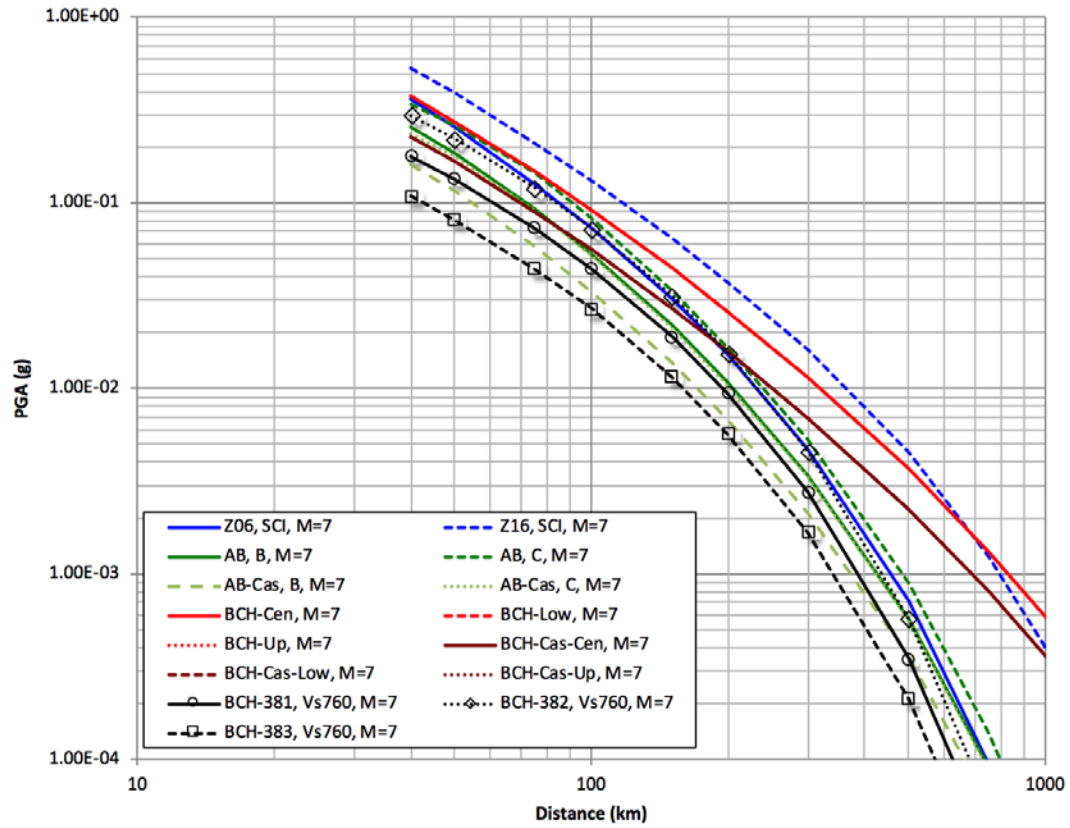


Figure 4.13(a) Median attenuation comparison for intraslab events, PGA, for M7, $V_{S30} = 760$ m/sec.

Slab: T=0.2s, Vs760, Mag=7

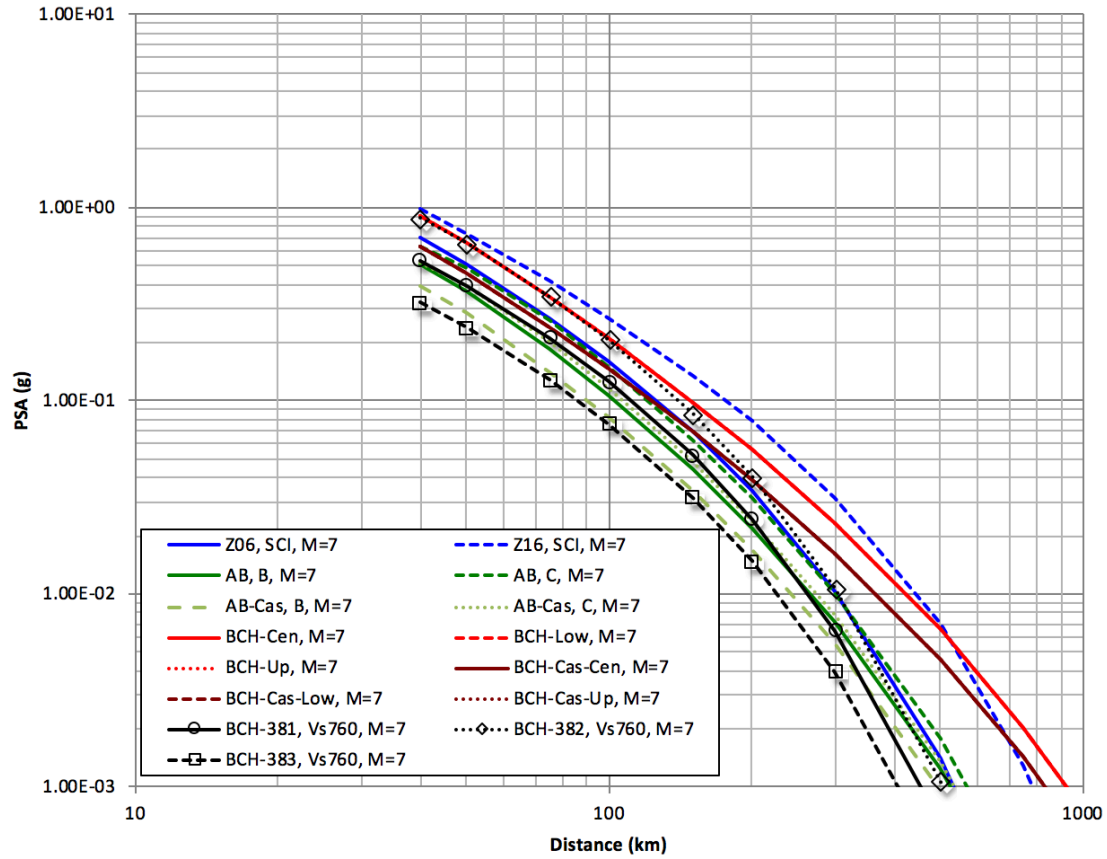


Figure 4.13(b) Median attenuation comparison for intraslab events, $T = 0.2$, for M7, $V_{s30} = 760$ m/sec.

Slab: T=1.0s, Vs760, Mag=7

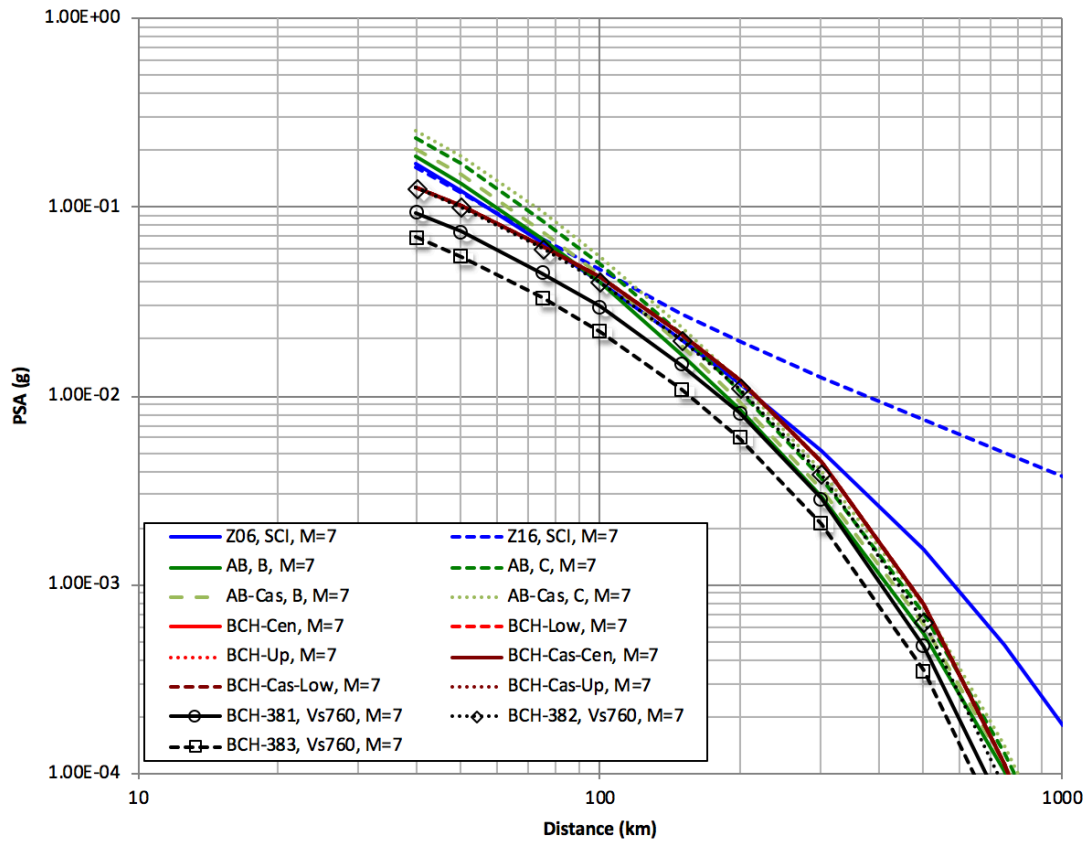


Figure 4.13(c) Median attenuation comparison for intraslab events, $T = 1$, for M7, $V_{S30} = 760$ m/sec.

Slab: T=3.0s, Vs760, Mag=7

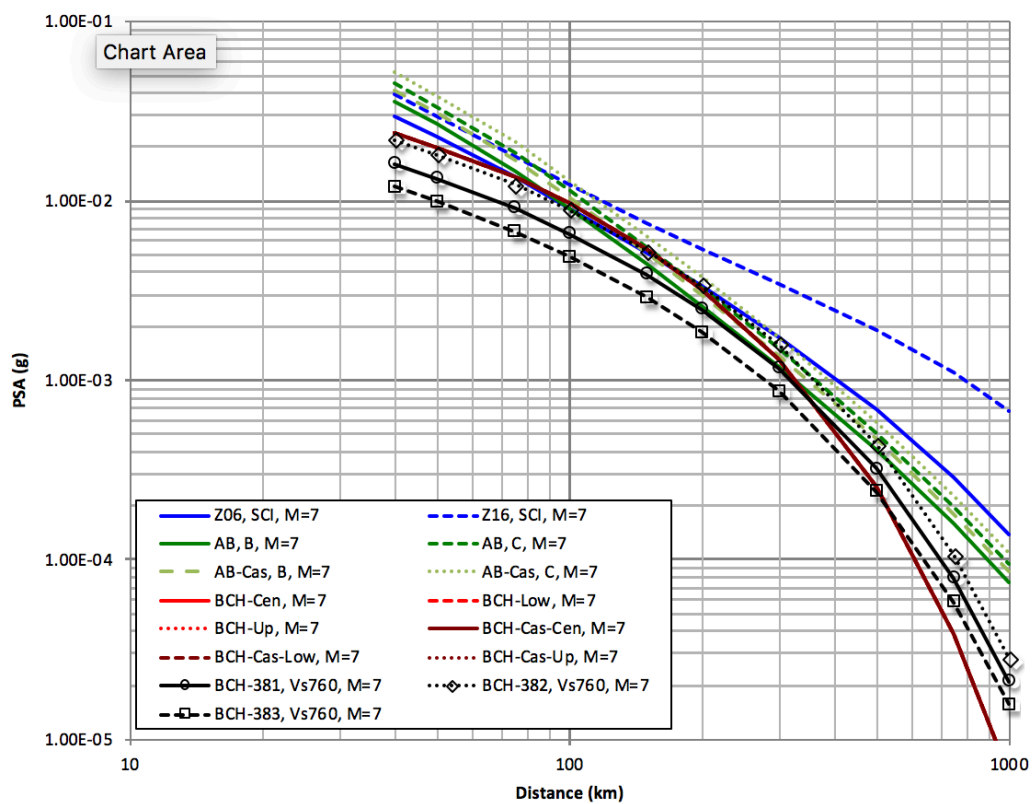


Figure 4.13(d) Median attenuation comparison for intraslab events, $T = 3$, for M7, $V_{S30} = 760$ m/sec.

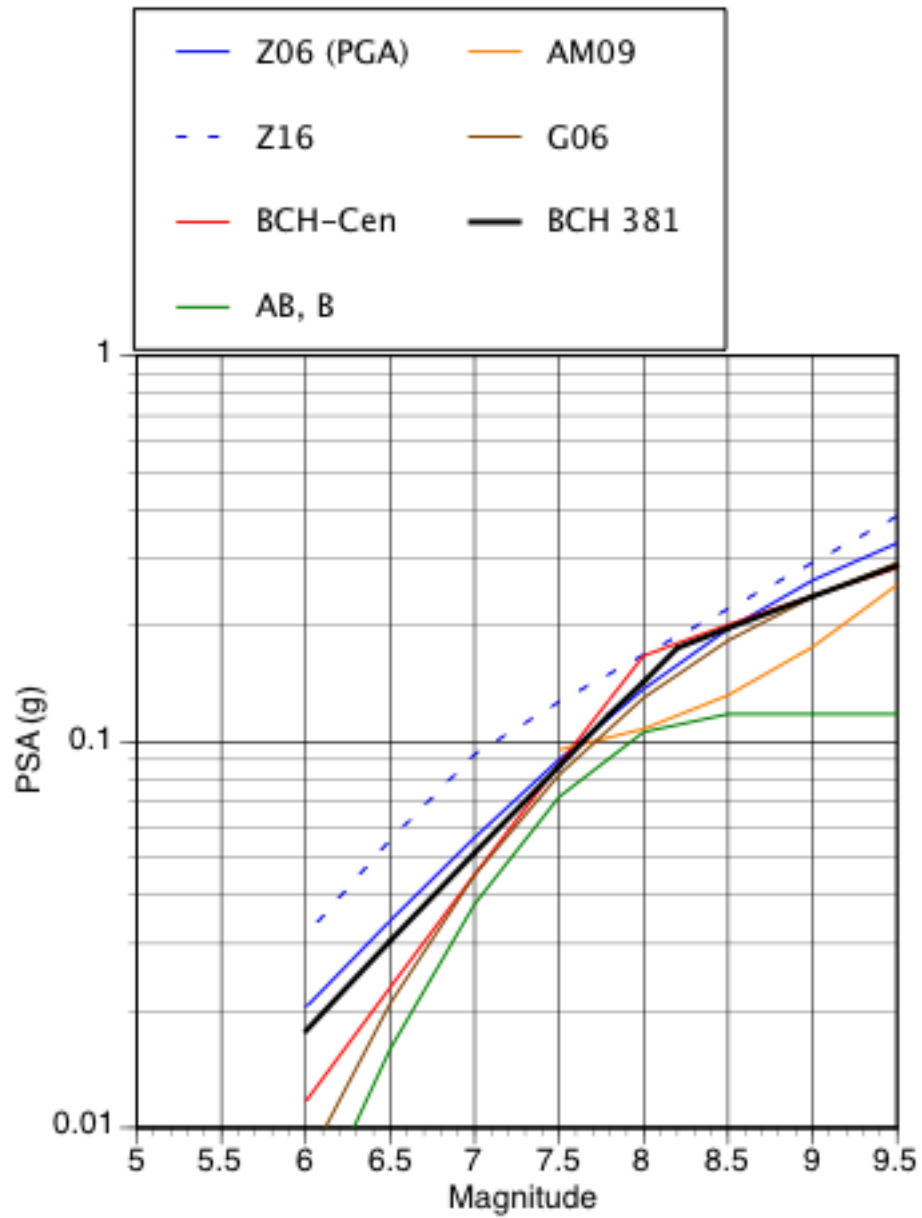


Figure 4.14(a) Magnitude scaling for PGA for interface earthquakes. ($R_{rup}=75$ km, $V_{S30}=760$ m/s)

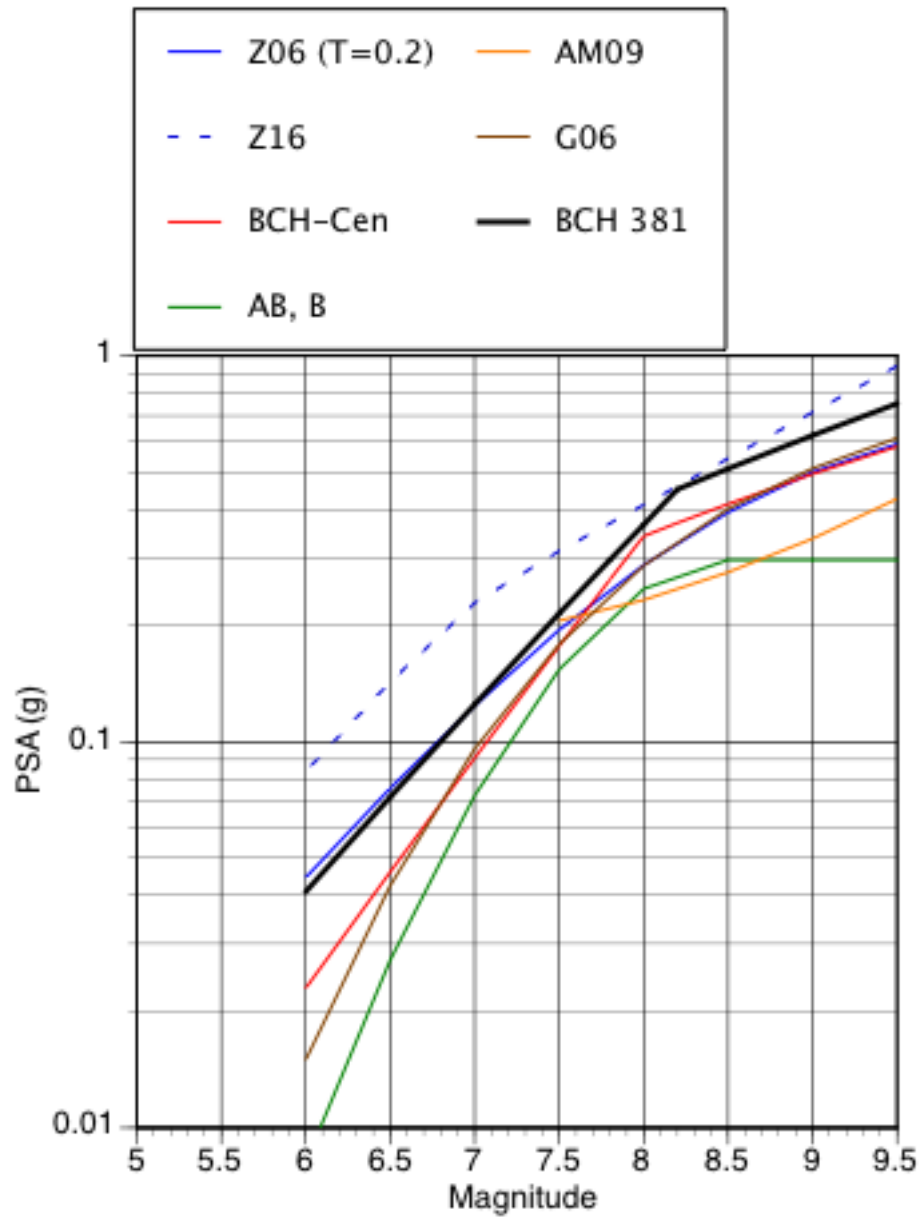


Figure 4.14(b) Magnitude scaling for T=0.2 sec for interface earthquakes. ($R_{rup}=75$ km, $V_{S30}=760$ m/s)

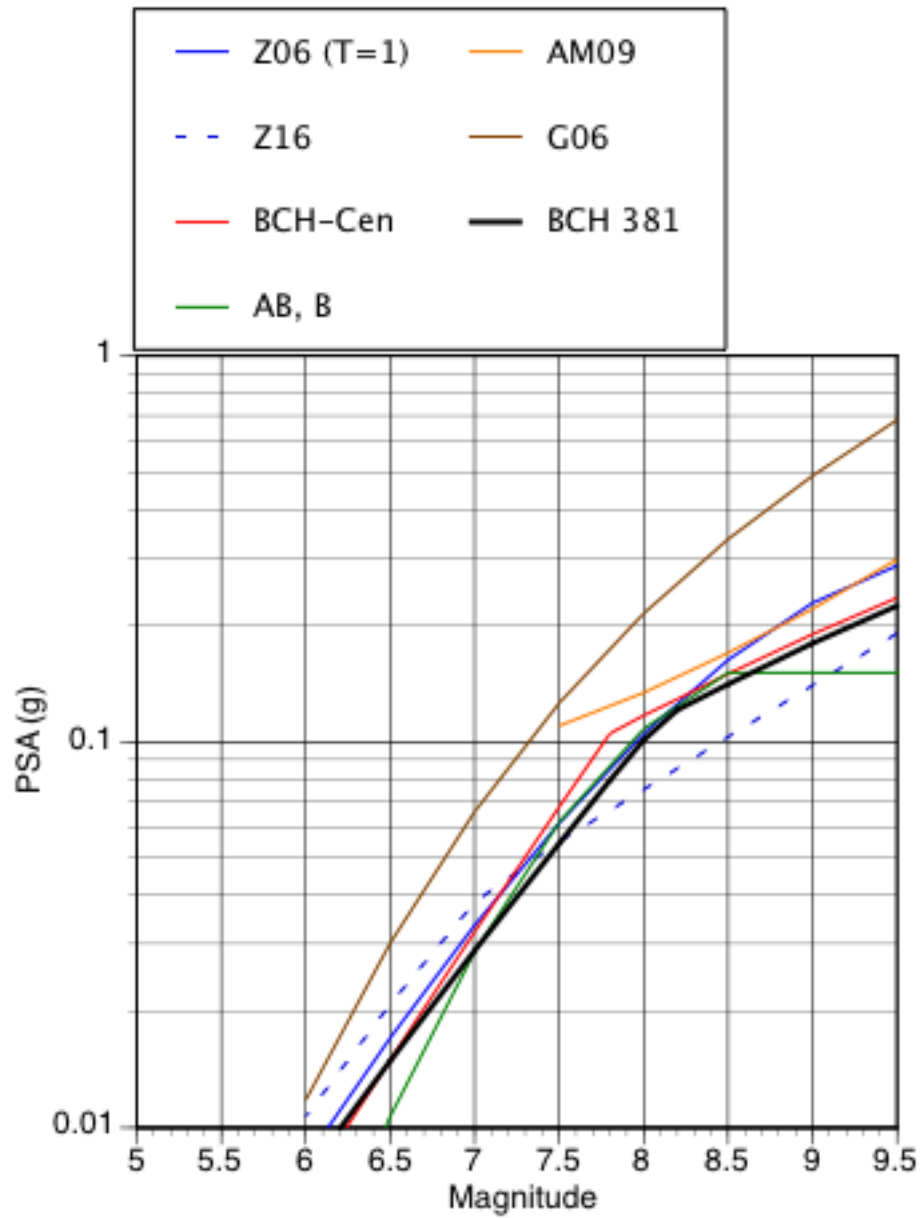


Figure 4.14(c) Magnitude scaling for T=1 sec for interface earthquakes. ($R_{rup}=75$ km, $V_{s30}=760$ m/s)

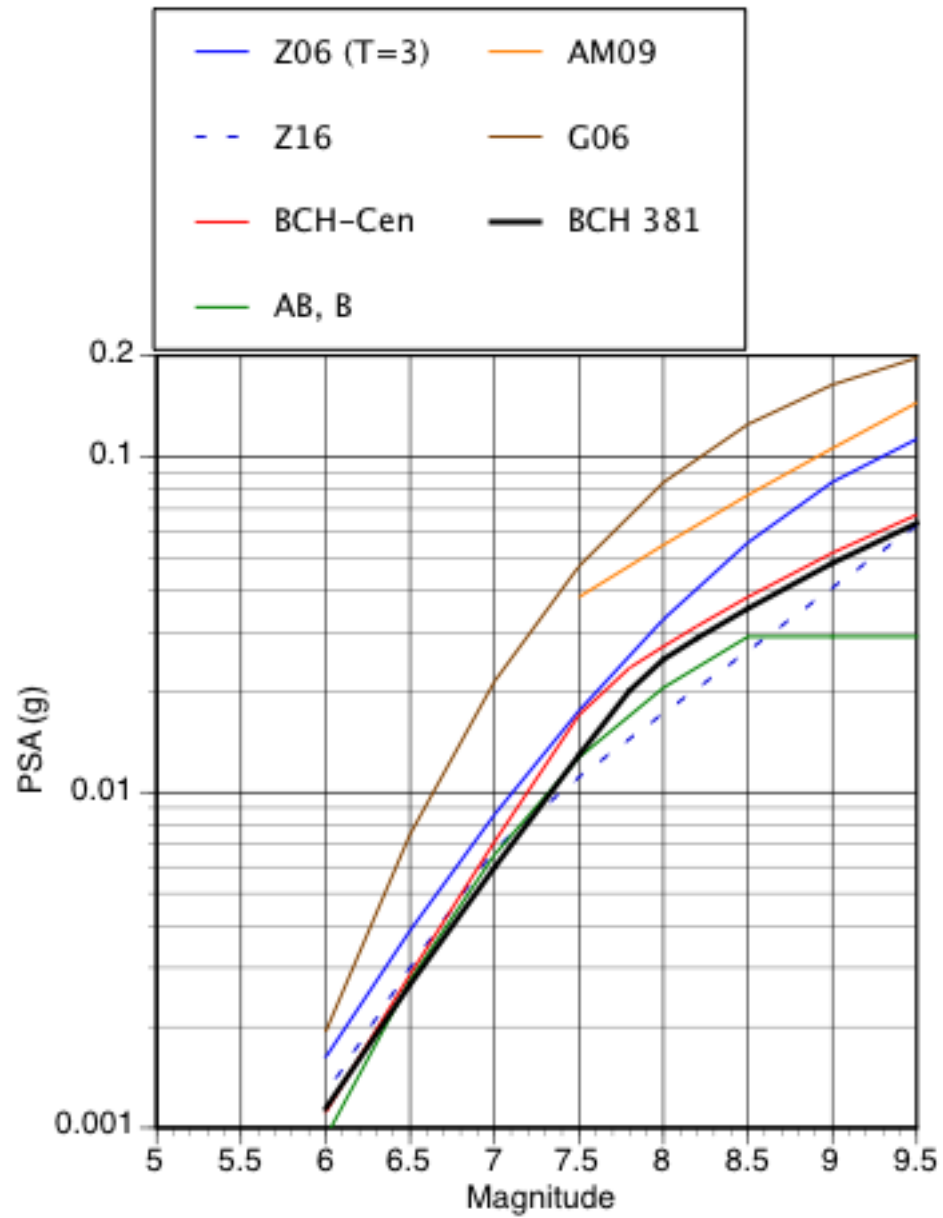


Figure 4.14(d) Magnitude scaling for $T=3$ sec for interface earthquakes. ($R_{rup}=75$ km, $V_{s30}=760$ m/s)

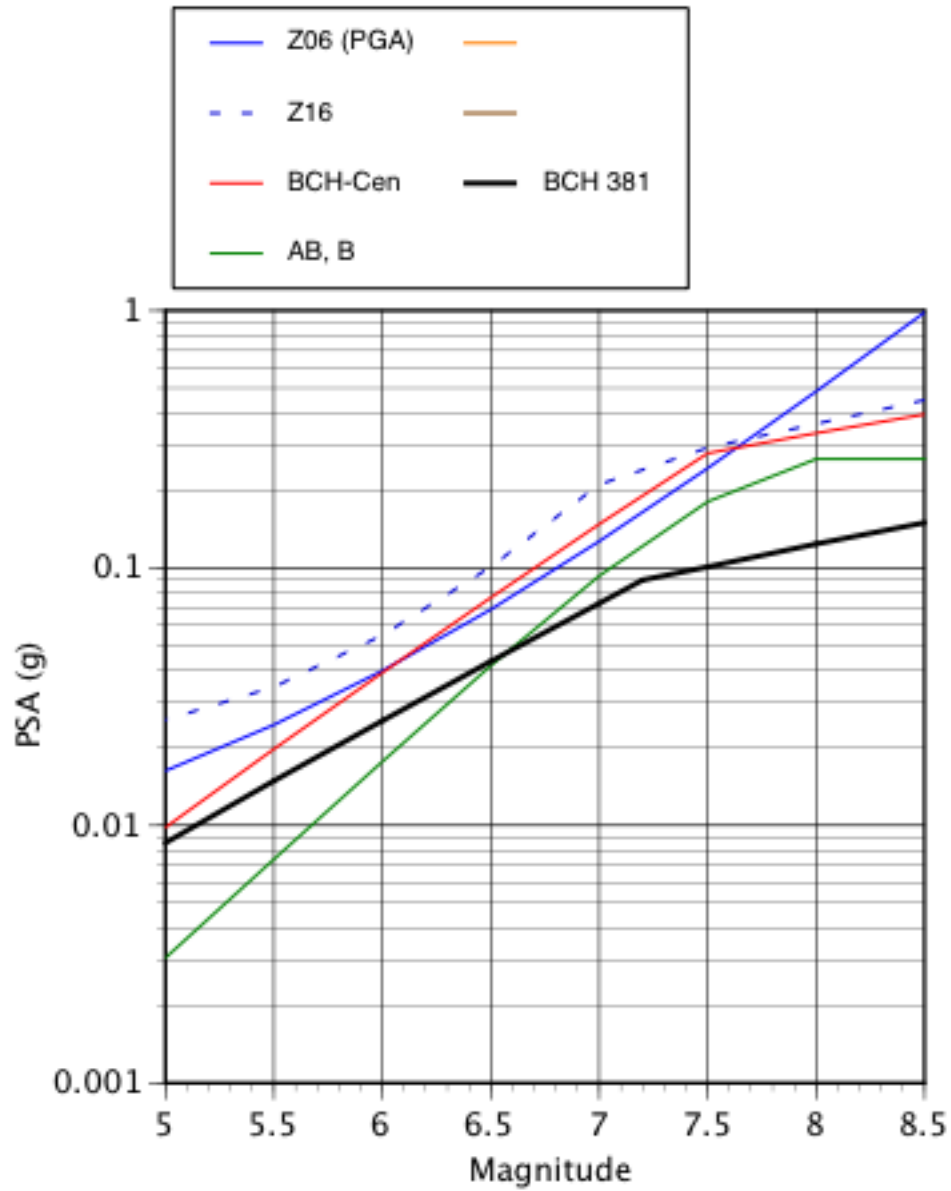


Figure 4.15(a) Magnitude scaling for PGA for intraslab earthquakes. ($R_{rup}=75$ km, $V_{s30}=760$ m/s, $Z_{TOR}=50$ km)

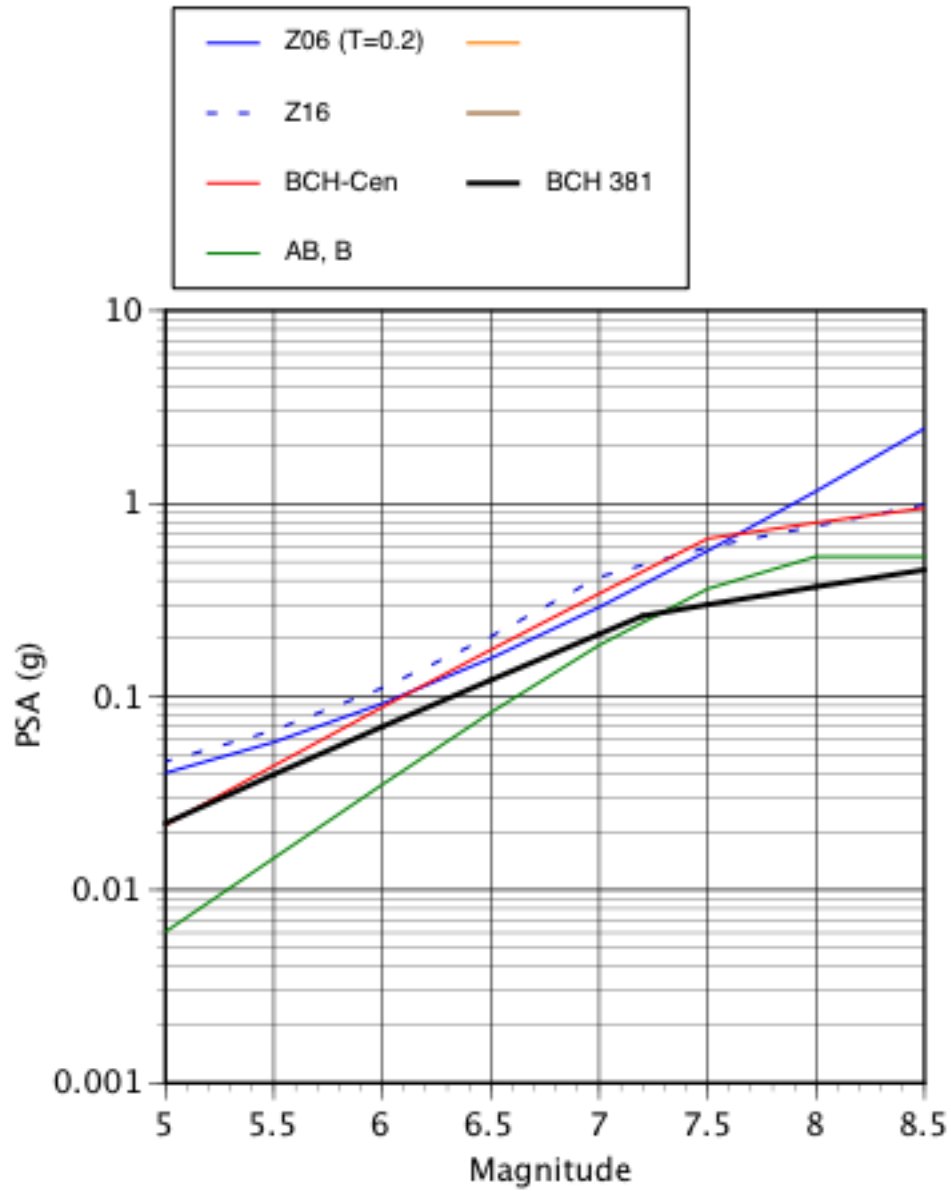


Figure 4.15(b) Magnitude scaling for $T=0.2$ sec for intraslab earthquakes. ($R_{rup}=75$ km, $V_{S30}=760$ m/s, $Z_{TOR}=50$ km)

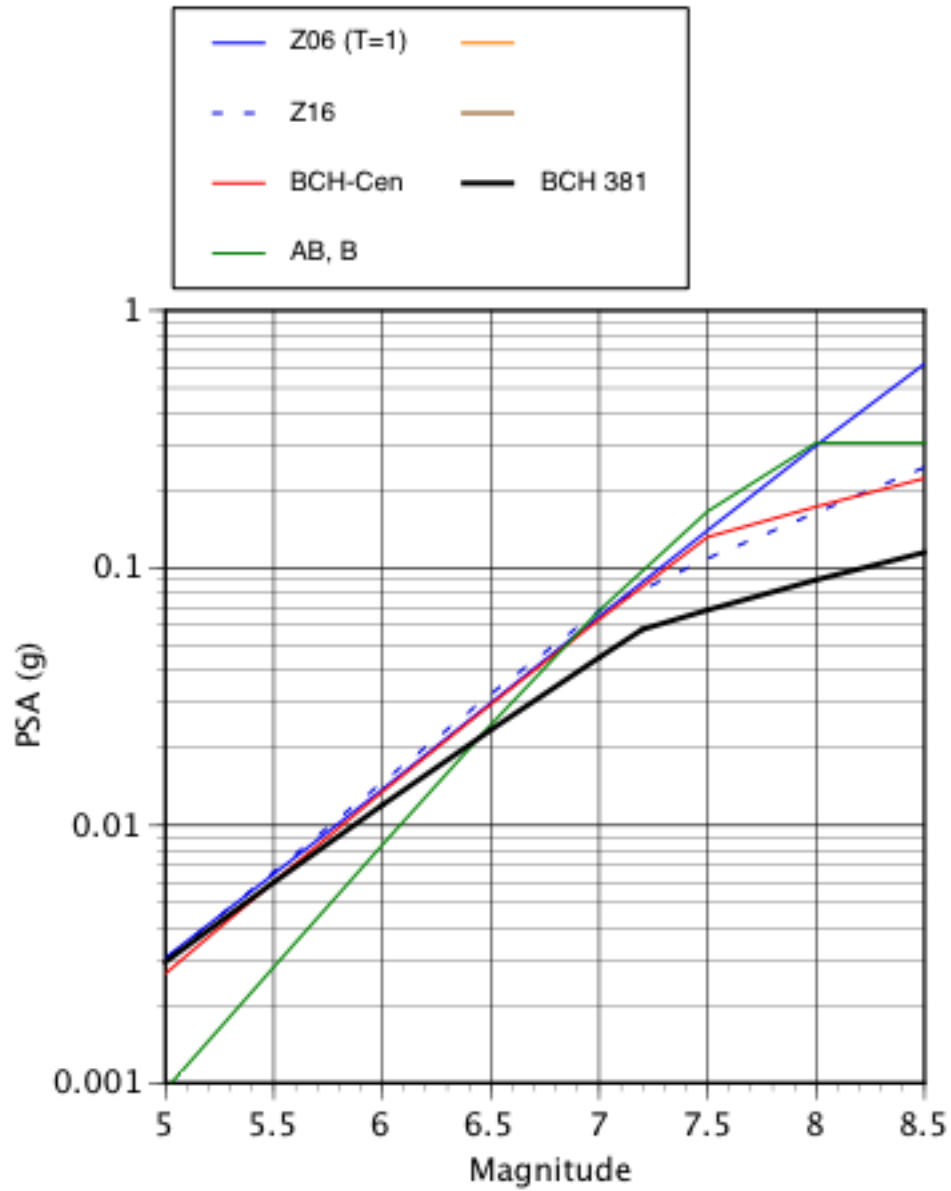


Figure 4.15(c) Magnitude scaling for $T=1$ sec for intraslab earthquakes. ($R_{rup}=75$ km, $V_{s30}=760$ m/s, $Z_{TOR}=50$ km)

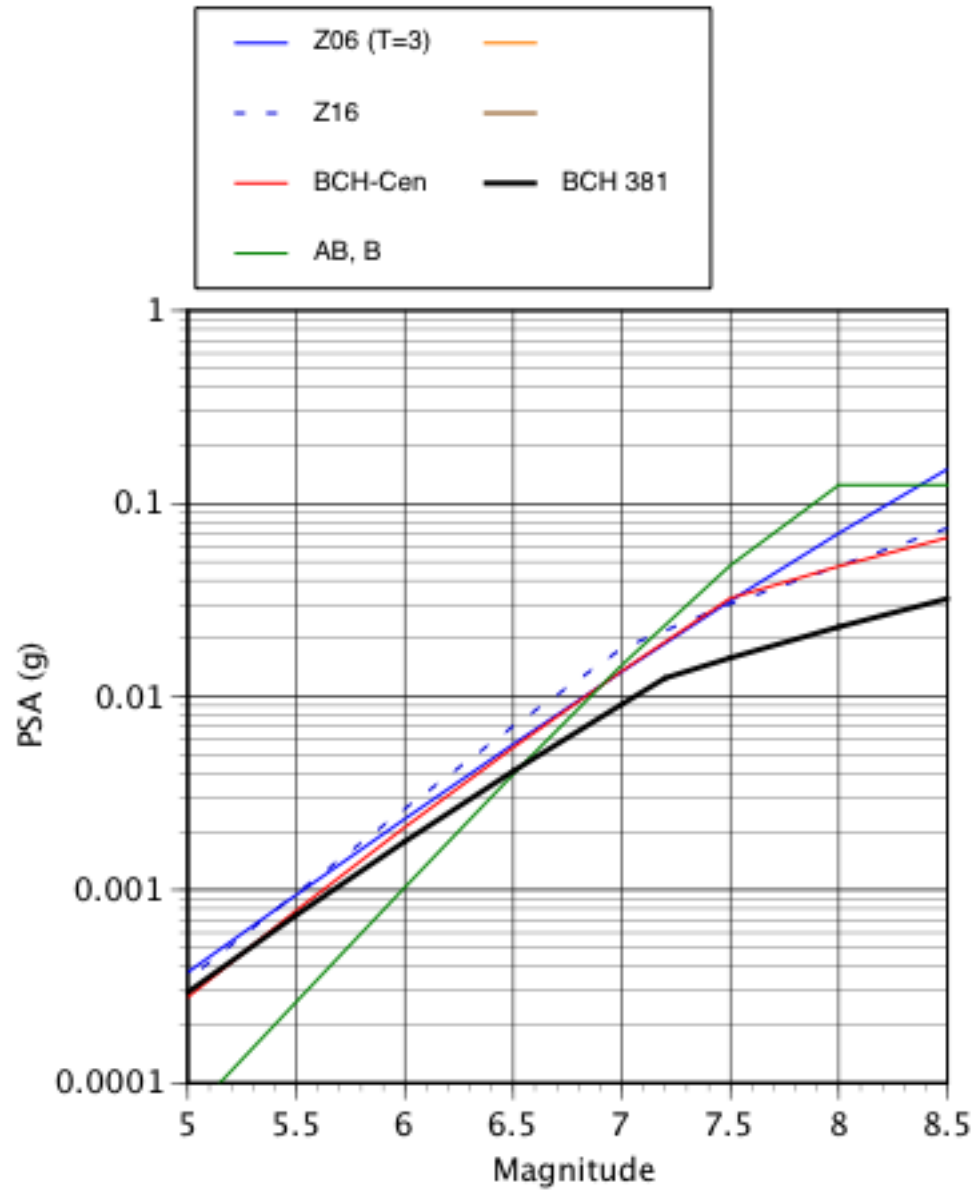


Figure 4.15(d) Magnitude scaling for T=3 sec for intraslab earthquakes. ($R_{rup}=75$ km, $V_{s30}=760$ m/s, $Z_{TOR}=50$ km)

Interface: Spectra, R075km, Vs760, Mag=8

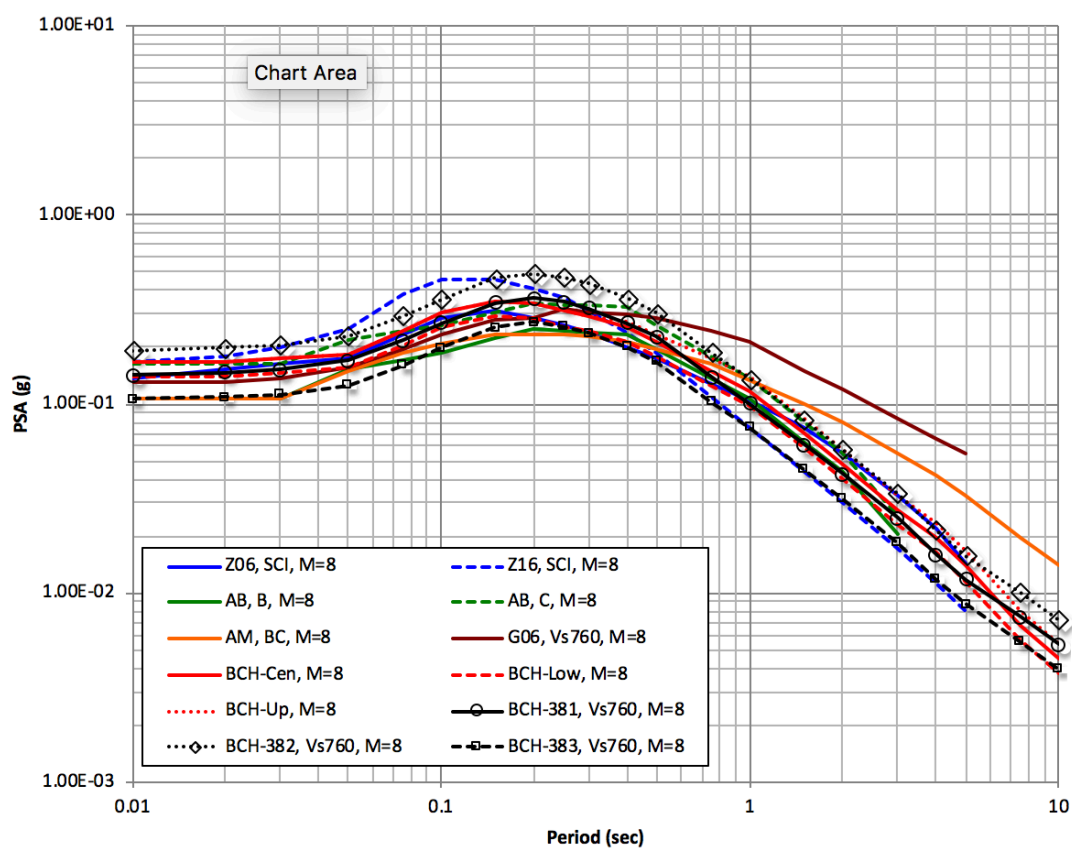


Figure 4.16 Median spectrum comparison for interface events, $R_{rup} = 75$ km, for M8, $V_{S30} = 760$ m/sec.

Interface: Spectra, R075km, Vs760, Mag=9

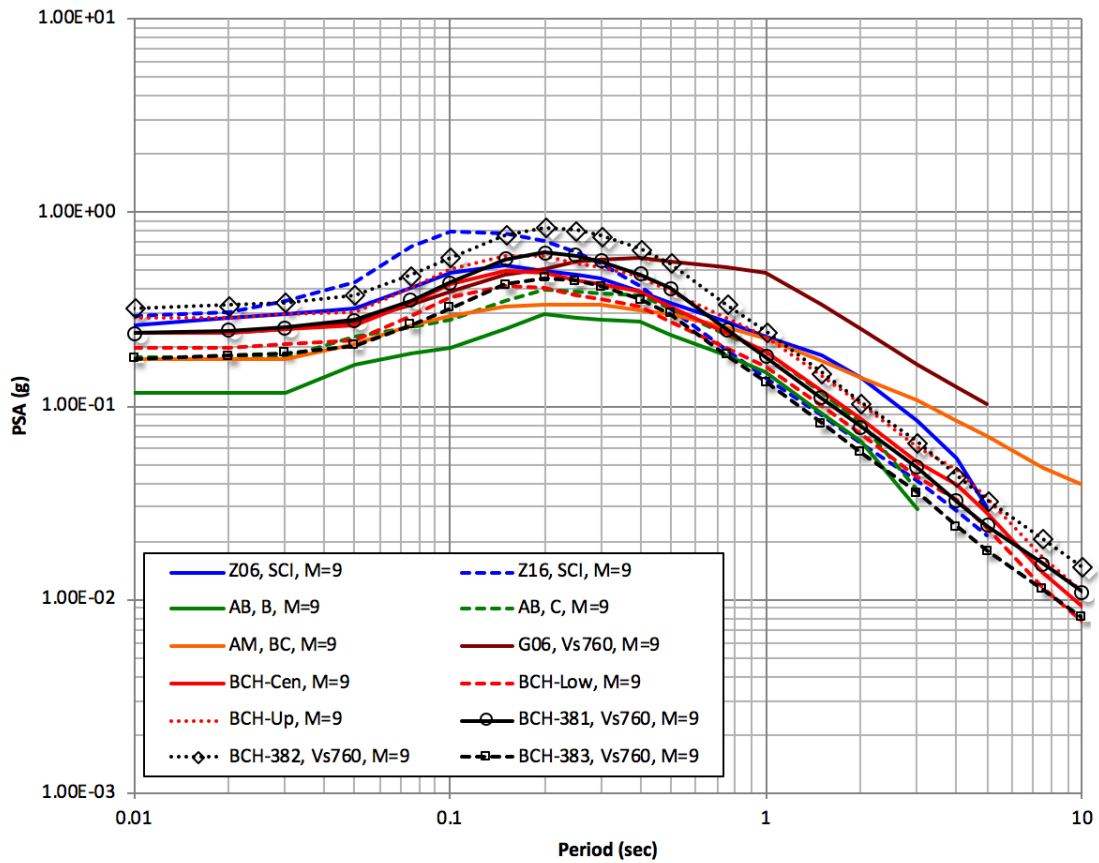


Figure 4.17 Median spectrum comparison for interface events, $R_{rup} = 75$ km, for M9, $V_{S30} = 760$ m/sec.

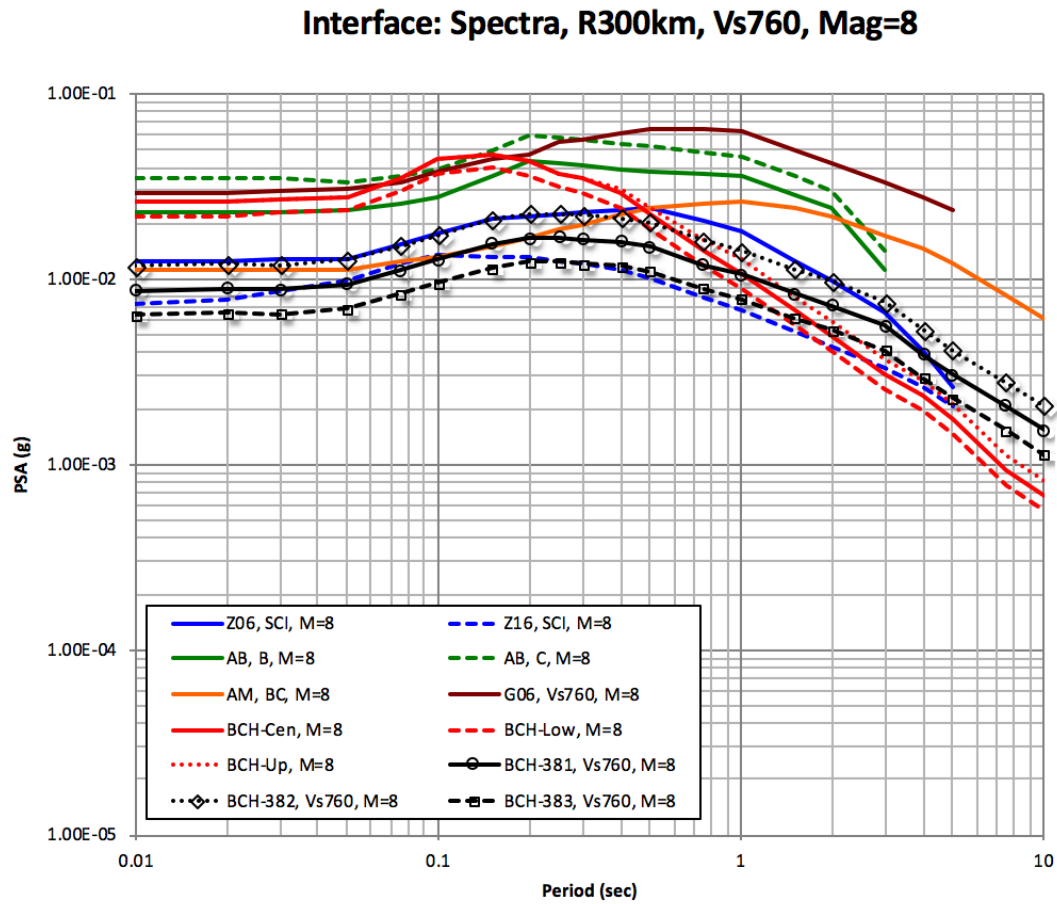


Figure 4.18 Median spectrum comparison for interface events, $R_{rup} = 300$ km, for $M = 8$, $V_{s30} = 760$ m/sec.

Interface: Spectra, R300km, Vs760, Mag=9

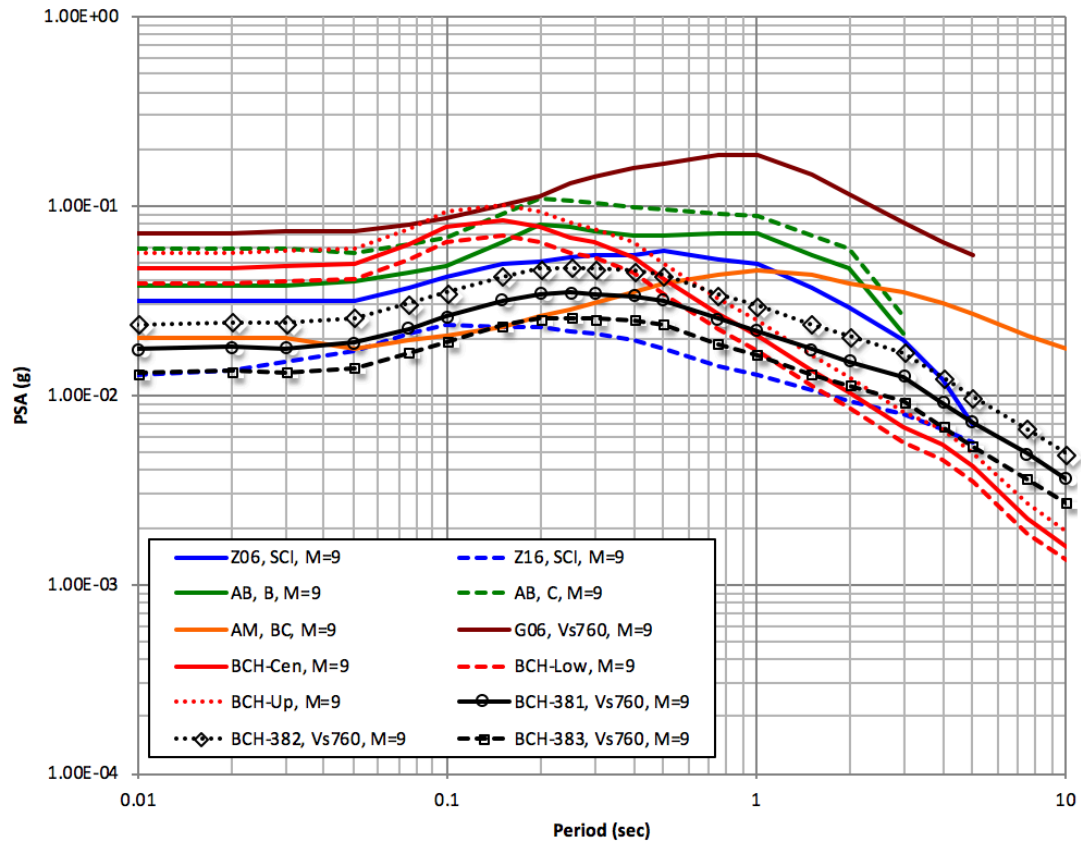


Figure 4.19 Median spectrum comparison for interface events, $R_{rup} = 300$ km, for M9, $V_{S30} = 760$ m/sec.

Slab: Spectra, R075km, Vs760, Mag=6.5

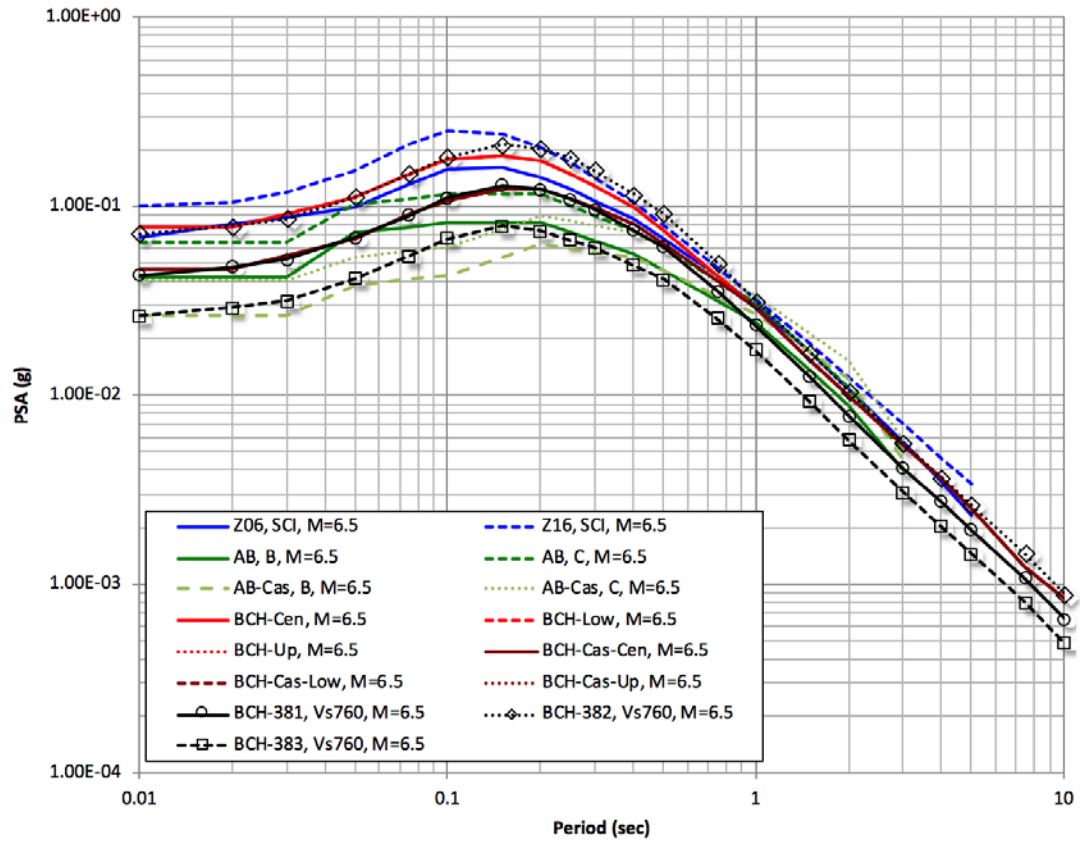


Figure 4.20 Median spectrum comparison for intraslab events, $R_{rup}=75$ km, for M6.5, $V_{S30} = 760$ m/sec.

Slab: Spectra, R075km, Vs760, Mag=7.5

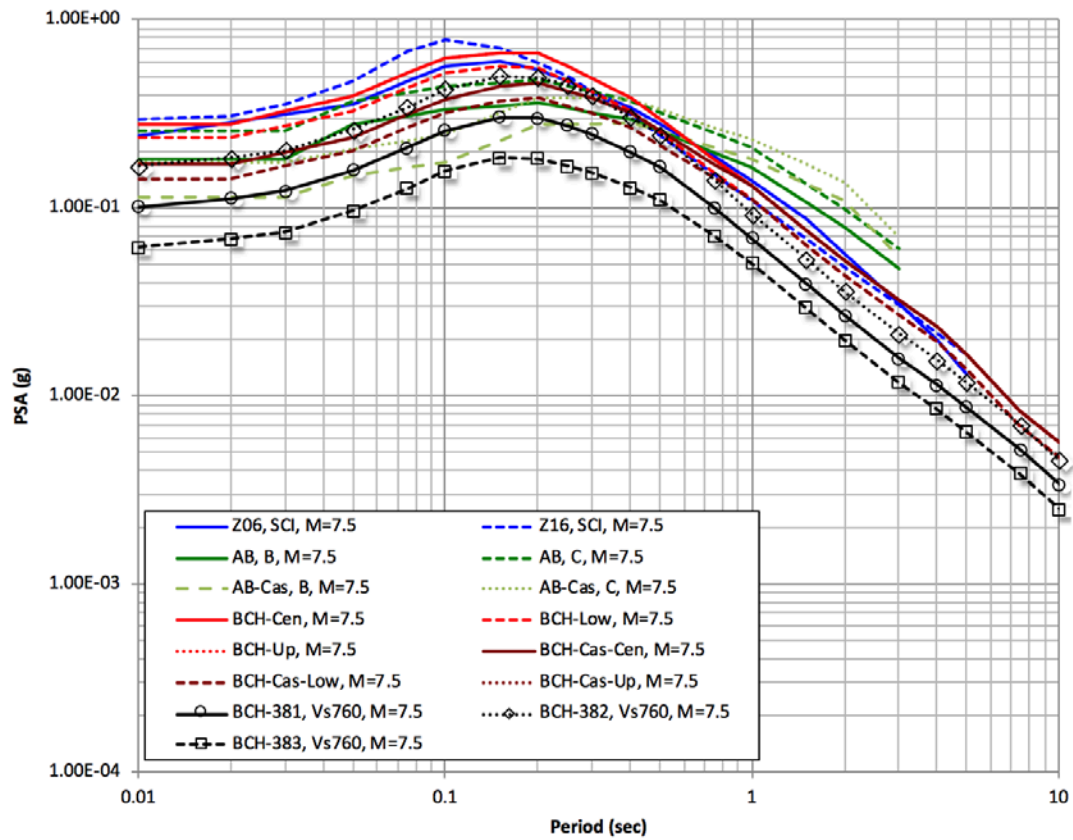


Figure 4.21 Median spectrum comparison for intraslab events, $R_{rup} = 75$ km, for M7.5, $V_{s30} = 760$ m/sec.

Slab: Spectra, R300km, Vs760, Mag=6.5

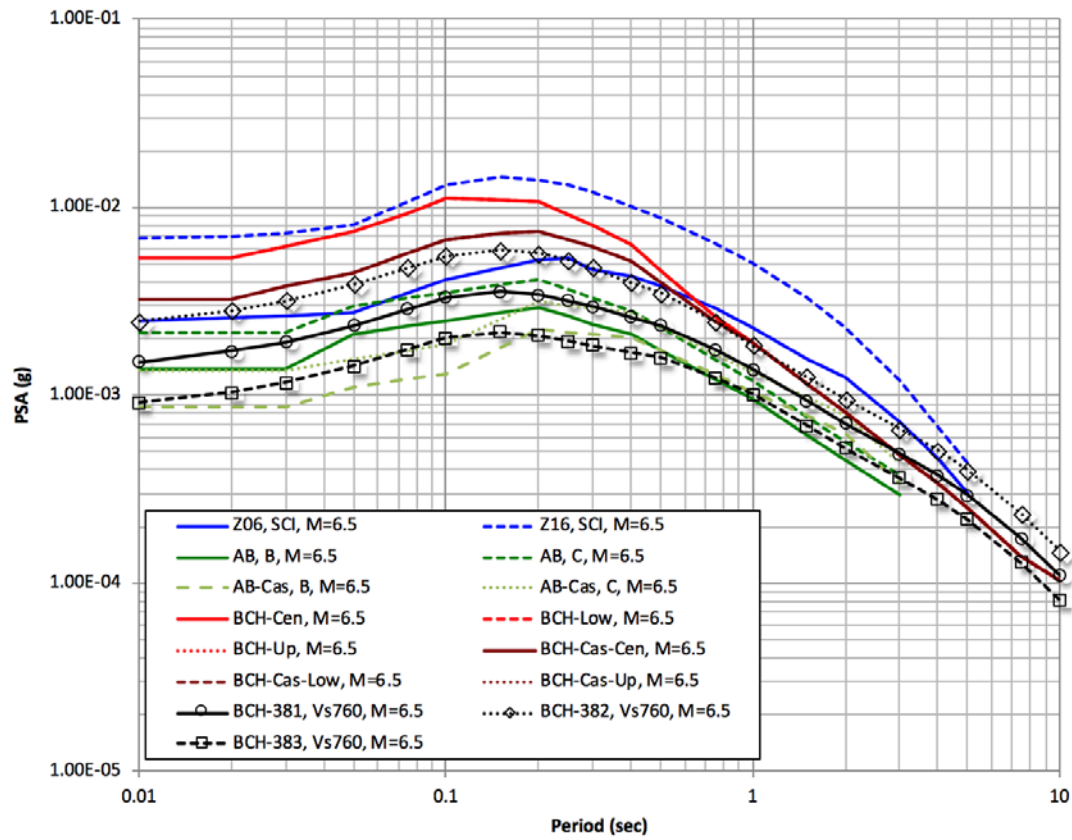


Figure 4.22 Median spectrum comparison for intraslab events, $R_{rup} = 300$ km, for M6.5, $V_{S30} = 760$ m/sec.

Slab: Spectra, R300km, Vs760, Mag=7.5

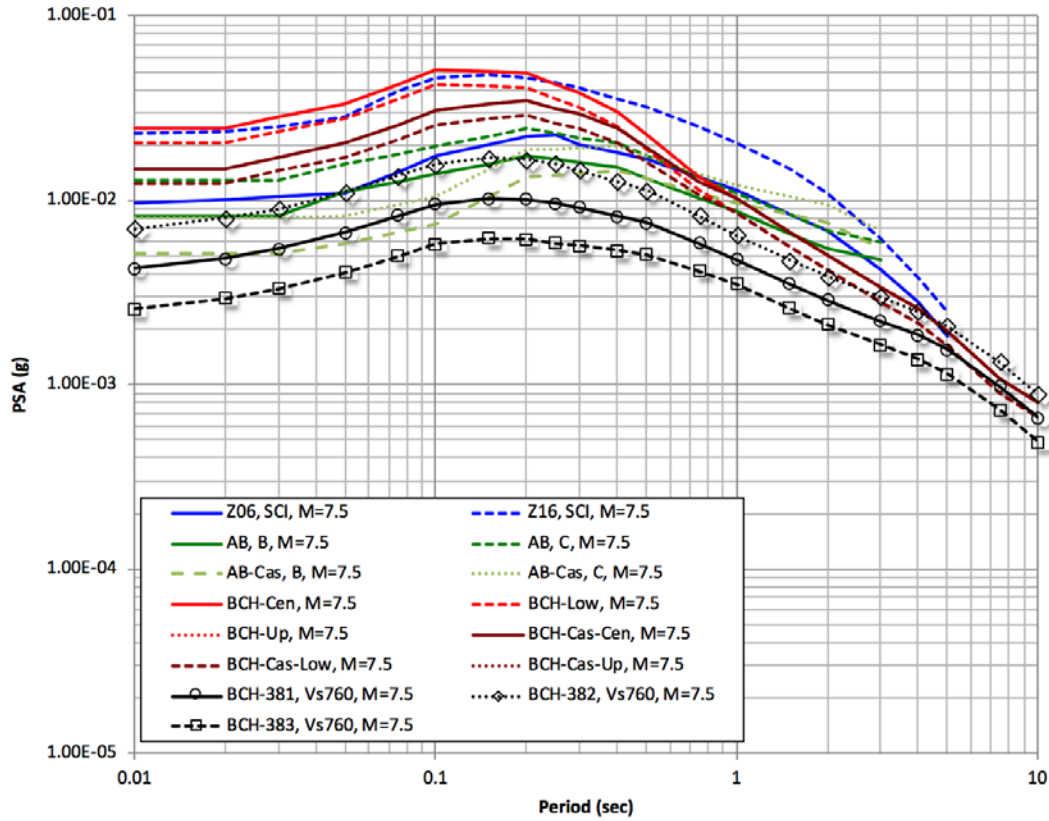


Figure 4.23 Median spectrum comparison for intraslab events, $R_{rup} = 300$ km, for M7.5, $V_{s30} = 760$ m/sec.

4.5 STANDARD DEVIATION

The standard deviation of the within-event residuals (ϕ) and the between-event residuals (τ) from the regression is shown in Figure 4.24. A check of the magnitude dependence of the ϕ and τ did not show a need for a magnitude-dependent model. A simple model with a period-independent and magnitude-independent ϕ is used. To avoid unusual shapes in the spectrum at different epsilon levels, the ϕ and τ are smoothed, as shown in Figure 4.24. The smoothed aleatory terms are listed in Table 4.5.

The nonlinear site response term is set to the PGA_{1000} -based model using in the 2016 BChydro GMM which was based on the nonlinear site model in Abrahamson and Silva (2008). The effect of the nonlinear site response on the ϕ and τ is modelled using the approach in Abrahamson and Silva (2008). The nonlinear ϕ and τ are given below:

$$\begin{aligned}
\varphi(T, P\hat{G}A_{1000}, V_{S30}) &= \varphi_0^2(T) + \left(\frac{\partial \ln \left(\text{Amp}(T, P\hat{G}A_{1000}, V_{S30}) \right)}{\partial (\ln PGA_{1000})} \right)^2 \varphi_B^2(T) \\
&+ 2 \left(\frac{\partial \ln \left(\text{Amp}(T, P\hat{G}A_{1000}, V_{S30}) \right)}{\partial (\ln PGA_{1000})} \right) \varphi_B(T) \varphi_B(PGA) \rho_w(T, PGA)
\end{aligned}$$

and

$$\begin{aligned}
\tau(T, P\hat{G}A_{1000}, V_{S30}) &= \tau_0^2(T) + \left(\frac{\partial \ln \left(\text{Amp}(T, P\hat{G}A_{1000}, V_{S30}) \right)}{\partial (\ln P\hat{G}A_{1000})} \right)^2 \tau_0^2(T) \\
&+ 2 \left(\frac{\partial \ln \left(\text{Amp}(T, P\hat{G}A_{1000}, V_{S30}) \right)}{\partial (\ln P\hat{G}A_{1000})} \right) \tau_0(T) \tau_0(PGA) \rho_B(T, PGA)
\end{aligned}$$

where

$$\frac{\partial \ln \left(\text{Amp}(T, P\hat{G}A_{1000}, V_{S30}) \right)}{\partial (\ln P\hat{G}A_{1000})} = \begin{cases} 0 & \text{for } V_{S30} \geq V_{LIN} \\ \frac{-b(T)P\hat{G}A_{1000}}{P\hat{G}A_{1000} + c} + \frac{b(T)P\hat{G}A_{1000}}{P\hat{G}A_{1000} + c \left(\frac{V_{S30}}{V_{LIN}} \right)^n} & \text{for } V_{S30} < V_{LIN} \end{cases}$$

and

$$\varphi_B(T) = \sqrt{\varphi_0^2(T) - \varphi_{amp}^2(T)}$$

Following Abrahamson and Silva (2008), a value of $\varphi_{amp}(T) = 0.3$ natural log units is assumed for all periods. The phi and tau values listed in Table 4.5 are the $\varphi_0(T)$ and $\tau_0(T)$ in the equations for the nonlinear site effects on phi and tau given above.

Table 4.5 Aleatory variability terms (in LN units)

Period (sec)	phi	tau
0.01	0.62	0.58
0.02	0.62	0.58
0.03	0.62	0.58
0.05	0.62	0.58
0.075	0.62	0.58
0.1	0.62	0.58
0.15	0.62	0.56
0.2	0.62	0.54
0.25	0.62	0.52
0.3	0.62	0.505
0.4	0.62	0.48
0.5	0.62	0.46
0.6	0.62	0.45
0.75	0.62	0.45
1.0	0.62	0.45
1.5	0.62	0.45
2.0	0.62	0.45
2.5	0.62	0.45
3.0	0.62	0.45
4.0	0.62	0.45
5.0	0.62	0.45
6.0	0.62	0.45
7.5	0.62	0.45
10.0	0.62	0.45

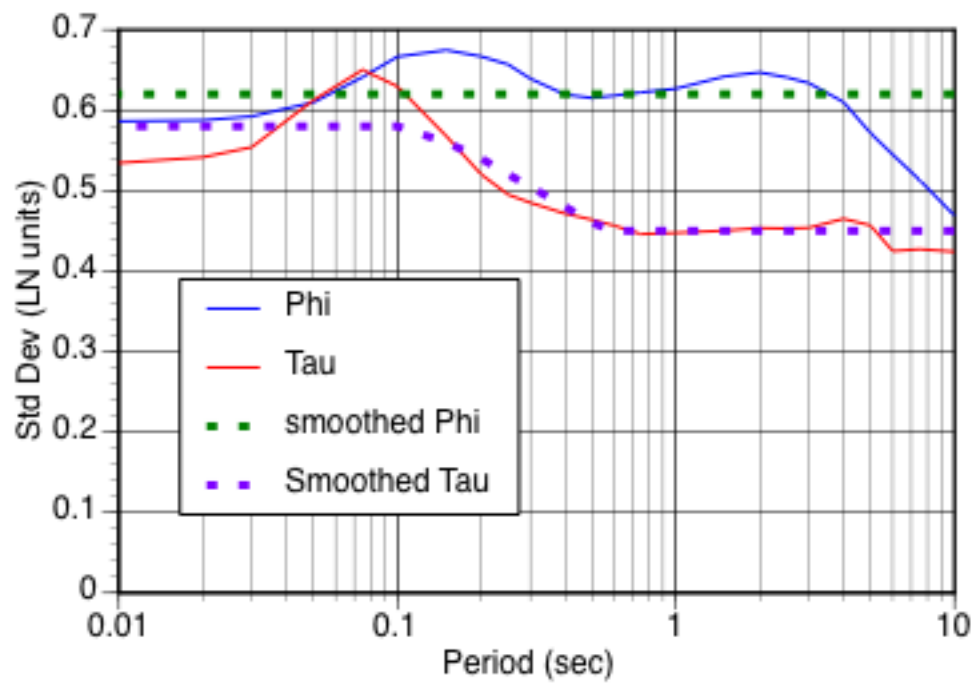


Figure 4.24 Smoothed phi and tau models.

5 Conclusions and Future Work

The updated BCHydro model is based on the expanded and improved NGA-SUB dataset and it includes the first order regional differences in the ground-motion scaling in terms of the V_{S30} scaling, linear R scaling, and a constant term. Due to these two changes, the model represents an improvement over the 2016 BCHydro GMM. The Updated BCHydro GMM is intended for application to the Cascadia region as part of the 2020 update to the national uniform-hazard maps. The ongoing NGA-SUB project will develop a suite of subduction GMMs that can be applied to other regions. These NGA-SUB GMMs will supersede this BCHydro updated GMM.

In developing this update of the BCHydro ground-motion model for subduction earthquakes, several technical issues were identified that were not resolved and should be addressed as part of the completion of the NGA-SUB project. These issues are listed below.

- On average, the short-period ground motion for the Cascadia earthquakes is much lower than for other regions. In this update, without a clear physical basis for this large reduction, the Cascadia GMM was increased to the global average. There is a need to determine the cause of the lower short-period ground motions in Cascadia.
- Basin effects were not included in the updated BCHydro model. Basin terms from empirical data are correlated with the V_{S30} scaling in the ground-motion model. The similarity or difference between basin scaling for different regions needs to be evaluated, then basin terms can be developed for Cascadia using either Cascadia data or global data for the basin scaling.
- The updated BCHydro model does not distinguish between forearc and backarc scaling. This is appropriate for Cascadia which did not show a significant difference in the attenuation rates for forearc and backarc stations, but in other regions of the world, this can be a large effect. The approach to modeling this effect in terms of the lengths of ray paths through forearc and backarc regions needs to be addressed.
- The magnitude scaling below the magnitude break point was modeled using the same scaling for interface and intraslab earthquakes. The event terms show that for the **M5** to **M6** range, the magnitude scaling for intraslab events is stronger than for interface events. The basis for using either the same magnitude scaling or different magnitude scaling for small magnitude interface and intraslab events should be revisited.

- The large magnitude scaling (above the break point) in the updated BCHydro model is based on finite-fault simulations for large interface earthquakes. This large scaling from the interface simulations was assumed to apply to the intraslab earthquakes as well. The new finite-fault simulations developed for intraslab earthquakes should be evaluated to determine if the large magnitude scaling from interface earthquakes is applicable to intraslab earthquakes.
- Site terms and single-station sigma was not evaluated in the updated BCHydro model. Because the locations of the subduction earthquakes often cover a limited azimuth range, the site terms may be strongly correlated with path terms. An evaluation of the trade-off between site and path terms is needed before developing single-station sigma models.
- The intraslab thickness was used to set the magnitude break for the intraslab scaling. Another approach would be to use the intraslab thickness to scale the difference between intraslab and interface events (the a_{10} term). The best use of the intraslab thickness to constrain the scaling of the intraslab ground motion needs further evaluation.
- Local site response depends on the level of shaking and the frequency content of the input rock motion as well as on the local site characteristics. The nonlinear site response scaling used for the updated BCH GMM was based on frequency content of rock motions generated by crustal events in active regions. The nonlinear site response scaling needs to be reevaluated using rock motions generated by subduction events.
- The analysis of ergodic site response for Cascadia in this study is preliminary and based on limited data. More complete analyses using additional data is needed to evaluate differences between VS30-scaling in Cascadia vs other regions of the United States. This will be considered in future ground motion analyses.

REFERENCES

- Abrahamson N.A., Gregor N., Addo K. (2016). BC Hydro ground motion prediction equations for subduction earthquakes, *Earthq. Spectra*, 32: 23–44.
- Abrahamson N.A., Youngs R.R. (1992). A stable algorithm for regression analyses using the random effects model, *Bull. Seismol. Soc. Am.*, 82: 505–510.
- Ancheta T.D., Darragh R.B., Stewart J.P., Seyhan E., Silva W.J., Chiou S.J., Wooddell K.E., Graves, R.W., Kottke A.R., Boore, D.M., Kishida T., and Donahue J.L. (2014). NGA-West2 Database, *Earthq. Spectra*, 30(3): 989–1005.
- Archuleta R., Ji C. (2018). Scaling of PGA and PGV deduced from numerical simulations of intraslab earthquakes, PEER Report, in preparation, Pacific Earthquake Engineering Research Center, University of California, Berkeley, CA.
- Atkinson, G.M., and Boore, G.M. 2003. Empirical ground-motion relationships for subduction-zone earthquakes and their application to Cascadia and other regions. *Bull. Seismol. Soc. Am.*, 93: 1703–1729.
- Atkinson, G.M., and Boore, G.M. 2008. Erratum to Empirical ground-motion relationships for subduction-zone earthquakes and their application to Cascadia and other regions. *Bull. Seismol. Soc. Am.*, 98, 2567–2569.
- Atkinson G.M., Macias M. (2009). Predicted ground motions for great interface earthquakes in the Cascadia subduction zone, *Bull. Seismol. Soc. Am.*, 99(3): 1552–1578.
- Gregor N.J., Silva W.J., Wong I.G., Youngs R.R. (2002). Ground-motion attenuation relationships for Cascadia subduction zone megathrust earthquakes based on a stochastic finite-fault modeling, *Bull. Seismol. Soc. Am.*, 92: 1923–1932. doi:10.1785/0120000260.
- Gregor N.J., Silva W.J., Wong I.G., and Youngs R.R. (2006). Updated Response Spectral Attenuation Relationship for Cascadia Subduction Zone Megathrust Earthquake, *Seism. Res. Letters*: 77, 2, 325–326.
- Gregor, N.J. Abrahamson N.A., Atkinson G.M., Boore D.M., Bozorgnia Y., Campbell K.W., Chiou S.J., Idriss I.M., Kamai R., Seyhan E., Silva, W.J. Stewart J.P. and Youngs R.R. (2014). Comparison of NGA-West2 GMPEs, *Earthq. Spectra*, 30(3): 1179–1197.
- Kishida T., Contreras V., Bozorgnia Y., Abrahamson N.A., Ahdi S.K., Ancheta T.D., Boore D.M., Campbell K.W., Chiou B., Darragh R., Gregor N., Kuehn N., Kwak D.Y., Kwok A.O., Lin P., Magistrale H., Mazzoni S., Muin S., Midorikawa S., Si H., Silva W.J., Stewart J.P., Wooddell K.E., Youngs R.R. (2018). NGA-Sub ground-motion database, *Proceedings, 11NCEE*, Los Angeles, CA.
- Zhao J.X., Zhang J., Asano A., Ohno Y., Oouchi T., Takahashi T., Ogawa H., Irikura K., Thio H.K., Somerville P.G., Fukushima Y., Fukushima Y. (2006). Attenuation relations of strong ground motion in Japan using site classification based on predominant period, *Bull. Seismol. Soc. Am.*, 96(3): 898–913.
- Zhao, J.X., Liang X., Jiang F., Xing H., Zhu M., Hou R., Zhang Y., Lan X., Rhoades D.A., Irikura K., Fukushima Y., and Somerville P.G. (2016). Ground-motion prediction equations for subduction interface earthquakes in Japan using site class and simple geometric attenuation functions, *Bull. Seismol. Soc. Am.*, 106 (4): 1518–1534.

PEER REPORTS

PEER reports are available as a free PDF download from http://peer.berkeley.edu/publications/peer_reports_complete.html. Printed hard copies of PEER reports can be ordered directly from our printer by following the instructions at http://peer.berkeley.edu/publications/peer_reports.html. For other related questions about the PEER Report Series, contact the Pacific Earthquake Engineering Research Center, 325 Davis Hall, Mail Code 1792, Berkeley, CA 94720. Tel.: (510) 642-3437; Fax: (510) 642-1655; Email: peer_center@berkeley.edu.

- PEER 2018/01** *PEER Annual Report 2017–2018*. Khalid Mosalam, Amarnath Kasalanati, and Selim Günay, June 2018.
- PEER 2017/12** *Experimental Investigation of the Behavior of Vintage and Retrofit Concentrically Braced Steel Frames under Cyclic Loading*. Barbara G. Simpson, Stephen A. Mahin, and Jiun-Wei Lai, December 2017.
- PEER 2017/11** *Preliminary Studies on the Dynamic Response of a Seismically Isolated Prototype Gen-IV Sodium-Cooled Fast Reactor (PGSFR)*. Benshun Shao, Andreas H. Schellenberg, Matthew J. Schoettler, and Stephen A. Mahin. December 2017.
- PEER 2017/10** *Development of Time Histories for IEEE693 Testing and Analysis (including Seismically Isolated Equipment)*. Shakhzod M. Takhirov, Eric Fujisaki, Leon Kempner, Michael Riley, and Brian Low. December 2017.
- PEER 2017/09** *“R” Package for Computation of Earthquake Ground-Motion Response Spectra*. Pengfei Wang, Jonathan P. Stewart, Yousef Bozorgnia, David M. Boore, and Tadahiro Kishida. December 2017.
- PEER 2017/08** *Influence of Kinematic SSI on Foundation Input Motions for Bridges on Deep Foundations*. Benjamin J. Turner, Scott J. Brandenburg, and Jonathan P. Stewart. November 2017.
- PEER 2017/07** *A Nonlinear Kinetic Model for Multi-Stage Friction Pendulum Systems*. Paul L. Drazin and Sanjay Govindjee, September 2017.
- PEER 2017/06** *Guidelines for Performance-Based Seismic Design of Tall Buildings, Version 2.02*. TBI Working Group led by co-chairs Ron Hamburger and Jack Moehle: Jack Baker, Jonathan Bray, C.B. Crouse, Greg Deierlein, John Hooper, Marshall Lew, Joe Maffei, Stephen Mahin, James Malley, Farzad Naeim, Jonathan Stewart, and John Wallace. May 2017.
- PEER 2017/05** *Recommendations for Ergodic Nonlinear Site Amplification in Central and Eastern North America*. Youssef M.A. Hashash, Joseph A. Harmon, Okan Ilhan, Grace A. Parker, and Jonathan P. Stewart. March 2017.
- PEER 2017/04** *Expert Panel Recommendations for Ergodic Site Amplification in Central and Eastern North America*. Jonathan P. Stewart, Grace A. Parker, Joseph P. Harmon, Gail M. Atkinson, David M. Boore, Robert B. Darragh, Walter J. Silva, and Youssef M.A. Hashash. March 2017.
- PEER 2017/03** *NGA-East Ground-Motion Models for the U.S. Geological Survey National Seismic Hazard Maps*. Christine A. Goulet, Yousef Bozorgnia, Nicolas Kuehn, Linda Al Atik, Robert R. Youngs, Robert W. Graves, and Gail M. Atkinson. March 2017.
- PEER 2017/02** *U.S.–New Zealand–Japan Workshop: Liquefaction-Induced Ground Movements Effects, University of California, Berkeley, California, 2–4 November 2016*. Jonathan D. Bray, Ross W. Boulanger, Misko Cubrinovski, Kohji Tokimatsu, Steven L. Kramer, Thomas O'Rourke, Ellen Rathje, Russell A. Green, Peter K. Robinson, and Christine Z. Beyzaei. March 2017.
- PEER 2017/01** *2016 PEER Annual Report*. Khalid M. Mosalam, Amarnath Kasalanati, and Grace Kang. March 2017.
- PEER 2016/10** *Performance-Based Robust Nonlinear Seismic Analysis with Application to Reinforced Concrete Bridge Systems*. Xiao Ling and Khalid M. Mosalam. December 2016.
- PEER 2016/08** *Resilience of Critical Structures, Infrastructure, and Communities*. Gian Paolo Cimellaro, Ali Zamani-Noori, Omar Kamouh, Vesna Terzic, and Stephen A. Mahin. December 2016.
- PEER 2016/07** *Hybrid Simulation Theory for a Classical Nonlinear Dynamical System*. Paul L. Drazin and Sanjay Govindjee. September 2016.
- PEER 2016/06** *California Earthquake Early Warning System Benefit Study*. Laurie A. Johnson, Sharyl Rabinovici, Grace S. Kang, and Stephen A. Mahin. July 2006.
- PEER 2016/05** *Ground-Motion Prediction Equations for Arias Intensity Consistent with the NGA-West2 Ground-Motion Models*. Charlotte Abrahamson, Hao-Jun Michael Shi, and Brian Yang. July 2016.

- PEER 2016/04** *The M_w 6.0 South Napa Earthquake of August 24, 2014: A Wake-Up Call for Renewed Investment in Seismic Resilience Across California.* Prepared for the California Seismic Safety Commission, Laurie A. Johnson and Stephen A. Mahin. May 2016.
- PEER 2016/03** *Simulation Confidence in Tsunami-Driven Overland Flow.* Patrick Lynett. May 2016.
- PEER 2016/02** *Semi-Automated Procedure for Windowing time Series and Computing Fourier Amplitude Spectra for the NGA-West2 Database.* Tadahiro Kishida, Olga-Joan Ktenidou, Robert B. Darragh, and Walter J. Silva. May 2016.
- PEER 2016/01** *A Methodology for the Estimation of Kappa (κ) from Large Datasets: Example Application to Rock Sites in the NGA-East Database and Implications on Design Motions.* Olga-Joan Ktenidou, Norman A. Abrahamson, Robert B. Darragh, and Walter J. Silva. April 2016.
- PEER 2015/13** *Self-Centering Precast Concrete Dual-Steel-Shell Columns for Accelerated Bridge Construction: Seismic Performance, Analysis, and Design.* Gabriele Guerrini, José I. Restrepo, Athanassios Vervelidis, and Milena Massari. December 2015.
- PEER 2015/12** *Shear-Flexure Interaction Modeling for Reinforced Concrete Structural Walls and Columns under Reversed Cyclic Loading.* Kristijan Kolozvari, Kutay Orakcal, and John Wallace. December 2015.
- PEER 2015/11** *Selection and Scaling of Ground Motions for Nonlinear Response History Analysis of Buildings in Performance-Based Earthquake Engineering.* N. Simon Kwong and Anil K. Chopra. December 2015.
- PEER 2015/10** *Structural Behavior of Column-Bent Cap Beam-Box Girder Systems in Reinforced Concrete Bridges Subjected to Gravity and Seismic Loads. Part II: Hybrid Simulation and Post-Test Analysis.* Mohamed A. Moustafa and Khalid M. Mosalam. November 2015.
- PEER 2015/09** *Structural Behavior of Column-Bent Cap Beam-Box Girder Systems in Reinforced Concrete Bridges Subjected to Gravity and Seismic Loads. Part I: Pre-Test Analysis and Quasi-Static Experiments.* Mohamed A. Moustafa and Khalid M. Mosalam. September 2015.
- PEER 2015/08** *NGA-East: Adjustments to Median Ground-Motion Models for Center and Eastern North America.* August 2015.
- PEER 2015/07** *NGA-East: Ground-Motion Standard-Deviation Models for Central and Eastern North America.* Linda Al Atik. June 2015.
- PEER 2015/06** *Adjusting Ground-Motion Intensity Measures to a Reference Site for which $V_{S30} = 3000$ m/sec.* David M. Boore. May 2015.
- PEER 2015/05** *Hybrid Simulation of Seismic Isolation Systems Applied to an APR-1400 Nuclear Power Plant.* Andreas H. Schellenberg, Alireza Sarebanha, Matthew J. Schoettler, Gilberto Mosqueda, Gianmario Benzoni, and Stephen A. Mahin. April 2015.
- PEER 2015/04** *NGA-East: Median Ground-Motion Models for the Central and Eastern North America Region.* April 2015.
- PEER 2015/03** *Single Series Solution for the Rectangular Fiber-Reinforced Elastomeric Isolator Compression Modulus.* James M. Kelly and Niel C. Van Engelen. March 2015.
- PEER 2015/02** *A Full-Scale, Single-Column Bridge Bent Tested by Shake-Table Excitation.* Matthew J. Schoettler, José I. Restrepo, Gabriele Guerrini, David E. Duck, and Francesco Carrea. March 2015.
- PEER 2015/01** *Concrete Column Blind Prediction Contest 2010: Outcomes and Observations.* Vesna Terzic, Matthew J. Schoettler, José I. Restrepo, and Stephen A. Mahin. March 2015.
- PEER 2014/20** *Stochastic Modeling and Simulation of Near-Fault Ground Motions for Performance-Based Earthquake Engineering.* Mayssa Dabaghi and Armen Der Kiureghian. December 2014.
- PEER 2014/19** *Seismic Response of a Hybrid Fiber-Reinforced Concrete Bridge Column Detailed for Accelerated Bridge Construction.* Wilson Nguyen, William Trono, Marios Panagiotou, and Claudia P. Ostertag. December 2014.
- PEER 2014/18** *Three-Dimensional Beam-Truss Model for Reinforced Concrete Walls and intraslabs Subjected to Cyclic Static or Dynamic Loading.* Yuan Lu, Marios Panagiotou, and Ioannis Koutromanos. December 2014.
- PEER 2014/17** *PEER NGA-East Database.* Christine A. Goulet, Tadahiro Kishida, Timothy D. Ancheta, Chris H. Cramer, Robert B. Darragh, Walter J. Silva, Youssef M.A. Hashash, Joseph Harmon, Jonathan P. Stewart, Katie E. Wooddell, and Robert R. Youngs. October 2014.
- PEER 2014/16** *Guidelines for Performing Hazard-Consistent One-Dimensional Ground Response Analysis for Ground Motion Prediction.* Jonathan P. Stewart, Kioumars Afshari, and Youssef M.A. Hashash. October 2014.
- PEER 2014/15** *NGA-East Regionalization Report: Comparison of Four Crustal Regions within Central and Eastern North America using Waveform Modeling and 5%-Damped Pseudo-Spectral Acceleration Response.* Jennifer Dreiling, Marius P. Isken, Walter D. Mooney, Martin C. Chapman, and Richard W. Godbee. October 2014.

- PEER 2014/14** *Scaling Relations between Seismic Moment and Rupture Area of Earthquakes in Stable Continental Regions.* Paul Somerville. August 2014.
- PEER 2014/13** *PEER Preliminary Notes and Observations on the August 24, 2014, South Napa Earthquake.* Grace S. Kang and Stephen A. Mahin, Editors. September 2014.
- PEER 2014/12** *Reference-Rock Site Conditions for Central and Eastern North America: Part II – Attenuation (Kappa) Definition.* Kenneth W. Campbell, Youssef M.A. Hashash, Byungmin Kim, Albert R. Kottke, Ellen M. Rathje, Walter J. Silva, and Jonathan P. Stewart. August 2014.
- PEER 2014/11** *Reference-Rock Site Conditions for Central and Eastern North America: Part I - Velocity Definition.* Youssef M.A. Hashash, Albert R. Kottke, Jonathan P. Stewart, Kenneth W. Campbell, Byungmin Kim, Ellen M. Rathje, Walter J. Silva, Sissy Nikolaou, and Cheryl Moss. August 2014.
- PEER 2014/10** *Evaluation of Collapse and Non-Collapse of Parallel Bridges Affected by Liquefaction and Lateral Spreading.* Benjamin Turner, Scott J. Brandenburg, and Jonathan P. Stewart. August 2014.
- PEER 2014/09** *PEER Arizona Strong-Motion Database and GMPEs Evaluation.* Tadahiro Kishida, Robert E. Kayen, Olga-Joan Ktenidou, Walter J. Silva, Robert B. Darragh, and Jennie Watson-Lamprey. June 2014.
- PEER 2014/08** *Unbonded Pretensioned Bridge Columns with Rocking Detail.* Jeffrey A. Schaefer, Bryan Kennedy, Marc O. Eberhard, and John F. Stanton. June 2014.
- PEER 2014/07** *Northridge 20 Symposium Summary Report: Impacts, Outcomes, and Next Steps.* May 2014.
- PEER 2014/06** *Report of the Tenth Planning Meeting of NEES/E-Defense Collaborative Research on Earthquake Engineering.* December 2013.
- PEER 2014/05** *Seismic Velocity Site Characterization of Thirty-One Chilean Seismometer Stations by Spectral Analysis of Surface Wave Dispersion.* Robert Kayen, Brad D. Carkin, Skye Corbet, Camilo Pinilla, Allan Ng, Edward Gorbis, and Christine Truong. April 2014.
- PEER 2014/04** *Effect of Vertical Acceleration on Shear Strength of Reinforced Concrete Columns.* Hyerin Lee and Khalid M. Mosalam. April 2014.
- PEER 2014/03** *Retest of Thirty-Year-Old Neoprene Isolation Bearings.* James M. Kelly and Niel C. Van Engelen. March 2014.
- PEER 2014/02** *Theoretical Development of Hybrid Simulation Applied to Plate Structures.* Ahmed A. Bakhty, Khalid M. Mosalam, and Sanjay Govindjee. January 2014.
- PEER 2014/01** *Performance-Based Seismic Assessment of Skewed Bridges.* Peyman Kaviani, Farzin Zareian, and Ertugrul Taciroglu. January 2014.
- PEER 2013/26** *Urban Earthquake Engineering.* Proceedings of the U.S.-Iran Seismic Workshop. December 2013.
- PEER 2013/25** *Earthquake Engineering for Resilient Communities: 2013 PEER Internship Program Research Report Collection.* Heidi Tremayne (Editor), Stephen A. Mahin (Editor), Jorge Archbold Monterossa, Matt Brosman, Shelly Dean, Katherine deLaveaga, Curtis Fong, Donovan Holder, Rakeeb Khan, Elizabeth Jachens, David Lam, Daniela Martinez Lopez, Mara Minner, Geffen Oren, Julia Pavicic, Melissa Quinonez, Lorena Rodriguez, Sean Salazar, Kelli Slaven, Vivian Steyert, Jenny Taing, and Salvador Tena. December 2013.
- PEER 2013/24** *NGA-West2 Ground Motion Prediction Equations for Vertical Ground Motions.* September 2013.
- PEER 2013/23** *Coordinated Planning and Preparedness for Fire Following Major Earthquakes.* Charles Scawthorn. November 2013.
- PEER 2013/22** *GEM-PEER Task 3 Project: Selection of a Global Set of Ground Motion Prediction Equations.* Jonathan P. Stewart, John Douglas, Mohammad B. Javanbarg, Carola Di Alessandro, Yousef Bozorgnia, Norman A. Abrahamson, David M. Boore, Kenneth W. Campbell, Elise Delavaud, Mustafa Erdik, and Peter J. Stafford. December 2013.
- PEER 2013/21** *Seismic Design and Performance of Bridges with Columns on Rocking Foundations.* Grigorios Antonellis and Marios Panagiotou. September 2013.
- PEER 2013/20** *Experimental and Analytical Studies on the Seismic Behavior of Conventional and Hybrid Braced Frames.* Jiun-Wei Lai and Stephen A. Mahin. September 2013.
- PEER 2013/19** *Toward Resilient Communities: A Performance-Based Engineering Framework for Design and Evaluation of the Built Environment.* Michael William Mieler, Bozidar Stojadinovic, Robert J. Budnitz, Stephen A. Mahin, and Mary C. Comerio. September 2013.
- PEER 2013/18** *Identification of Site Parameters that Improve Predictions of Site Amplification.* Ellen M. Rathje and Sara Navidi. July 2013.

- PEER 2013/17** *Response Spectrum Analysis of Concrete Gravity Dams Including Dam-Water-Foundation Interaction.* Arnkjell Løkke and Anil K. Chopra. July 2013.
- PEER 2013/16** *Effect of Hoop Reinforcement Spacing on the Cyclic Response of Large Reinforced Concrete Special Moment Frame Beams.* Marios Panagiotou, Tea Visnjic, Grigorios Antonellis, Panagiotis Galanis, and Jack P. Moehle. June 2013.
- PEER 2013/15** *A Probabilistic Framework to Include the Effects of Near-Fault Directivity in Seismic Hazard Assessment.* Shrey Kumar Shahi, Jack W. Baker. October 2013.
- PEER 2013/14** *Hanging-Wall Scaling using Finite-Fault Simulations.* Jennifer L. Donahue and Norman A. Abrahamson. September 2013.
- PEER 2013/13** *Semi-Empirical Nonlinear Site Amplification and its Application in NEHRP Site Factors.* Jonathan P. Stewart and Emel Seyhan. November 2013.
- PEER 2013/12** *Nonlinear Horizontal Site Response for the NGA-West2 Project.* Ronnie Kamai, Norman A. Abramson, Walter J. Silva. May 2013.
- PEER 2013/11** *Epistemic Uncertainty for NGA-West2 Models.* Linda Al Atik and Robert R. Youngs. May 2013.
- PEER 2013/10** *NGA-West 2 Models for Ground-Motion Directionality.* Shrey K. Shahi and Jack W. Baker. May 2013.
- PEER 2013/09** *Final Report of the NGA-West2 Directivity Working Group.* Paul Spudich, Jeffrey R. Bayless, Jack W. Baker, Brian S.J. Chiou, Badie Rowshandel, Shrey Shahi, and Paul Somerville. May 2013.
- PEER 2013/08** *NGA-West2 Model for Estimating Average Horizontal Values of Pseudo-Absolute Spectral Accelerations Generated by Crustal Earthquakes.* I. M. Idriss. May 2013.
- PEER 2013/07** *Update of the Chiou and Youngs NGA Ground Motion Model for Average Horizontal Component of Peak Ground Motion and Response Spectra.* Brian Chiou and Robert Youngs. May 2013.
- PEER 2013/06** *NGA-West2 Campbell-Bozorgnia Ground Motion Model for the Horizontal Components of PGA, PGV, and 5%-Damped Elastic Pseudo-Acceleration Response Spectra for Periods Ranging from 0.01 to 10 sec.* Kenneth W. Campbell and Yousef Bozorgnia. May 2013.
- PEER 2013/05** *NGA-West 2 Equations for Predicting Response Spectral Accelerations for Shallow Crustal Earthquakes.* David M. Boore, Jonathan P. Stewart, Emel Seyhan, and Gail M. Atkinson. May 2013.
- PEER 2013/04** *Update of the AS08 Ground-Motion Prediction Equations Based on the NGA-West2 Data Set.* Norman Abrahamson, Walter Silva, and Ronnie Kamai. May 2013.
- PEER 2013/03** *PEER NGA-West2 Database.* Timothy D. Ancheta, Robert B. Darragh, Jonathan P. Stewart, Emel Seyhan, Walter J. Silva, Brian S.J. Chiou, Katie E. Wooddell, Robert W. Graves, Albert R. Kottke, David M. Boore, Tadahiro Kishida, and Jennifer L. Donahue. May 2013.
- PEER 2013/02** *Hybrid Simulation of the Seismic Response of Squat Reinforced Concrete Shear Walls.* Catherine A. Whyte and Bozidar Stojadinovic. May 2013.
- PEER 2013/01** *Housing Recovery in Chile: A Qualitative Mid-program Review.* Mary C. Comerio. February 2013.
- PEER 2012/08** *Guidelines for Estimation of Shear Wave Velocity.* Bernard R. Wair, Jason T. DeJong, and Thomas Shantz. December 2012.
- PEER 2012/07** *Earthquake Engineering for Resilient Communities: 2012 PEER Internship Program Research Report Collection.* Heidi Tremayne (Editor), Stephen A. Mahin (Editor), Collin Anderson, Dustin Cook, Michael Erceg, Carlos Esparza, Jose Jimenez, Dorian Krausz, Andrew Lo, Stephanie Lopez, Nicole McCurdy, Paul Shipman, Alexander Strum, Eduardo Vega. December 2012.
- PEER 2012/06** *Fragilities for Precarious Rocks at Yucca Mountain.* Matthew D. Purvance, Rasool Anooshehpour, and James N. Brune. December 2012.
- PEER 2012/05** *Development of Simplified Analysis Procedure for Piles in Laterally Spreading Layered Soils.* Christopher R. McGann, Pedro Arduino, and Peter Mackenzie-Helnwein. December 2012.
- PEER 2012/04** *Unbonded Pre-Tensioned Columns for Bridges in Seismic Regions.* Phillip M. Davis, Todd M. Janes, Marc O. Eberhard, and John F. Stanton. December 2012.
- PEER 2012/03** *Experimental and Analytical Studies on Reinforced Concrete Buildings with Seismically Vulnerable Beam-Column Joints.* Sangjoon Park and Khalid M. Mosalam. October 2012.
- PEER 2012/02** *Seismic Performance of Reinforced Concrete Bridges Allowed to Uplift during Multi-Directional Excitation.* Andres Oscar Espinoza and Stephen A. Mahin. July 2012.

- PEER 2012/01** *Spectral Damping Scaling Factors for Shallow Crustal Earthquakes in Active Tectonic Regions.* Sanaz Rezaeian, Yousef Bozorgnia, I. M. Idriss, Kenneth Campbell, Norman Abrahamson, and Walter Silva. July 2012.
- PEER 2011/10** *Earthquake Engineering for Resilient Communities: 2011 PEER Internship Program Research Report Collection.* Heidi Faison and Stephen A. Mahin, Editors. December 2011.
- PEER 2011/09** *Calibration of Semi-Stochastic Procedure for Simulating High-Frequency Ground Motions.* Jonathan P. Stewart, Emel Seyhan, and Robert W. Graves. December 2011.
- PEER 2011/08** *Water Supply in regard to Fire Following Earthquake.* Charles Scawthorn. November 2011.
- PEER 2011/07** *Seismic Risk Management in Urban Areas.* Proceedings of a U.S.-Iran-Turkey Seismic Workshop. September 2011.
- PEER 2011/06** *The Use of Base Isolation Systems to Achieve Complex Seismic Performance Objectives.* Troy A. Morgan and Stephen A. Mahin. July 2011.
- PEER 2011/05** *Case Studies of the Seismic Performance of Tall Buildings Designed by Alternative Means.* Task 12 Report for the Tall Buildings Initiative. Jack Moehle, Yousef Bozorgnia, Nirmal Jayaram, Pierson Jones, Mohsen Rahnama, Niles Shome, Zeynep Tuna, John Wallace, Tony Yang, and Farzin Zareian. July 2011.
- PEER 2011/04** *Recommended Design Practice for Pile Foundations in Laterally Spreading Ground.* Scott A. Ashford, Ross W. Boulanger, and Scott J. Brandenberg. June 2011.
- PEER 2011/03** *New Ground Motion Selection Procedures and Selected Motions for the PEER Transportation Research Program.* Jack W. Baker, Ting Lin, Shrey K. Shahi, and Nirmal Jayaram. March 2011.
- PEER 2011/02** *A Bayesian Network Methodology for Infrastructure Seismic Risk Assessment and Decision Support.* Michelle T. Bensi, Armen Der Kiureghian, and Daniel Straub. March 2011.
- PEER 2011/01** *Demand Fragility Surfaces for Bridges in Liquefied and Laterally Spreading Ground.* Scott J. Brandenberg, Jian Zhang, Pirooz Kashighandi, Yili Huo, and Minxing Zhao. March 2011.
- PEER 2010/05** *Guidelines for Performance-Based Seismic Design of Tall Buildings.* Developed by the Tall Buildings Initiative. November 2010.
- PEER 2010/04** *Application Guide for the Design of Flexible and Rigid Bus Connections between Substation Equipment Subjected to Earthquakes.* Jean-Bernard Dastous and Armen Der Kiureghian. September 2010.
- PEER 2010/03** *Shear Wave Velocity as a Statistical Function of Standard Penetration Test Resistance and Vertical Effective Stress at Caltrans Bridge Sites.* Scott J. Brandenberg, Naresh Bellana, and Thomas Shantz. June 2010.
- PEER 2010/02** *Stochastic Modeling and Simulation of Ground Motions for Performance-Based Earthquake Engineering.* Sanaz Rezaeian and Armen Der Kiureghian. June 2010.
- PEER 2010/01** *Structural Response and Cost Characterization of Bridge Construction Using Seismic Performance Enhancement Strategies.* Ady Aviram, Božidar Stojadinović, Gustavo J. Parra-Montesinos, and Kevin R. Mackie. March 2010.
- PEER 2009/03** *The Integration of Experimental and Simulation Data in the Study of Reinforced Concrete Bridge Systems Including Soil-Foundation-Structure Interaction.* Matthew Dryden and Gregory L. Fenves. November 2009.
- PEER 2009/02** *Improving Earthquake Mitigation through Innovations and Applications in Seismic Science, Engineering, Communication, and Response.* Proceedings of a U.S.-Iran Seismic Workshop. October 2009.
- PEER 2009/01** *Evaluation of Ground Motion Selection and Modification Methods: Predicting Median Interstory Drift Response of Buildings.* Curt B. Haselton, Editor. June 2009.
- PEER 2008/10** *Technical Manual for Strata.* Albert R. Kottke and Ellen M. Rathje. February 2009.
- PEER 2008/09** *NGA Model for Average Horizontal Component of Peak Ground Motion and Response Spectra.* Brian S.-J. Chiou and Robert R. Youngs. November 2008.
- PEER 2008/08** *Toward Earthquake-Resistant Design of Concentrically Braced Steel Structures.* Patxi Uriz and Stephen A. Mahin. November 2008.
- PEER 2008/07** *Using OpenSees for Performance-Based Evaluation of Bridges on Liquefiable Soils.* Stephen L. Kramer, Pedro Arduino, and HyungSuk Shin. November 2008.
- PEER 2008/06** *Shaking Table Tests and Numerical Investigation of Self-Centering Reinforced Concrete Bridge Columns.* Hyung IL Jeong, Junichi Sakai, and Stephen A. Mahin. September 2008.
- PEER 2008/05** *Performance-Based Earthquake Engineering Design Evaluation Procedure for Bridge Foundations Undergoing Liquefaction-Induced Lateral Ground Displacement.* Christian A. Ledezma and Jonathan D. Bray. August 2008.

- PEER 2008/04** *Benchmarking of Nonlinear Geotechnical Ground Response Analysis Procedures.* Jonathan P. Stewart, Annie On-Lei Kwok, Youssef M. A. Hashash, Neven Matasovic, Robert Pyke, Zhiliang Wang, and Zhaohui Yang. August 2008.
- PEER 2008/03** *Guidelines for Nonlinear Analysis of Bridge Structures in California.* Ady Aviram, Kevin R. Mackie, and Božidar Stojadinović. August 2008.
- PEER 2008/02** *Treatment of Uncertainties in Seismic-Risk Analysis of Transportation Systems.* Evangelos Stergiou and Anne S. Kiremidjian. July 2008.
- PEER 2008/01** *Seismic Performance Objectives for Tall Buildings.* William T. Holmes, Charles Kircher, William Petak, and Nabih Youssef. August 2008.
- PEER 2007/12** *An Assessment to Benchmark the Seismic Performance of a Code-Conforming Reinforced Concrete Moment-Frame Building.* Curt Haselton, Christine A. Goulet, Judith Mitrani-Reiser, James L. Beck, Gregory G. Deierlein, Keith A. Porter, Jonathan P. Stewart, and Ertugrul Taciroglu. August 2008.
- PEER 2007/11** *Bar Buckling in Reinforced Concrete Bridge Columns.* Wayne A. Brown, Dawn E. Lehman, and John F. Stanton. February 2008.
- PEER 2007/10** *Computational Modeling of Progressive Collapse in Reinforced Concrete Frame Structures.* Mohamed M. Talaat and Khalid M. Mosalam. May 2008.
- PEER 2007/09** *Integrated Probabilistic Performance-Based Evaluation of Benchmark Reinforced Concrete Bridges.* Kevin R. Mackie, John-Michael Wong, and Božidar Stojadinović. January 2008.
- PEER 2007/08** *Assessing Seismic Collapse Safety of Modern Reinforced Concrete Moment-Frame Buildings.* Curt B. Haselton and Gregory G. Deierlein. February 2008.
- PEER 2007/07** *Performance Modeling Strategies for Modern Reinforced Concrete Bridge Columns.* Michael P. Berry and Marc O. Eberhard. April 2008.
- PEER 2007/06** *Development of Improved Procedures for Seismic Design of Buried and Partially Buried Structures.* Linda Al Atik and Nicholas Sitar. June 2007.
- PEER 2007/05** *Uncertainty and Correlation in Seismic Risk Assessment of Transportation Systems.* Renee G. Lee and Anne S. Kiremidjian. July 2007.
- PEER 2007/04** *Numerical Models for Analysis and Performance-Based Design of Shallow Foundations Subjected to Seismic Loading.* Sivapalan Gajan, Tara C. Hutchinson, Bruce L. Kutter, Prishati Raychowdhury, José A. Ugalde, and Jonathan P. Stewart. May 2008.
- PEER 2007/03** *Beam-Column Element Model Calibrated for Predicting Flexural Response Leading to Global Collapse of RC Frame Buildings.* Curt B. Haselton, Abbie B. Liel, Sarah Taylor Lange, and Gregory G. Deierlein. May 2008.
- PEER 2007/02** *Campbell-Bozorgnia NGA Ground Motion Relations for the Geometric Mean Horizontal Component of Peak and Spectral Ground Motion Parameters.* Kenneth W. Campbell and Yousef Bozorgnia. May 2007.
- PEER 2007/01** *Boore-Atkinson NGA Ground Motion Relations for the Geometric Mean Horizontal Component of Peak and Spectral Ground Motion Parameters.* David M. Boore and Gail M. Atkinson. May 2007.
- PEER 2006/12** *Societal Implications of Performance-Based Earthquake Engineering.* Peter J. May. May 2007.
- PEER 2006/11** *Probabilistic Seismic Demand Analysis Using Advanced Ground Motion Intensity Measures, Attenuation Relationships, and Near-Fault Effects.* Polsak Tothong and C. Allin Cornell. March 2007.
- PEER 2006/10** *Application of the PEER PBEE Methodology to the I-880 Viaduct.* Sashi Kunnath. February 2007.
- PEER 2006/09** *Quantifying Economic Losses from Travel Forgone Following a Large Metropolitan Earthquake.* James Moore, Sungbin Cho, Yue Yue Fan, and Stuart Werner. November 2006.
- PEER 2006/08** *Vector-Valued Ground Motion Intensity Measures for Probabilistic Seismic Demand Analysis.* Jack W. Baker and C. Allin Cornell. October 2006.
- PEER 2006/07** *Analytical Modeling of Reinforced Concrete Walls for Predicting Flexural and Coupled-Shear-Flexural Responses.* Kutay Orakcal, Leonardo M. Massone, and John W. Wallace. October 2006.
- PEER 2006/06** *Nonlinear Analysis of a Soil-Drilled Pier System under Static and Dynamic Axial Loading.* Gang Wang and Nicholas Sitar. November 2006.
- PEER 2006/05** *Advanced Seismic Assessment Guidelines.* Paolo Bazzurro, C. Allin Cornell, Charles Menun, Maziar Motahari, and Nicolas Luco. September 2006.

- PEER 2006/04** *Probabilistic Seismic Evaluation of Reinforced Concrete Structural Components and Systems*. Tae Hyung Lee and Khalid M. Mosalam. August 2006.
- PEER 2006/03** *Performance of Lifelines Subjected to Lateral Spreading*. Scott A. Ashford and Teerawut Juirnarongrit. July 2006.
- PEER 2006/02** *Pacific Earthquake Engineering Research Center Highway Demonstration Project*. Anne Kiremidjian, James Moore, Yue Yue Fan, Nesrin Basoz, Ozgur Yazali, and Meredith Williams. April 2006.
- PEER 2006/01** *Bracing Berkeley. A Guide to Seismic Safety on the UC Berkeley Campus*. Mary C. Comerio, Stephen Tobriner, and Ariane Fehrenkamp. January 2006.
- PEER 2005/17** *Earthquake Simulation Tests on Reducing Residual Displacements of Reinforced Concrete Bridges*. Junichi Sakai, Stephen A Mahin, and Andres Espinoza. December 2005.
- PEER 2005/16** *Seismic Response and Reliability of Electrical Substation Equipment and Systems*. Junho Song, Armen Der Kiureghian, and Jerome L. Sackman. April 2006.
- PEER 2005/15** *CPT-Based Probabilistic Assessment of Seismic Soil Liquefaction Initiation*. R. E. S. Moss, R. B. Seed, R. E. Kayen, J. P. Stewart, and A. Der Kiureghian. April 2006.
- PEER 2005/14** *Workshop on Modeling of Nonlinear Cyclic Load-Deformation Behavior of Shallow Foundations*. Bruce L. Kutter, Geoffrey Martin, Tara Hutchinson, Chad Harden, Sivapalan Gajan, and Justin Phalen. March 2006.
- PEER 2005/13** *Stochastic Characterization and Decision Bases under Time-Dependent Aftershock Risk in Performance-Based Earthquake Engineering*. Gee Liek Yeo and C. Allin Cornell. July 2005.
- PEER 2005/12** *PEER Testbed Study on a Laboratory Building: Exercising Seismic Performance Assessment*. Mary C. Comerio, Editor. November 2005.
- PEER 2005/11** *Van Nuys Hotel Building Testbed Report: Exercising Seismic Performance Assessment*. Helmut Krawinkler, Editor. October 2005.
- PEER 2005/10** *First NEES/E-Defense Workshop on Collapse Simulation of Reinforced Concrete Building Structures*. September 2005.
- PEER 2005/09** *Test Applications of Advanced Seismic Assessment Guidelines*. Joe Maffei, Karl Telleen, Danya Mohr, William Holmes, and Yuki Nakayama. August 2006.
- PEER 2005/08** *Damage Accumulation in Lightly Confined Reinforced Concrete Bridge Columns*. R. Tyler Ranf, Jared M. Nelson, Zach Price, Marc O. Eberhard, and John F. Stanton. April 2006.
- PEER 2005/07** *Experimental and Analytical Studies on the Seismic Response of Freestanding and Anchored Laboratory Equipment*. Dimitrios Konstantinidis and Nicos Makris. January 2005.
- PEER 2005/06** *Global Collapse of Frame Structures under Seismic Excitations*. Luis F. Ibarra and Helmut Krawinkler. September 2005.
- PEER 2005/05** *Performance Characterization of Bench- and Shelf-Mounted Equipment*. Samit Ray Chaudhuri and Tara C. Hutchinson. May 2006.
- PEER 2005/04** *Numerical Modeling of the Nonlinear Cyclic Response of Shallow Foundations*. Chad Harden, Tara Hutchinson, Geoffrey R. Martin, and Bruce L. Kutter. August 2005.
- PEER 2005/03** *A Taxonomy of Building Components for Performance-Based Earthquake Engineering*. Keith A. Porter. September 2005.
- PEER 2005/02** *Fragility Basis for California Highway Overpass Bridge Seismic Decision Making*. Kevin R. Mackie and Božidar Stojadinović. June 2005.
- PEER 2005/01** *Empirical Characterization of Site Conditions on Strong Ground Motion*. Jonathan P. Stewart, Yoojoong Choi, and Robert W. Graves. June 2005.
- PEER 2004/09** *Electrical Substation Equipment Interaction: Experimental Rigid Conductor Studies*. Christopher Stearns and André Filiatrault. February 2005.
- PEER 2004/08** *Seismic Qualification and Fragility Testing of Line Break 550-kV Disconnect Switches*. Shakhzod M. Takhirov, Gregory L. Fenves, and Eric Fujisaki. January 2005.
- PEER 2004/07** *Ground Motions for Earthquake Simulator Qualification of Electrical Substation Equipment*. Shakhzod M. Takhirov, Gregory L. Fenves, Eric Fujisaki, and Don Clyde. January 2005.
- PEER 2004/06** *Performance-Based Regulation and Regulatory Regimes*. Peter J. May and Chris Koski. September 2004.

- PEER 2004/05** *Performance-Based Seismic Design Concepts and Implementation: Proceedings of an International Workshop.* Peter Fajfar and Helmut Krawinkler, Editors. September 2004.
- PEER 2004/04** *Seismic Performance of an Instrumented Tilt-up Wall Building.* James C. Anderson and Vitelmo V. Bertero. July 2004.
- PEER 2004/03** *Evaluation and Application of Concrete Tilt-up Assessment Methodologies.* Timothy Graf and James O. Malley. October 2004.
- PEER 2004/02** *Analytical Investigations of New Methods for Reducing Residual Displacements of Reinforced Concrete Bridge Columns.* Junichi Sakai and Stephen A. Mahin. August 2004.
- PEER 2004/01** *Seismic Performance of Masonry Buildings and Design Implications.* Kerri Anne Taeko Tokoro, James C. Anderson, and Vitelmo V. Bertero. February 2004.
- PEER 2003/18** *Performance Models for Flexural Damage in Reinforced Concrete Columns.* Michael Berry and Marc Eberhard. August 2003.
- PEER 2003/17** *Predicting Earthquake Damage in Older Reinforced Concrete Beam-Column Joints.* Catherine Pagni and Laura Lowes. October 2004.
- PEER 2003/16** *Seismic Demands for Performance-Based Design of Bridges.* Kevin Mackie and Božidar Stojadinović. August 2003.
- PEER 2003/15** *Seismic Demands for Nondeteriorating Frame Structures and Their Dependence on Ground Motions.* Ricardo Antonio Medina and Helmut Krawinkler. May 2004.
- PEER 2003/14** *Finite Element Reliability and Sensitivity Methods for Performance-Based Earthquake Engineering.* Terje Haukaas and Armen Der Kiureghian. April 2004.
- PEER 2003/13** *Effects of Connection Hysteretic Degradation on the Seismic Behavior of Steel Moment-Resisting Frames.* Janise E. Rodgers and Stephen A. Mahin. March 2004.
- PEER 2003/12** *Implementation Manual for the Seismic Protection of Laboratory Contents: Format and Case Studies.* William T. Holmes and Mary C. Comerio. October 2003.
- PEER 2003/11** *Fifth U.S.-Japan Workshop on Performance-Based Earthquake Engineering Methodology for Reinforced Concrete Building Structures.* February 2004.
- PEER 2003/10** *A Beam-Column Joint Model for Simulating the Earthquake Response of Reinforced Concrete Frames.* Laura N. Lowes, Nilanjan Mitra, and Arash Altoontash. February 2004.
- PEER 2003/09** *Sequencing Repairs after an Earthquake: An Economic Approach.* Marco Casari and Simon J. Wilkie. April 2004.
- PEER 2003/08** *A Technical Framework for Probability-Based Demand and Capacity Factor Design (DCFD) Seismic Formats.* Fatemeh Jalayer and C. Allin Cornell. November 2003.
- PEER 2003/07** *Uncertainty Specification and Propagation for Loss Estimation Using FOSM Methods.* Jack W. Baker and C. Allin Cornell. September 2003.
- PEER 2003/06** *Performance of Circular Reinforced Concrete Bridge Columns under Bidirectional Earthquake Loading.* Mahmoud M. Hachem, Stephen A. Mahin, and Jack P. Moehle. February 2003.
- PEER 2003/05** *Response Assessment for Building-Specific Loss Estimation.* Eduardo Miranda and Shahram Taghavi. September 2003.
- PEER 2003/04** *Experimental Assessment of Columns with Short Lap Splices Subjected to Cyclic Loads.* Murat Melek, John W. Wallace, and Joel Conte. April 2003.
- PEER 2003/03** *Probabilistic Response Assessment for Building-Specific Loss Estimation.* Eduardo Miranda and Hesameddin Aslani. September 2003.
- PEER 2003/02** *Software Framework for Collaborative Development of Nonlinear Dynamic Analysis Program.* Jun Peng and Kincho H. Law. September 2003.
- PEER 2003/01** *Shake Table Tests and Analytical Studies on the Gravity Load Collapse of Reinforced Concrete Frames.* Kenneth John Elwood and Jack P. Moehle. November 2003.
- PEER 2002/24** *Performance of Beam to Column Bridge Joints Subjected to a Large Velocity Pulse.* Natalie Gibson, André Filiatrault, and Scott A. Ashford. April 2002.
- PEER 2002/23** *Effects of Large Velocity Pulses on Reinforced Concrete Bridge Columns.* Greg L. Orozco and Scott A. Ashford. April 2002.
- PEER 2002/22** *Characterization of Large Velocity Pulses for Laboratory Testing.* Kenneth E. Cox and Scott A. Ashford. April 2002.

- PEER 2002/21** *Fourth U.S.-Japan Workshop on Performance-Based Earthquake Engineering Methodology for Reinforced Concrete Building Structures.* December 2002.
- PEER 2002/20** *Barriers to Adoption and Implementation of PBEE Innovations.* Peter J. May. August 2002.
- PEER 2002/19** *Economic-Engineered Integrated Models for Earthquakes: Socioeconomic Impacts.* Peter Gordon, James E. Moore II, and Harry W. Richardson. July 2002.
- PEER 2002/18** *Assessment of Reinforced Concrete Building Exterior Joints with Substandard Details.* Chris P. Pantelides, Jon Hansen, Justin Nadauld, and Lawrence D. Reaveley. May 2002.
- PEER 2002/17** *Structural Characterization and Seismic Response Analysis of a Highway Overcrossing Equipped with Elastomeric Bearings and Fluid Dampers: A Case Study.* Nicos Makris and Jian Zhang. November 2002.
- PEER 2002/16** *Estimation of Uncertainty in Geotechnical Properties for Performance-Based Earthquake Engineering.* Allen L. Jones, Steven L. Kramer, and Pedro Arduino. December 2002.
- PEER 2002/15** *Seismic Behavior of Bridge Columns Subjected to Various Loading Patterns.* Asadollah Esmaeily-Gh. and Yan Xiao. December 2002.
- PEER 2002/14** *Inelastic Seismic Response of Extended Pile Shaft Supported Bridge Structures.* T.C. Hutchinson, R.W. Boulanger, Y.H. Chai, and I.M. Idriss. December 2002.
- PEER 2002/13** *Probabilistic Models and Fragility Estimates for Bridge Components and Systems.* Paolo Gardoni, Armen Der Kiureghian, and Khalid M. Mosalam. June 2002.
- PEER 2002/12** *Effects of Fault Dip and Slip Rake on Near-Source Ground Motions: Why Chi-Chi Was a Relatively Mild M7.6 Earthquake.* Brad T. Aagaard, John F. Hall, and Thomas H. Heaton. December 2002.
- PEER 2002/11** *Analytical and Experimental Study of Fiber-Reinforced Strip Isolators.* James M. Kelly and Shakhzod M. Takhirov. September 2002.
- PEER 2002/10** *Centrifuge Modeling of Settlement and Lateral Spreading with Comparisons to Numerical Analyses.* Sivapalan Gajan and Bruce L. Kutter. January 2003.
- PEER 2002/09** *Documentation and Analysis of Field Case Histories of Seismic Compression during the 1994 Northridge, California, Earthquake.* Jonathan P. Stewart, Patrick M. Smith, Daniel H. Whang, and Jonathan D. Bray. October 2002.
- PEER 2002/08** *Component Testing, Stability Analysis and Characterization of Buckling-Restrained Unbonded BracesTM.* Cameron Black, Nicos Makris, and Ian Aiken. September 2002.
- PEER 2002/07** *Seismic Performance of Pile-Wharf Connections.* Charles W. Roeder, Robert Graff, Jennifer Soderstrom, and Jun Han Yoo. December 2001.
- PEER 2002/06** *The Use of Benefit-Cost Analysis for Evaluation of Performance-Based Earthquake Engineering Decisions.* Richard O. Zerbe and Anthony Falit-Baiamonte. September 2001.
- PEER 2002/05** *Guidelines, Specifications, and Seismic Performance Characterization of Nonstructural Building Components and Equipment.* André Filiatrault, Constantin Christopoulos, and Christopher Stearns. September 2001.
- PEER 2002/04** *Consortium of Organizations for Strong-Motion Observation Systems and the Pacific Earthquake Engineering Research Center Lifelines Program: Invited Workshop on Archiving and Web Dissemination of Geotechnical Data, 4-5 October 2001.* September 2002.
- PEER 2002/03** *Investigation of Sensitivity of Building Loss Estimates to Major Uncertain Variables for the Van Nuys Testbed.* Keith A. Porter, James L. Beck, and Rustem V. Shaikhutdinov. August 2002.
- PEER 2002/02** *The Third U.S.-Japan Workshop on Performance-Based Earthquake Engineering Methodology for Reinforced Concrete Building Structures.* July 2002.
- PEER 2002/01** *Nonstructural Loss Estimation: The UC Berkeley Case Study.* Mary C. Comerio and John C. Stallmeyer. December 2001.
- PEER 2001/16** *Statistics of SDF-System Estimate of Roof Displacement for Pushover Analysis of Buildings.* Anil K. Chopra, Rakesh K. Goel, and Chatpan Chintanapakdee. December 2001.
- PEER 2001/15** *Damage to Bridges during the 2001 Nisqually Earthquake.* R. Tyler Ranf, Marc O. Eberhard, and Michael P. Berry. November 2001.
- PEER 2001/14** *Rocking Response of Equipment Anchored to a Base Foundation.* Nicos Makris and Cameron J. Black. September 2001.
- PEER 2001/13** *Modeling Soil Liquefaction Hazards for Performance-Based Earthquake Engineering.* Steven L. Kramer and Ahmed-W. Elgamal. February 2001.

- PEER 2001/12** *Development of Geotechnical Capabilities in OpenSees.* Boris Jeremić. September 2001.
- PEER 2001/11** *Analytical and Experimental Study of Fiber-Reinforced Elastomeric Isolators.* James M. Kelly and Shakhzod M. Takhirov. September 2001.
- PEER 2001/10** *Amplification Factors for Spectral Acceleration in Active Regions.* Jonathan P. Stewart, Andrew H. Liu, Yoojoong Choi, and Mehmet B. Baturay. December 2001.
- PEER 2001/09** *Ground Motion Evaluation Procedures for Performance-Based Design.* Jonathan P. Stewart, Shyh-Jeng Chiou, Jonathan D. Bray, Robert W. Graves, Paul G. Somerville, and Norman A. Abrahamson. September 2001.
- PEER 2001/08** *Experimental and Computational Evaluation of Reinforced Concrete Bridge Beam-Column Connections for Seismic Performance.* Clay J. Naito, Jack P. Moehle, and Khalid M. Mosalam. November 2001.
- PEER 2001/07** *The Rocking Spectrum and the Shortcomings of Design Guidelines.* Nicos Makris and Dimitrios Konstantinidis. August 2001.
- PEER 2001/06** *Development of an Electrical Substation Equipment Performance Database for Evaluation of Equipment Fragilities.* Thalia Agninos. April 1999.
- PEER 2001/05** *Stiffness Analysis of Fiber-Reinforced Elastomeric Isolators.* Hsiang-Chuan Tsai and James M. Kelly. May 2001.
- PEER 2001/04** *Organizational and Societal Considerations for Performance-Based Earthquake Engineering.* Peter J. May. April 2001.
- PEER 2001/03** *A Modal Pushover Analysis Procedure to Estimate Seismic Demands for Buildings: Theory and Preliminary Evaluation.* Anil K. Chopra and Rakesh K. Goel. January 2001.
- PEER 2001/02** *Seismic Response Analysis of Highway Overcrossings Including Soil-Structure Interaction.* Jian Zhang and Nicos Makris. March 2001.
- PEER 2001/01** *Experimental Study of Large Seismic Steel Beam-to-Column Connections.* Egor P. Popov and Shakhzod M. Takhirov. November 2000.
- PEER 2000/10** *The Second U.S.-Japan Workshop on Performance-Based Earthquake Engineering Methodology for Reinforced Concrete Building Structures.* March 2000.
- PEER 2000/09** *Structural Engineering Reconnaissance of the August 17, 1999 Earthquake: Kocaeli (Izmit), Turkey.* Halil Sezen, Kenneth J. Elwood, Andrew S. Whittaker, Khalid Mosalam, John J. Wallace, and John F. Stanton. December 2000.
- PEER 2000/08** *Behavior of Reinforced Concrete Bridge Columns Having Varying Aspect Ratios and Varying Lengths of Confinement.* Anthony J. Calderone, Dawn E. Lehman, and Jack P. Moehle. January 2001.
- PEER 2000/07** *Cover-Plate and Flange-Plate Reinforced Steel Moment-Resisting Connections.* Taejin Kim, Andrew S. Whittaker, Amir S. Gilani, Vitelmo V. Bertero, and Shakhzod M. Takhirov. September 2000.
- PEER 2000/06** *Seismic Evaluation and Analysis of 230-kV Disconnect Switches.* Amir S. J. Gilani, Andrew S. Whittaker, Gregory L. Fenves, Chun-Hao Chen, Henry Ho, and Eric Fujisaki. July 2000.
- PEER 2000/05** *Performance-Based Evaluation of Exterior Reinforced Concrete Building Joints for Seismic Excitation.* Chandra Clyde, Chris P. Pantelides, and Lawrence D. Reaveley. July 2000.
- PEER 2000/04** *An Evaluation of Seismic Energy Demand: An Attenuation Approach.* Chung-Che Chou and Chia-Ming Uang. July 1999.
- PEER 2000/03** *Framing Earthquake Retrofitting Decisions: The Case of Hillside Homes in Los Angeles.* Detlof von Winterfeldt, Nels Roselund, and Alicia Kitsuse. March 2000.
- PEER 2000/02** *U.S.-Japan Workshop on the Effects of Near-Field Earthquake Shaking.* Andrew Whittaker, Editor. July 2000.
- PEER 2000/01** *Further Studies on Seismic Interaction in Interconnected Electrical Substation Equipment.* Armen Der Kiureghian, Kee-Jeung Hong, and Jerome L. Sackman. November 1999.
- PEER 1999/14** *Seismic Evaluation and Retrofit of 230-kV Porcelain Transformer Bushings.* Amir S. Gilani, Andrew S. Whittaker, Gregory L. Fenves, and Eric Fujisaki. December 1999.
- PEER 1999/13** *Building Vulnerability Studies: Modeling and Evaluation of Tilt-up and Steel Reinforced Concrete Buildings.* John W. Wallace, Jonathan P. Stewart, and Andrew S. Whittaker, Editors. December 1999.
- PEER 1999/12** *Rehabilitation of Nonductile RC Frame Building Using Encasement Plates and Energy-Dissipating Devices.* Mehrdad Sasani, Vitelmo V. Bertero, James C. Anderson. December 1999.
- PEER 1999/11** *Performance Evaluation Database for Concrete Bridge Components and Systems under Simulated Seismic Loads.* Yael D. Hose and Frieder Seible. November 1999.

- PEER 1999/10** *U.S.-Japan Workshop on Performance-Based Earthquake Engineering Methodology for Reinforced Concrete Building Structures.* December 1999.
- PEER 1999/09** *Performance Improvement of Long Period Building Structures Subjected to Severe Pulse-Type Ground Motions.* James C. Anderson, Vitelmo V. Bertero, and Raul Bertero. October 1999.
- PEER 1999/08** *Envelopes for Seismic Response Vectors.* Charles Menun and Armen Der Kiureghian. July 1999.
- PEER 1999/07** *Documentation of Strengths and Weaknesses of Current Computer Analysis Methods for Seismic Performance of Reinforced Concrete Members.* William F. Cofer. November 1999.
- PEER 1999/06** *Rocking Response and Overturning of Anchored Equipment under Seismic Excitations.* Nicos Makris and Jian Zhang. November 1999.
- PEER 1999/05** *Seismic Evaluation of 550 kV Porcelain Transformer Bushings.* Amir S. Gilani, Andrew S. Whittaker, Gregory L. Fenves, and Eric Fujisaki. October 1999.
- PEER 1999/04** *Adoption and Enforcement of Earthquake Risk-Reduction Measures.* Peter J. May, Raymond J. Burby, T. Jens Feeley, and Robert Wood. August 1999.
- PEER 1999/03** *Task 3 Characterization of Site Response General Site Categories.* Adrian Rodriguez-Marek, Jonathan D. Bray and Norman Abrahamson. February 1999.
- PEER 1999/02** *Capacity-Demand-Diagram Methods for Estimating Seismic Deformation of Inelastic Structures: SDF Systems.* Anil K. Chopra and Rakesh Goel. April 1999.
- PEER 1999/01** *Interaction in Interconnected Electrical Substation Equipment Subjected to Earthquake Ground Motions.* Armen Der Kiureghian, Jerome L. Sackman, and Kee-Jeung Hong. February 1999.
- PEER 1998/08** *Behavior and Failure Analysis of a Multiple-Frame Highway Bridge in the 1994 Northridge Earthquake.* Gregory L. Fenves and Michael Ellery. December 1998.
- PEER 1998/07** *Empirical Evaluation of Inertial Soil-Structure Interaction Effects.* Jonathan P. Stewart, Raymond B. Seed, and Gregory L. Fenves. November 1998.
- PEER 1998/06** *Effect of Damping Mechanisms on the Response of Seismic Isolated Structures.* Nicos Makris and Shih-Po Chang. November 1998.
- PEER 1998/05** *Rocking Response and Overturning of Equipment under Horizontal Pulse-Type Motions.* Nicos Makris and Yiannis Roussos. October 1998.
- PEER 1998/04** *Pacific Earthquake Engineering Research Invitational Workshop Proceedings, May 14–15, 1998: Defining the Links between Planning, Policy Analysis, Economics and Earthquake Engineering.* Mary Comerio and Peter Gordon. September 1998.
- PEER 1998/03** *Repair/Upgrade Procedures for Welded Beam to Column Connections.* James C. Anderson and Xiaojing Duan. May 1998.
- PEER 1998/02** *Seismic Evaluation of 196 kV Porcelain Transformer Bushings.* Amir S. Gilani, Juan W. Chavez, Gregory L. Fenves, and Andrew S. Whittaker. May 1998.
- PEER 1998/01** *Seismic Performance of Well-Confined Concrete Bridge Columns.* Dawn E. Lehman and Jack P. Moehle. December 2000.

PEER REPORTS: ONE HUNDRED SERIES

The following PEER reports are available by Internet only at http://peer.berkeley.edu/publications/peer_reports_complete.html.

- PEER 2012/103** *Performance-Based Seismic Demand Assessment of Concentrically Braced Steel Frame Buildings*. Chui-Hsin Chen and Stephen A. Mahin. December 2012.
- PEER 2012/102** *Procedure to Restart an Interrupted Hybrid Simulation: Addendum to PEER Report 2010/103*. Vesna Terzic and Božidar Stojadinovic. October 2012.
- PEER 2012/101** *Mechanics of Fiber Reinforced Bearings*. James M. Kelly and Andrea Calabrese. February 2012.
- PEER 2011/107** *Nonlinear Site Response and Seismic Compression at Vertical Array Strongly Shaken by 2007 Niigata-ken Chuetsu-oki Earthquake*. Eric Yee, Jonathan P. Stewart, and Kohji Tokimatsu. December 2011.
- PEER 2011/106** *Self Compacting Hybrid Fiber Reinforced Concrete Composites for Bridge Columns*. Pardeep Kumar, Gabriel Jen, William Trono, Marios Panagiotou, and Claudia Ostertag. September 2011.
- PEER 2011/105** *Stochastic Dynamic Analysis of Bridges Subjected to Spatially Varying Ground Motions*. Katerina Konakli and Armen Der Kiureghian. August 2011.
- PEER 2011/104** *Design and Instrumentation of the 2010 E-Defense Four-Story Reinforced Concrete and Post-Tensioned Concrete Buildings*. Takuya Nagae, Kenichi Tahara, Taizo Matsumori, Hitoshi Shiohara, Toshimi Kabeyasawa, Susumu Kono, Minehiro Nishiyama (Japanese Research Team) and John Wallace, Wassim Ghannoum, Jack Moehle, Richard Sause, Wesley Keller, Zeynep Tuna (U.S. Research Team). June 2011.
- PEER 2011/103** *In-Situ Monitoring of the Force Output of Fluid Dampers: Experimental Investigation*. Dimitrios Konstantinidis, James M. Kelly, and Nicos Makris. April 2011.
- PEER 2011/102** *Ground-Motion Prediction Equations 1964–2010*. John Douglas. April 2011.
- PEER 2011/101** *Report of the Eighth Planning Meeting of NEES/E-Defense Collaborative Research on Earthquake Engineering*. Convened by the Hyogo Earthquake Engineering Research Center (NIED), NEES Consortium, Inc. February 2011.
- PEER 2010/111** *Modeling and Acceptance Criteria for Seismic Design and Analysis of Tall Buildings*. Task 7 Report for the Tall Buildings Initiative - Published jointly by the Applied Technology Council. October 2010.
- PEER 2010/110** *Seismic Performance Assessment and Probabilistic Repair Cost Analysis of Precast Concrete Cladding Systems for Multistory Buildings*. Jeffrey P. Hunt and Božidar Stojadinovic. November 2010.
- PEER 2010/109** *Report of the Seventh Joint Planning Meeting of NEES/E-Defense Collaboration on Earthquake Engineering. Held at the E-Defense, Miki, and Shin-Kobe, Japan, September 18–19, 2009*. August 2010.
- PEER 2010/108** *Probabilistic Tsunami Hazard in California*. Hong Kie Thio, Paul Somerville, and Jascha Polet, preparers. October 2010.
- PEER 2010/107** *Performance and Reliability of Exposed Column Base Plate Connections for Steel Moment-Resisting Frames*. Ady Aviram, Božidar Stojadinovic, and Armen Der Kiureghian. August 2010.
- PEER 2010/106** *Verification of Probabilistic Seismic Hazard Analysis Computer Programs*. Patricia Thomas, Ivan Wong, and Norman Abrahamson. May 2010.
- PEER 2010/105** *Structural Engineering Reconnaissance of the April 6, 2009, Abruzzo, Italy, Earthquake, and Lessons Learned*. M. Selim Günay and Khalid M. Mosalam. April 2010.
- PEER 2010/104** *Simulating the Inelastic Seismic Behavior of Steel Braced Frames, Including the Effects of Low-Cycle Fatigue*. Yuli Huang and Stephen A. Mahin. April 2010.
- PEER 2010/103** *Post-Earthquake Traffic Capacity of Modern Bridges in California*. Vesna Terzic and Božidar Stojadinović. March 2010.
- PEER 2010/102** *Analysis of Cumulative Absolute Velocity (CAV) and JMA Instrumental Seismic Intensity (I_{JMA}) Using the PEER–NGA Strong Motion Database*. Kenneth W. Campbell and Yousef Bozorgnia. February 2010.
- PEER 2010/101** *Rocking Response of Bridges on Shallow Foundations*. Jose A. Ugalde, Bruce L. Kutter, and Boris Jeremic. April 2010.
- PEER 2009/109** *Simulation and Performance-Based Earthquake Engineering Assessment of Self-Centering Post-Tensioned Concrete Bridge Systems*. Won K. Lee and Sarah L. Billington. December 2009.
- PEER 2009/108** *PEER Lifelines Geotechnical Virtual Data Center*. J. Carl Stepp, Daniel J. Ponti, Loren L. Turner, Jennifer N. Swift, Sean Devlin, Yang Zhu, Jean Benoit, and John Bobbitt. September 2009.

- PEER 2009/107** *Experimental and Computational Evaluation of Current and Innovative In-Span Hinge Details in Reinforced Concrete Box-Girder Bridges: Part 2: Post-Test Analysis and Design Recommendations.* Matias A. Hube and Khalid M. Mosalam. December 2009.
- PEER 2009/106** *Shear Strength Models of Exterior Beam-Column Joints without Transverse Reinforcement.* Sangjoon Park and Khalid M. Mosalam. November 2009.
- PEER 2009/105** *Reduced Uncertainty of Ground Motion Prediction Equations through Bayesian Variance Analysis.* Robb Eric S. Moss. November 2009.
- PEER 2009/104** *Advanced Implementation of Hybrid Simulation.* Andreas H. Schellenberg, Stephen A. Mahin, Gregory L. Fenves. November 2009.
- PEER 2009/103** *Performance Evaluation of Innovative Steel Braced Frames.* T. Y. Yang, Jack P. Moehle, and Božidar Stojadinovic. August 2009.
- PEER 2009/102** *Reinvestigation of Liquefaction and Nonliquefaction Case Histories from the 1976 Tangshan Earthquake.* Robb Eric Moss, Robert E. Kayen, Liyuan Tong, Songyu Liu, Guojun Cai, and Jiaer Wu. August 2009.
- PEER 2009/101** *Report of the First Joint Planning Meeting for the Second Phase of NEES/E-Defense Collaborative Research on Earthquake Engineering.* Stephen A. Mahin et al. July 2009.
- PEER 2008/104** *Experimental and Analytical Study of the Seismic Performance of Retaining Structures.* Linda Al Atik and Nicholas Sitar. January 2009.
- PEER 2008/103** *Experimental and Computational Evaluation of Current and Innovative In-Span Hinge Details in Reinforced Concrete Box-Girder Bridges. Part 1: Experimental Findings and Pre-Test Analysis.* Matias A. Hube and Khalid M. Mosalam. January 2009.
- PEER 2008/102** *Modeling of Unreinforced Masonry Infill Walls Considering In-Plane and Out-of-Plane Interaction.* Stephen Kadosiewicz and Khalid M. Mosalam. January 2009.
- PEER 2008/101** *Seismic Performance Objectives for Tall Buildings.* William T. Holmes, Charles Kircher, William Petak, and Nabih Youssef. August 2008.
- PEER 2007/101** *Generalized Hybrid Simulation Framework for Structural Systems Subjected to Seismic Loading.* Tarek Elkhoraibi and Khalid M. Mosalam. July 2007.
- PEER 2007/100** *Seismic Evaluation of Reinforced Concrete Buildings Including Effects of Masonry Infill Walls.* Alidad Hashemi and Khalid M. Mosalam. July 2007.

The Pacific Earthquake Engineering Research Center (PEER) is a multi-institutional research and education center with headquarters at the University of California, Berkeley. Investigators from over 20 universities, several consulting companies, and researchers at various state and federal government agencies contribute to research programs focused on performance-based earthquake engineering.

These research programs aim to identify and reduce the risks from major earthquakes to life safety and to the economy by including research in a wide variety of disciplines including structural and geotechnical engineering, geology/seismology, lifelines, transportation, architecture, economics, risk management, and public policy.

PEER is supported by federal, state, local, and regional agencies, together with industry partners.



PEER Core Institutions:

University of California, Berkeley (Lead Institution)
California Institute of Technology
Oregon State University
Stanford University
University of California, Davis
University of California, Irvine
University of California, Los Angeles
University of California, San Diego
University of Southern California
University of Washington

PEER reports can be ordered at http://peer.berkeley.edu/publications/peer_reports.html or by contacting

Pacific Earthquake Engineering Research Center
University of California, Berkeley
325 Davis Hall, Mail Code 1792
Berkeley, CA 94720-1792
Tel: 510-642-3437
Fax: 510-642-1655
Email: peer_center@berkeley.edu

ISSN 1547-0587X